



Simulation of runaway electrons with MHD modes

Masatoshi Yagi

National Institutes for Quantum and Radiological
Science and Technology, Japan

in collaboration with A. Matsuyama and N. Aiba

March 20-24, 2017, Aix-Marseille University

Outline

1. Introduction (including activity in Rokkasho)
2. Avalanche mechanisms of runaway electron generation
3. Simulation of runaway beam current profile with MHD modes
4. Effects of stochastic magnetic fields
5. Summary and conclusion

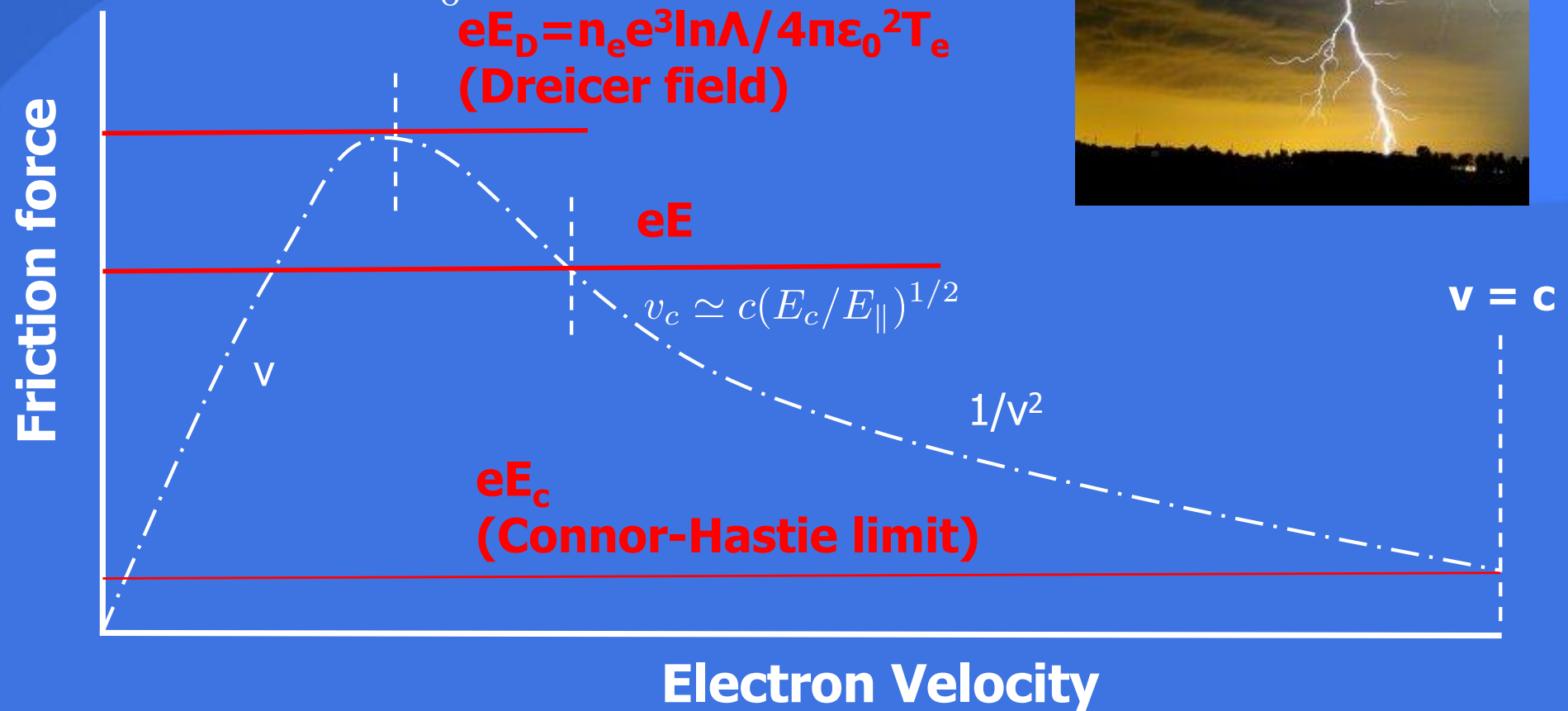
Runaway electrons

<https://science.nasa.gov/science-news/>

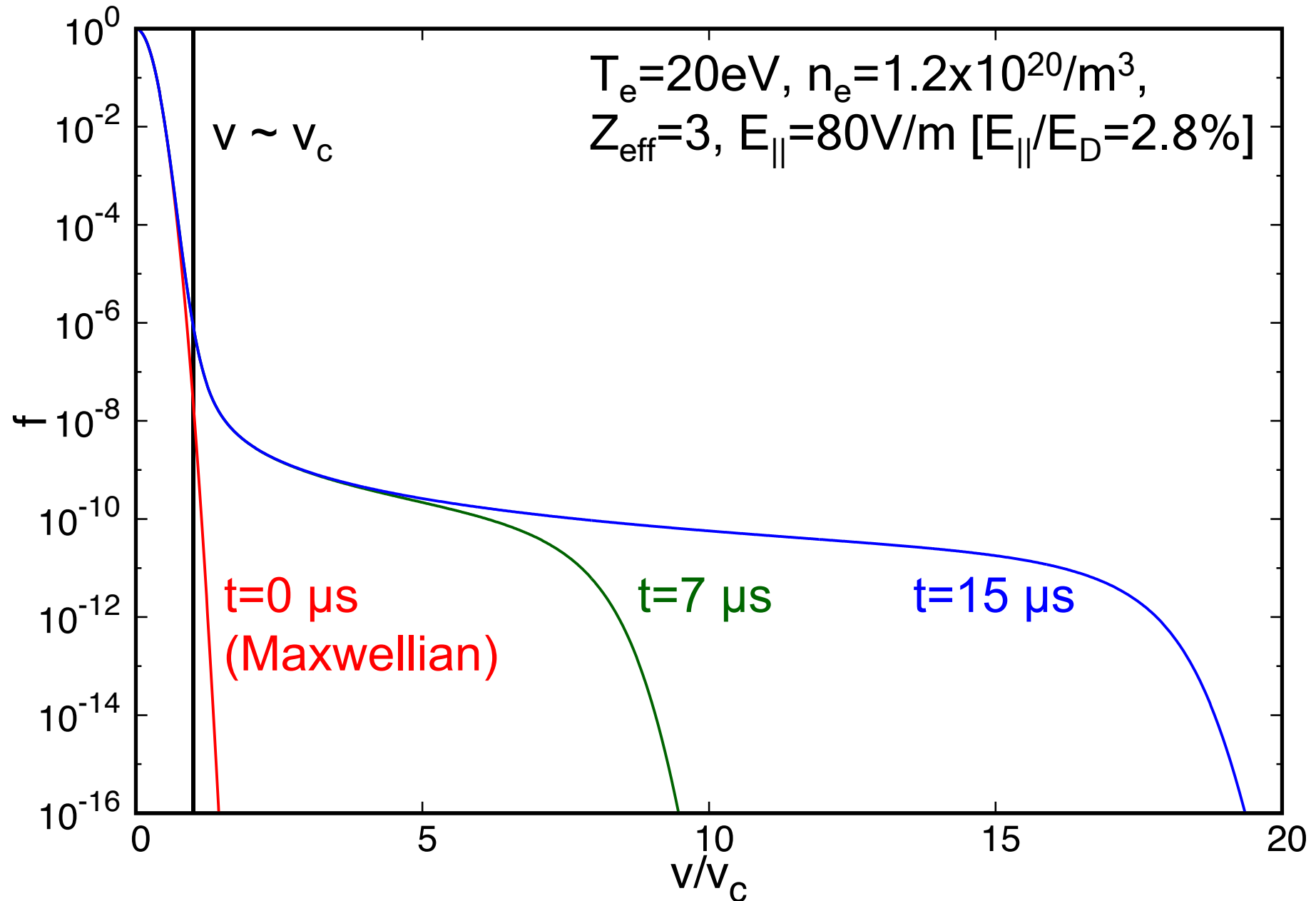
Electrons run away when electric field exceeds absolute threshold for runaway electrons determined by relativistic constraint (Connor & Hastie, NF1975)

$$E_c = \frac{n_e e^3 \ln \Lambda}{4\pi \epsilon_0^2 m_e c^2}$$

$eE_D = n_e e^3 \ln \Lambda / 4\pi \epsilon_0^2 T_e$
(Dreicer field)



Dreicer acceleration - formation of velocity space tail



Localized RE wall loads must be avoided in ITER

- ◆ Runaway mitigation has become high priority issue in ITER

- ◆ Characteristics of REs in ITER (simulation)

 - Up to 2/3 of pre-disruption plasma current

 - Average kinetic energy $\sim 10\text{-}20$ MeV

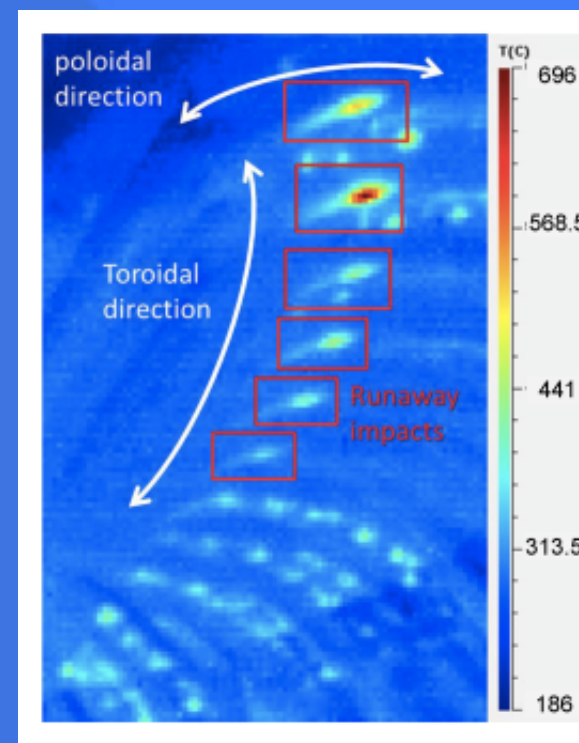
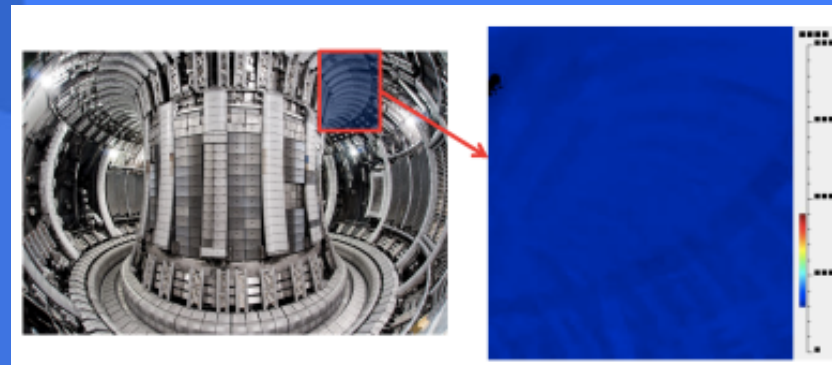
- ◆ Wall loads due to high energy electrons

ITER: 0.5MA RE = 1 MJ

melt layer depth of Be > 1 mm

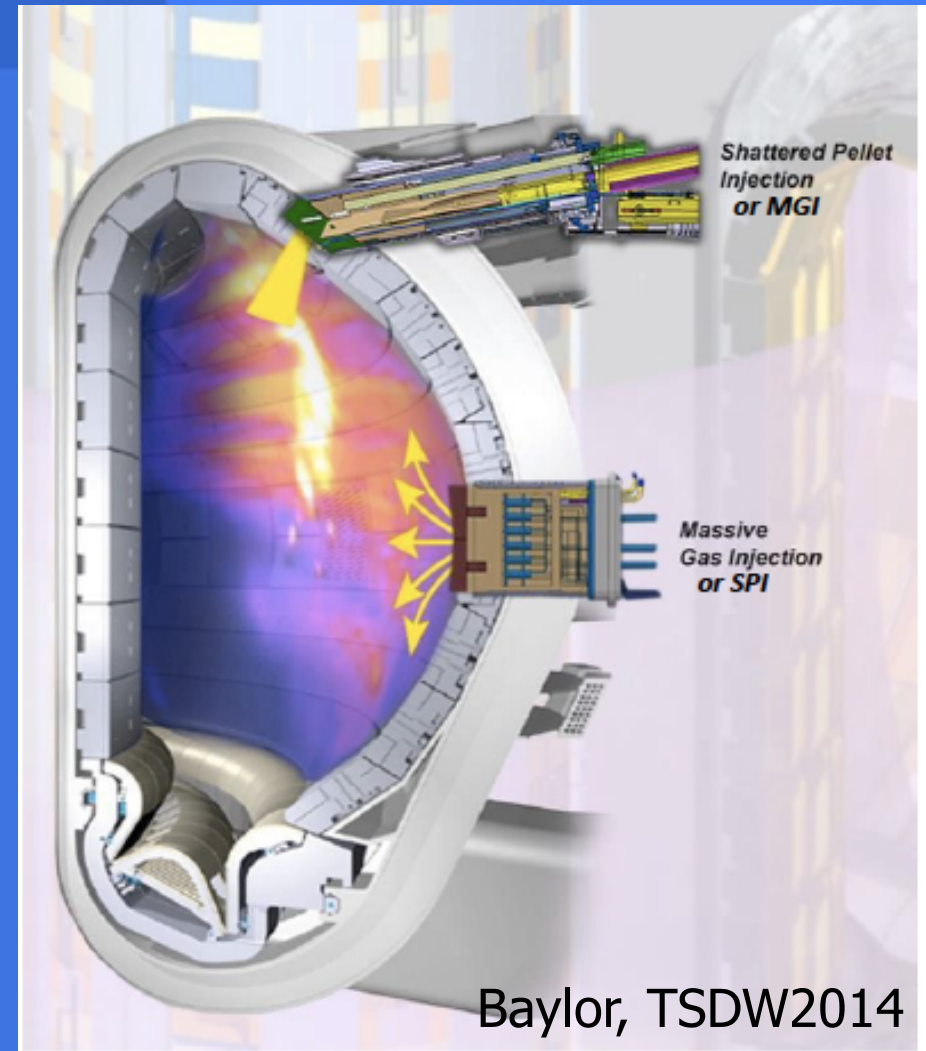
(energy distributed equally on 36 BMs)

[Lehnen, US-J MHD-WS2014]



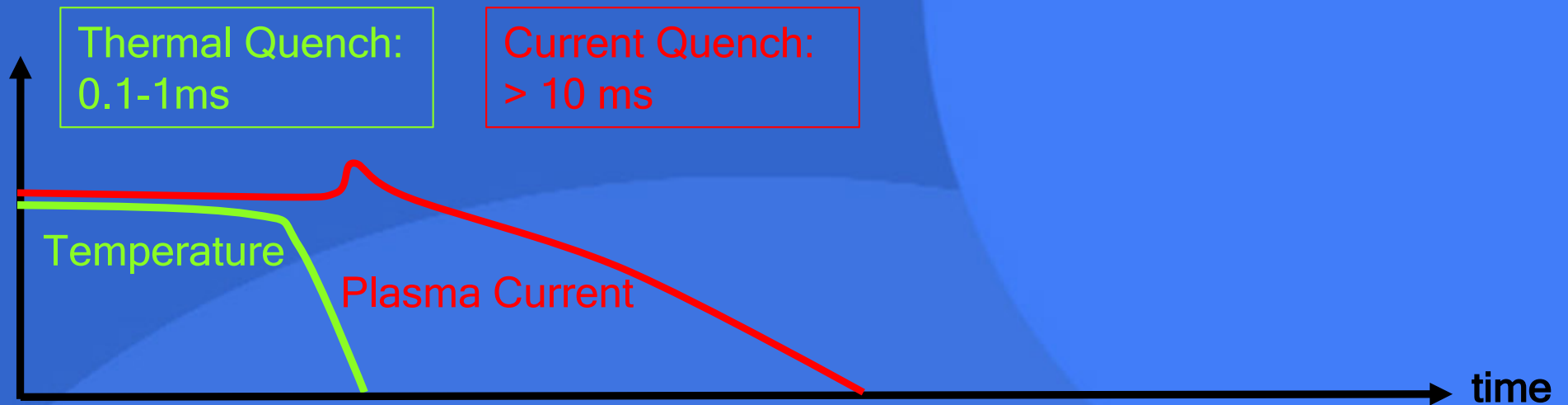
RE mitigation must be compatible with heat and electromagnetic loads mitigation

- ◆ Massive impurity injection is used to mitigate heat and electromagnetic loads
 - Dissipate thermal stored energy by radiation
 - Avoid coupling to the wall through eddy and halo currents with increasing plasma resistivity
- ◆ Short current quench time tends to higher loop voltage and runaway electrons
 - Mitigation scheme must be optimized to be compatible with RE mitigation.

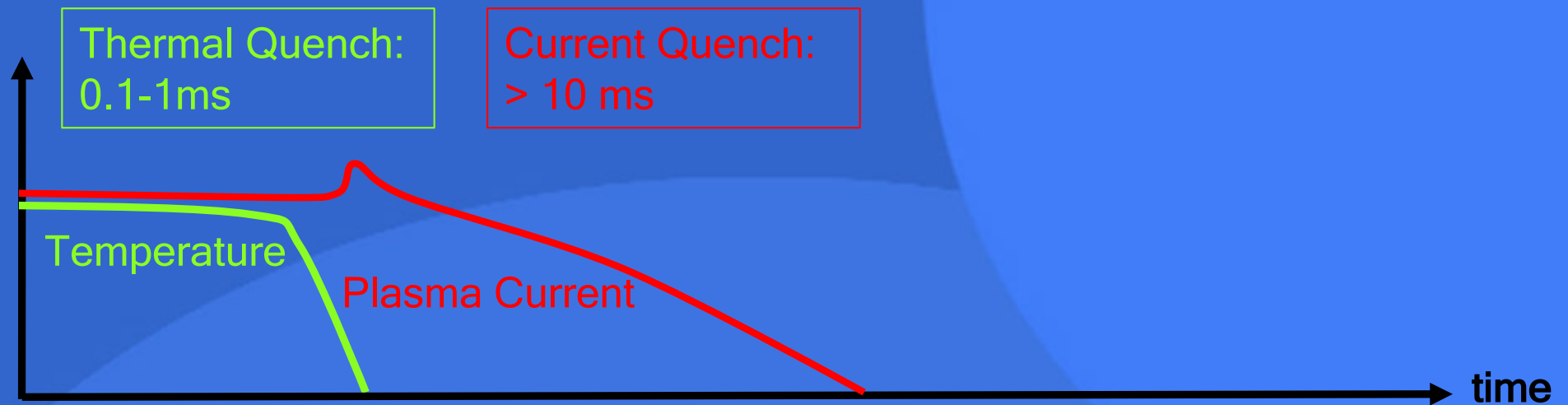


Avalanche mechanism of runaway electron generation

Mechanism of runaway electron generation during major disruptions

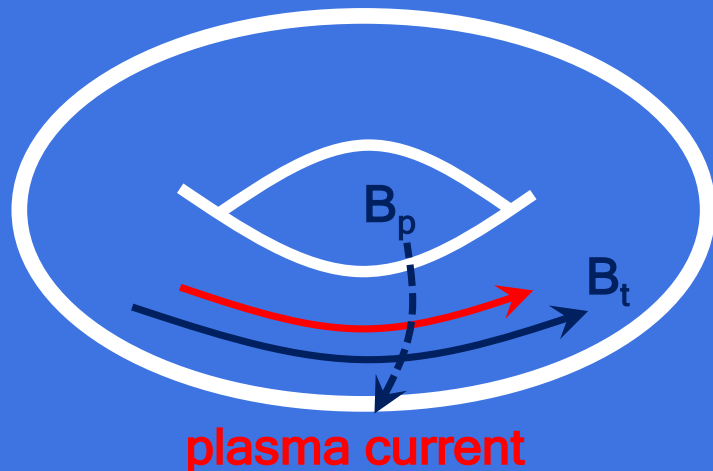


Mechanism of runaway electron generation during major disruptions

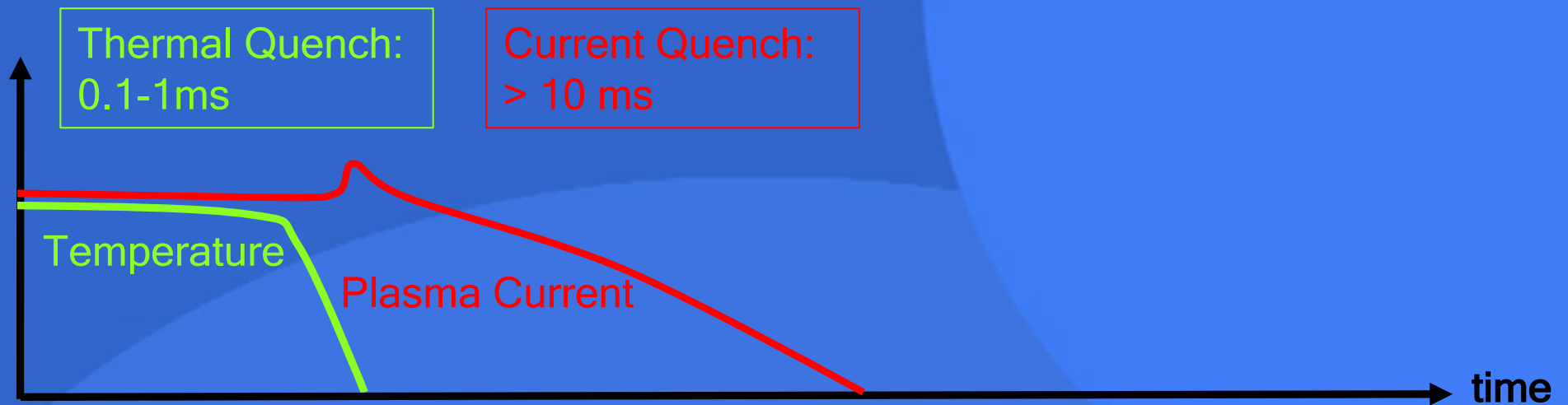


Normal tokamak discharge

- high temperature (1-10 keV)
- low resistivity ($\eta=1/S < 10^{-8}$)

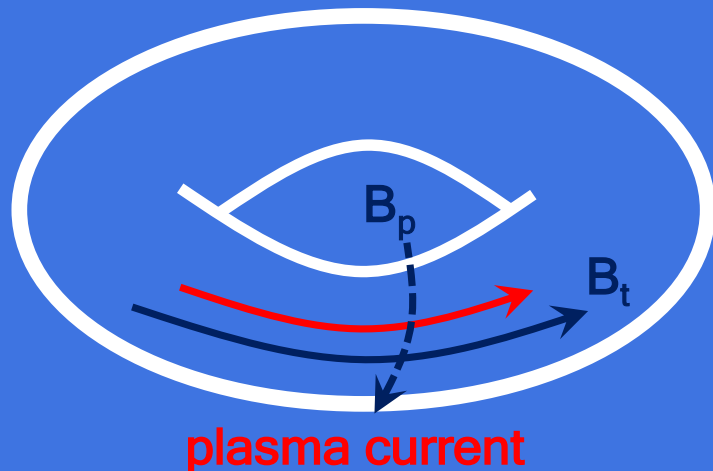


Mechanism of runaway electron generation during major disruptions



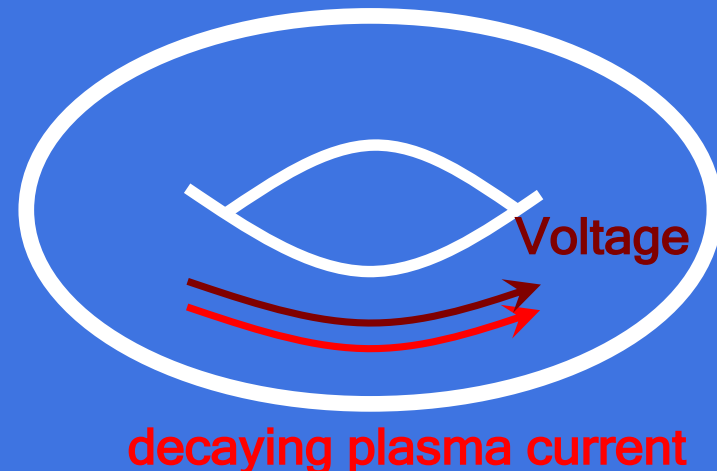
Normal tokamak discharge

- high temperature (1-10 keV)
- low resistivity ($\eta=1/S < 10^{-8}$)

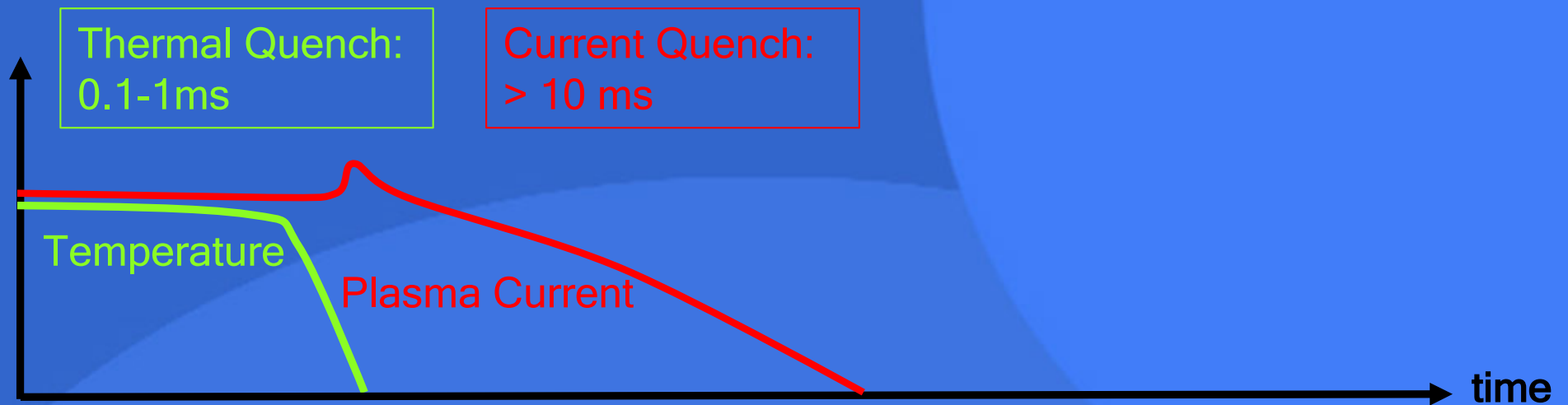


Post-disruption plasma

- low temperature ($\sim 10\text{eV}$)
- high resistivity ($\eta=1/S = 10^{-5}-10^{-6}$)

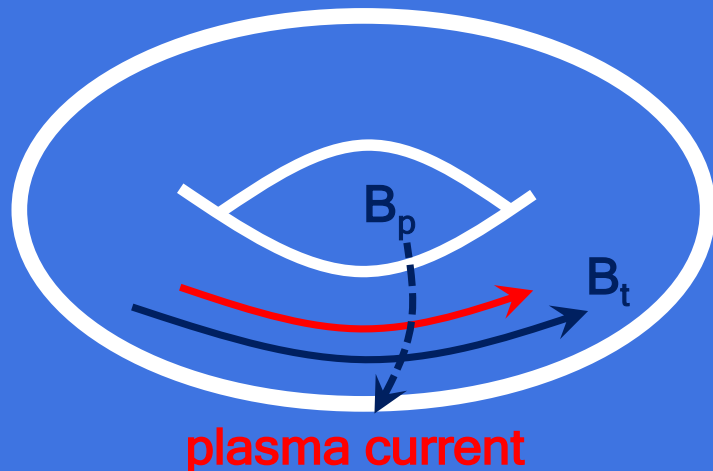


Mechanism of runaway electron generation during major disruptions



Normal tokamak discharge

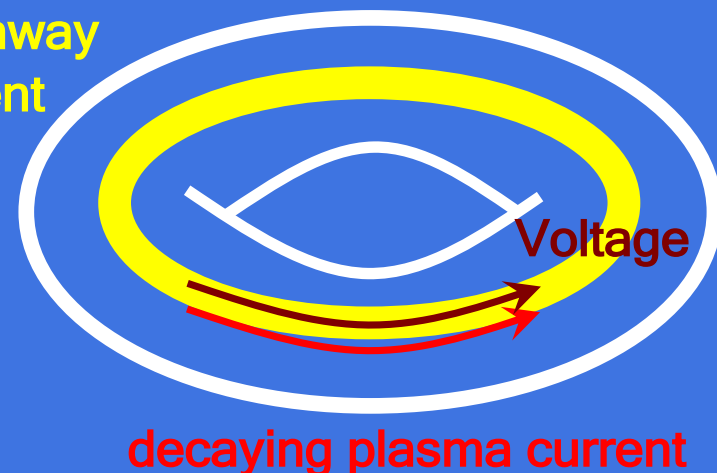
- high temperature (1-10 keV)
- low resistivity ($\eta=1/S < 10^{-8}$)



Post-disruption plasma

- low temperature ($\sim 10\text{eV}$)
- high resistivity ($\eta=1/S = 10^{-5}-10^{-6}$)

Runaway current

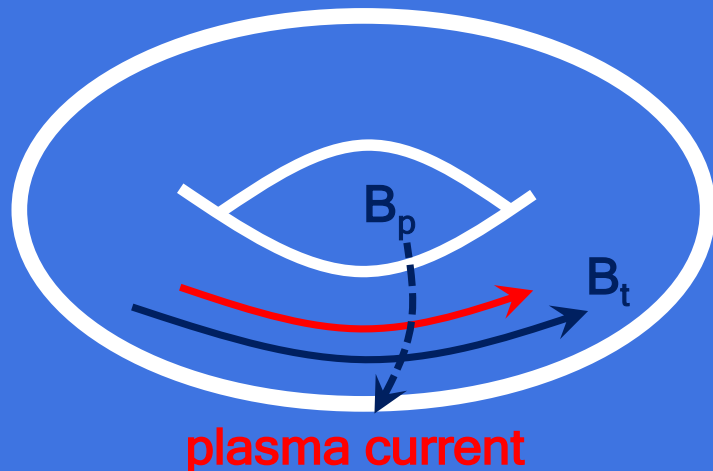


Mechanism of runaway electron generation during major disruptions



Normal tokamak discharge

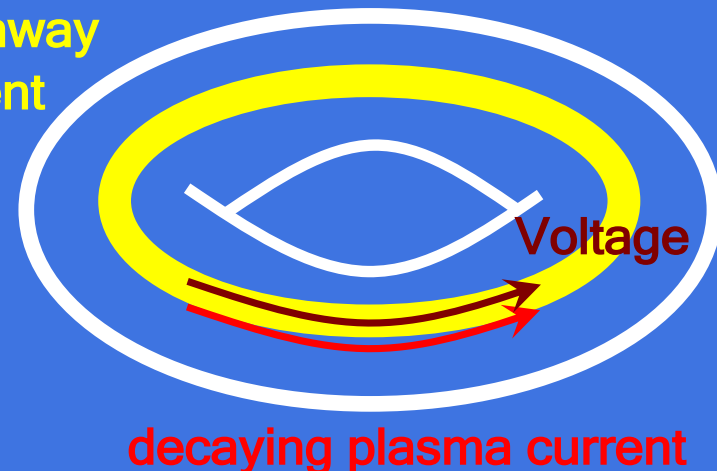
- high temperature (1-10 keV)
- low resistivity ($\eta=1/S < 10^{-8}$)



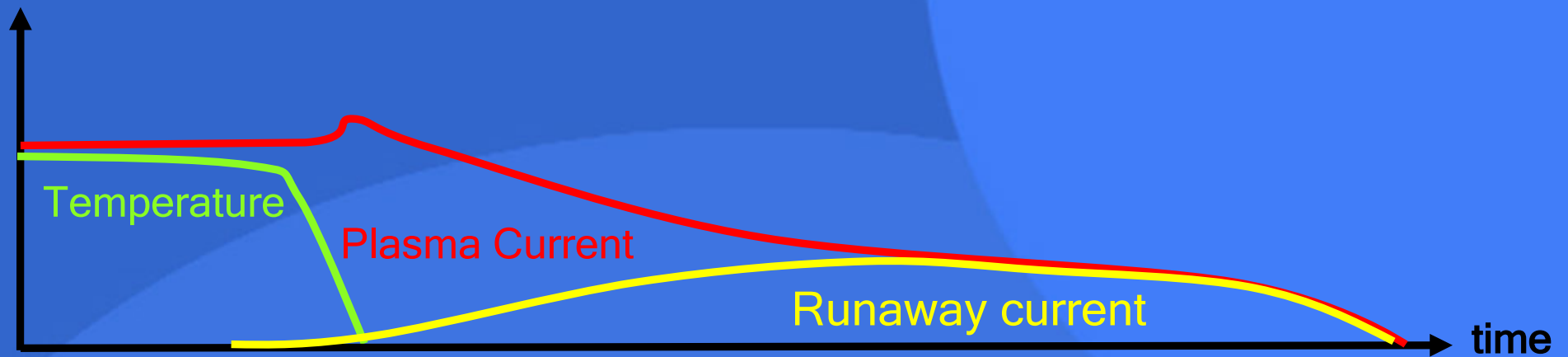
Post-disruption plasma

- low temperature ($\sim 10\text{eV}$)
- high resistivity ($\eta=1/S = 10^{-5}-10^{-6}$)

Runaway current

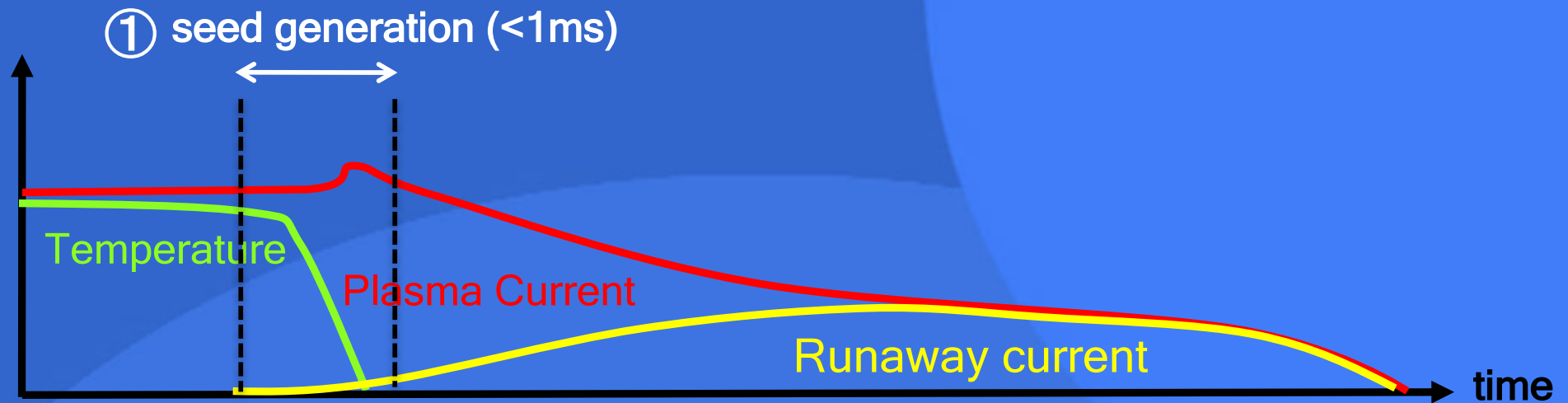


Mechanism of runaway electron generation during major disruptions



- Mechanism of runaway beam formation

Mechanism of runaway electron generation during major disruptions

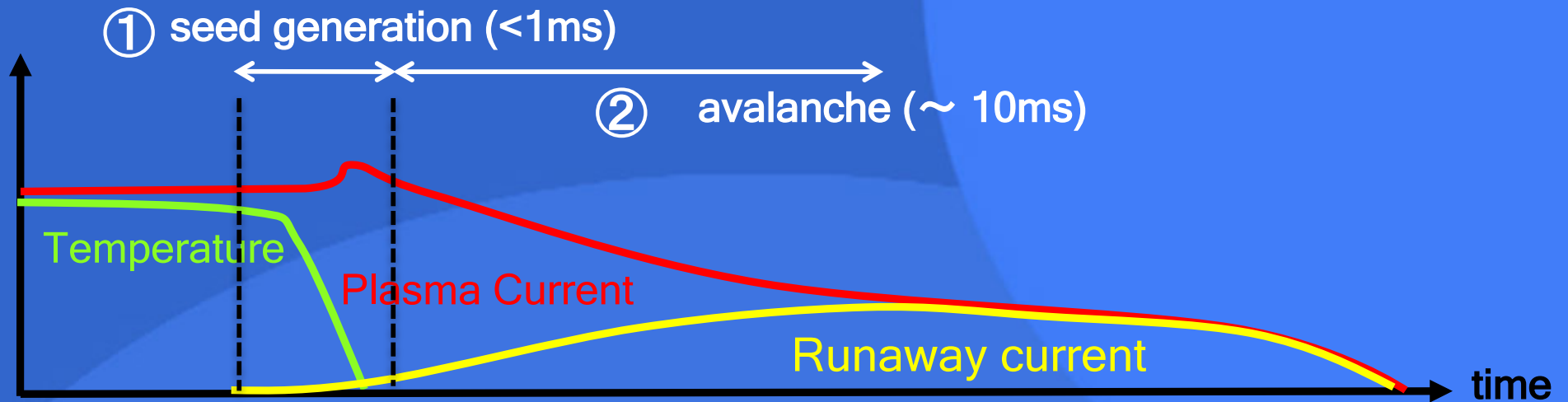


- Mechanism of runaway beam formation

- ① Seed generation:

- Dreicer acceleration
 - Hot-tail generation

Mechanism of runaway electron generation during major disruptions



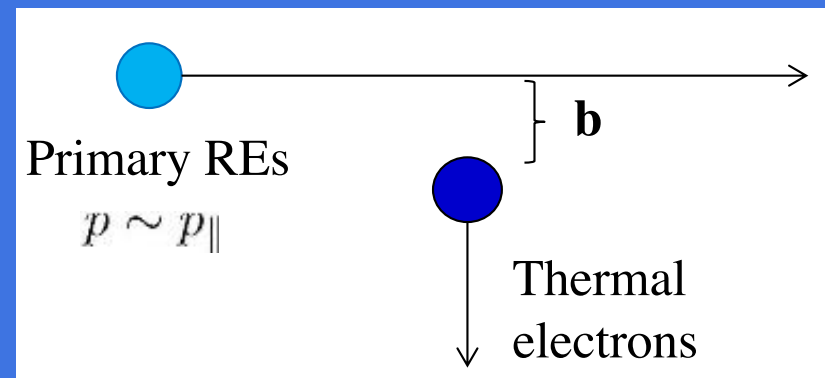
- Mechanism of runaway beam formation

- ① Seed generation:

- Dreicer acceleration
 - Hot-tail generation

- ② Avalanche growth

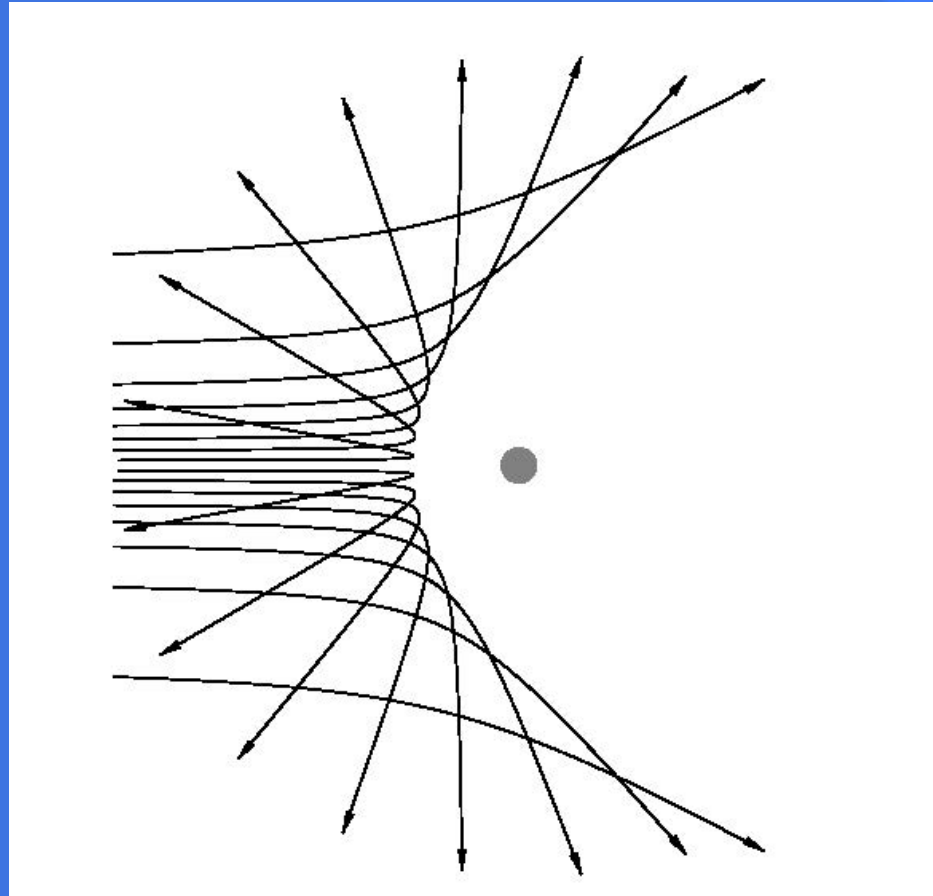
- Secondary generation by close collisions



Large angle scattering

Coulomb collisions

{ Small angle scattering
Large angle scattering
~ smaller by up to $O(1/\ln\Lambda)$

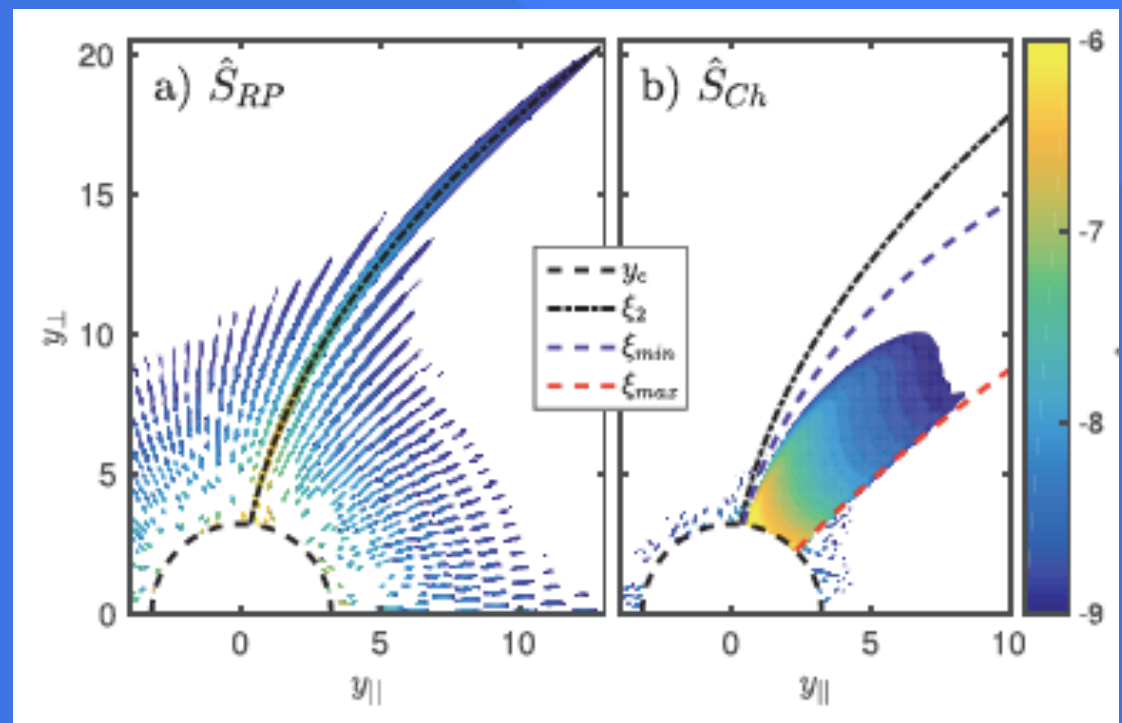


Fast avalanche growth [Rosenbluth-Putvinski, NF1997]

- ◆ The theory assume strong electric field $E \gg E_c$, and that primary electrons are highly relativistic $\gamma \gg 1$.

$$\left(\frac{\partial f}{\partial t}\right)_{\text{avl}} = \frac{n_r \delta(\lambda - \lambda_2) \sqrt{1 - \lambda b}}{\tau \ln \Lambda} \frac{1}{p^2} \frac{\partial}{\partial p} \left(\frac{1}{1 - \sqrt{1 + p^2}} \right) \quad \lambda_2 b = \frac{2}{\sqrt{1 + p^2} + 1}$$

$$\rightarrow \frac{dn_r}{dt} \approx n_r \sqrt{\frac{\pi}{2}} \frac{E/E_c - 1}{3\tau \ln \Lambda} \frac{1}{\tau \ln \Lambda} \quad \text{frequency of hard collisions}$$



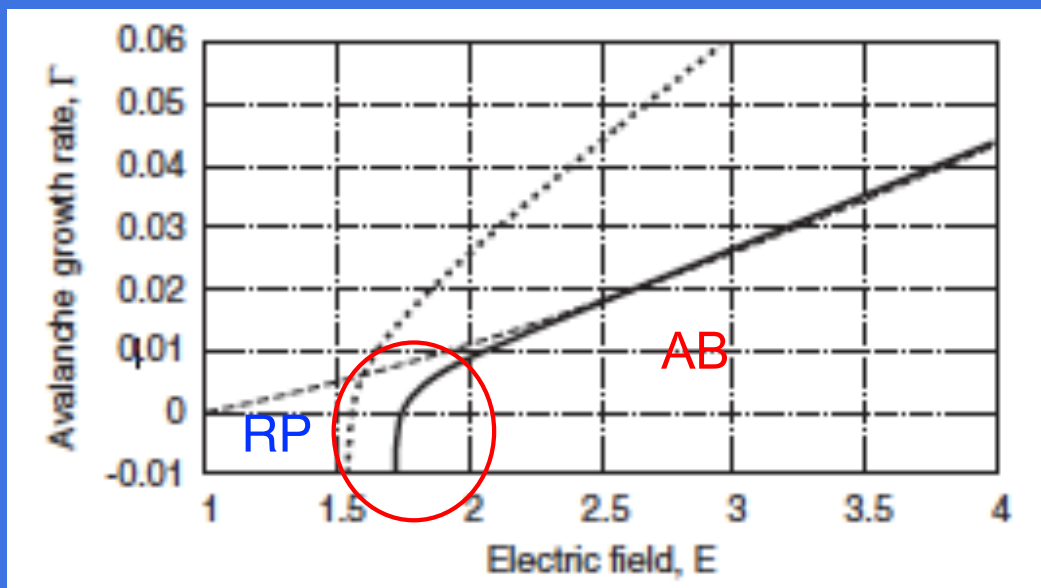
Stahl, NF2016

Near-critical field theory [Aleynikov&Breizman, PRL2015]

- ◆ Weak electric field $E \sim E_c$, and that finite energy of primary electrons are taken into account for calculating electron-electron collisions.

$$\Gamma_{\text{avl}} \equiv \frac{d \log n_{\text{RE}}}{dt} = n_e v_1 \int_{\epsilon_c}^{1/2} \frac{d\sigma_M(\epsilon; \gamma_1)}{d\epsilon} d\epsilon \quad \epsilon = \frac{\gamma - 1}{\gamma_1 - 1} \quad x = \frac{1}{\epsilon(1 - \epsilon)}$$

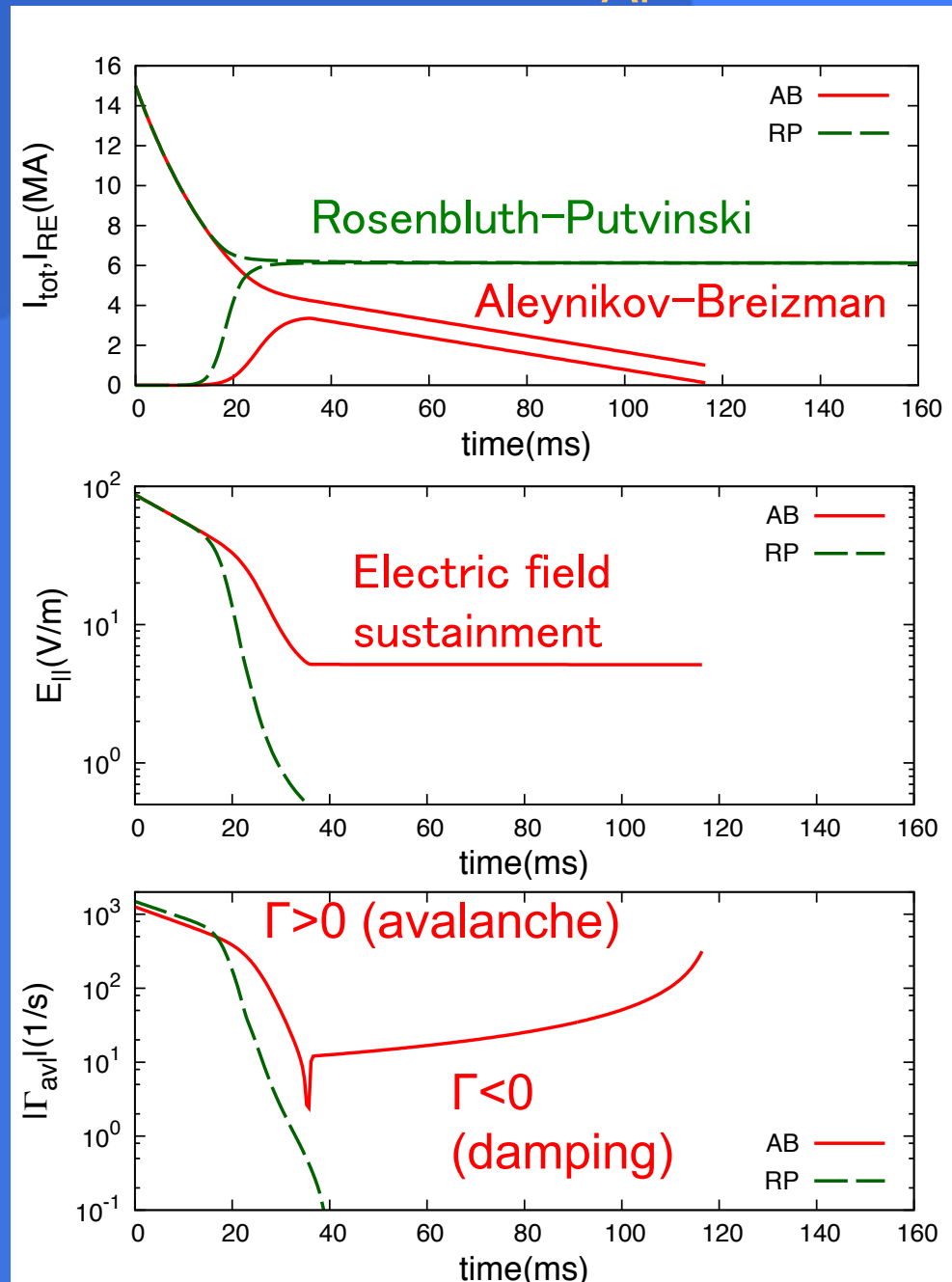
$$\frac{d\sigma_M(\epsilon; \gamma_1)}{d\epsilon} = 2\pi r_0^2 \frac{\gamma_1^2}{(\gamma_1 - 1)^2(\gamma_1 + 1)} \left[x^2 - 3x + \left(\frac{\gamma_1 - 1}{\gamma_1} \right)^2 (1 + x) \right]$$



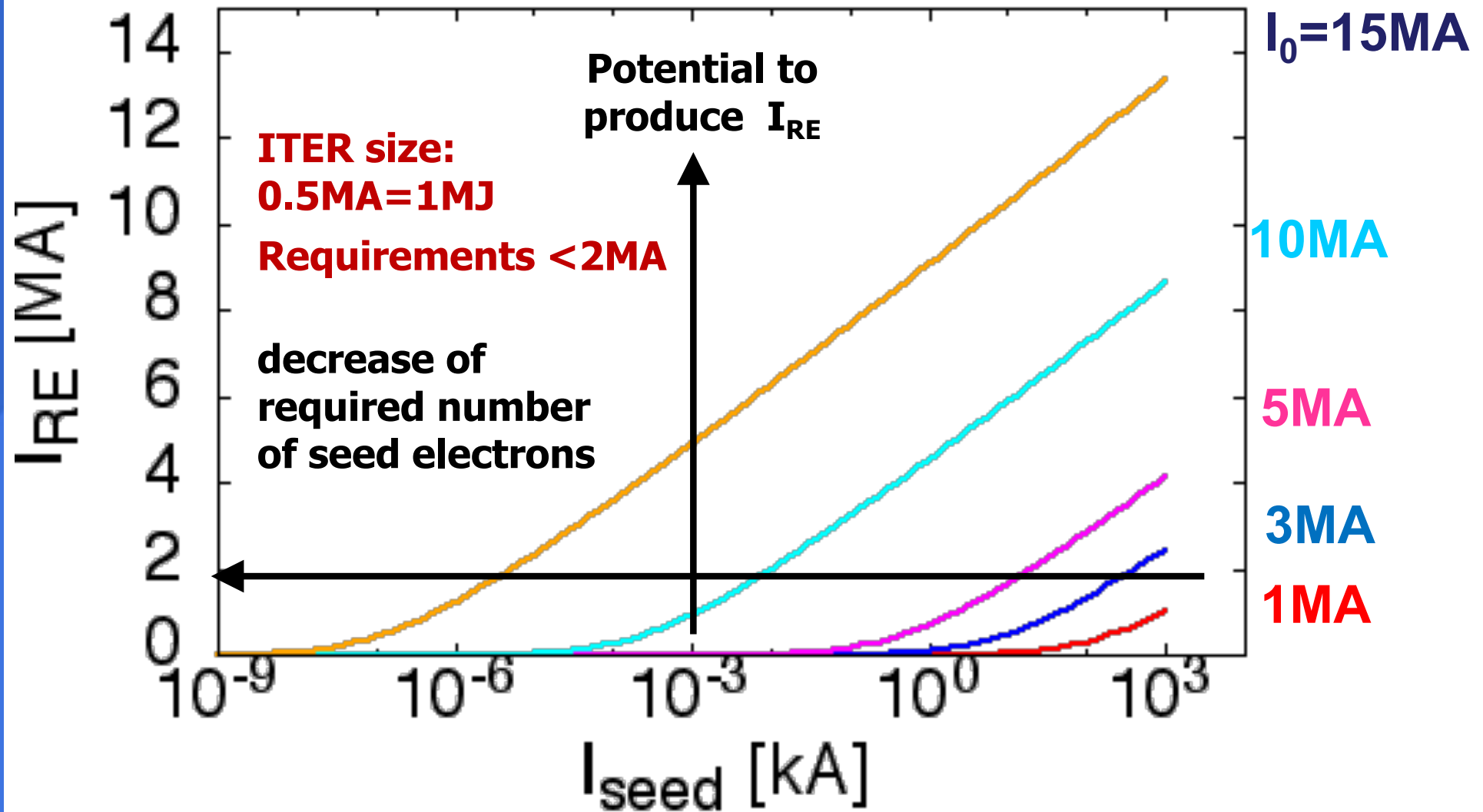
$\Gamma < 0$ (damping):
when primary electrons lose energy due to close collision

$\Gamma \sim 0$ (marginal stability):
→ electric field is sustained for avalanche to be marginally stable [Breizman, NF2014]

Comparison between R-P and A-B models for ITER 15MA scale simulation with $n_{Ar} = 2 \times 10^{20}/m^3$



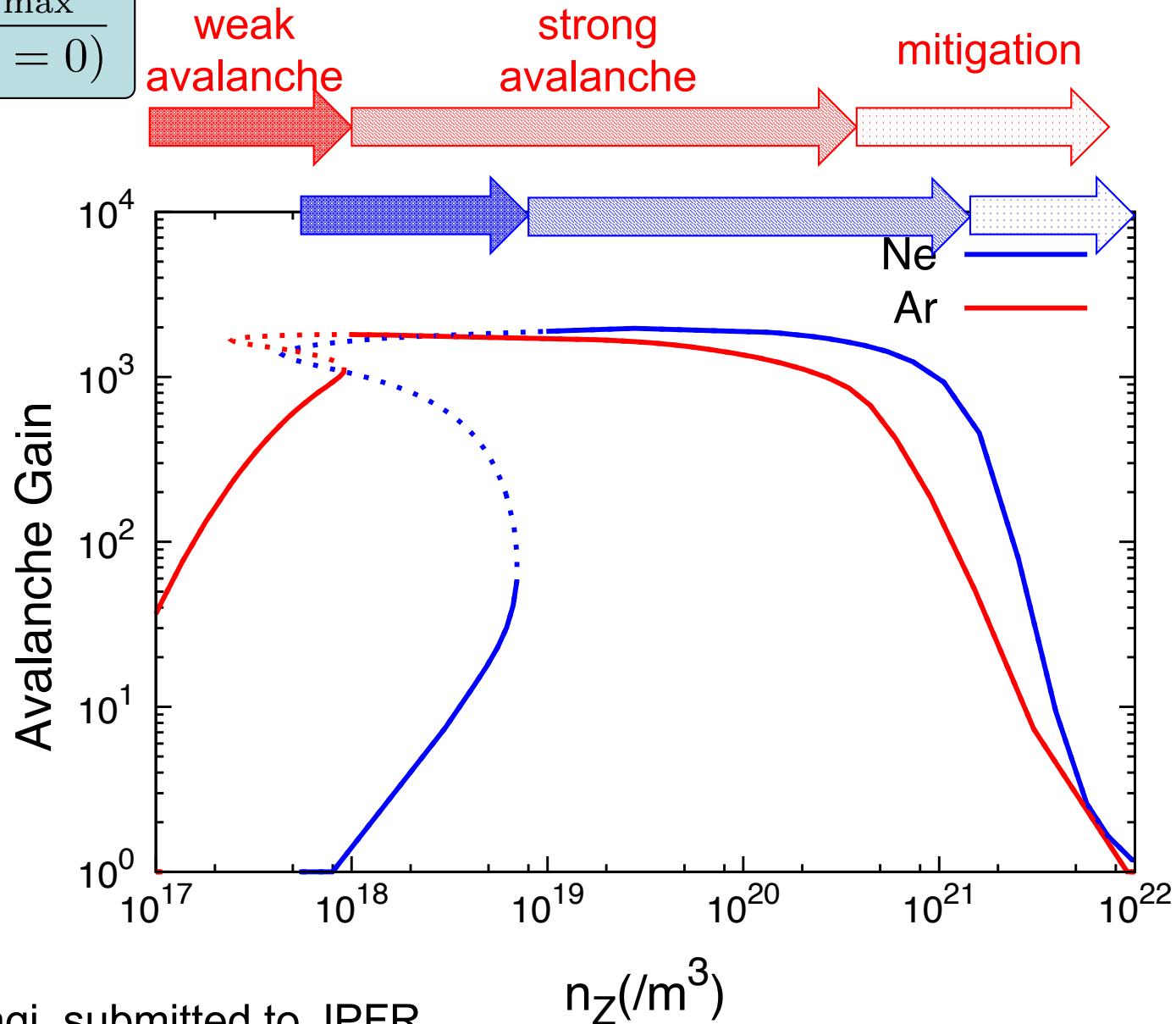
Avalanche generation becomes dominant mechanisms in ITER



$L \sim L_{ext} \sim \mu_0 R_0, R = 6.2 \text{ m}, Z_{eff} = 3, \ln \Lambda = 18$

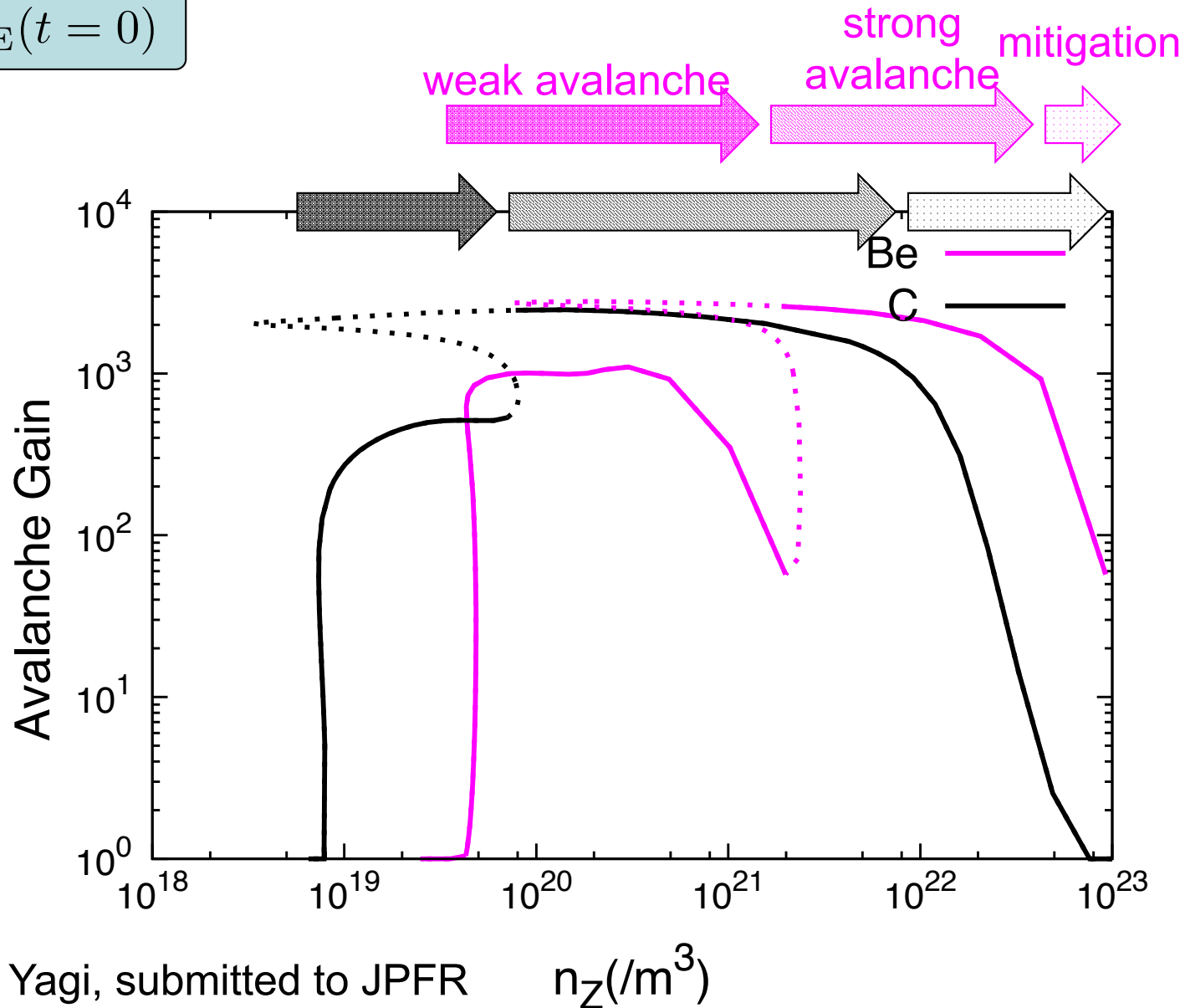
Dependence of the avalanche gain on impurity species - mitigation by noble gas injection

$$\text{Gain} = \frac{I_{\text{RE,max}}}{I_{\text{RE}}(t=0)}$$

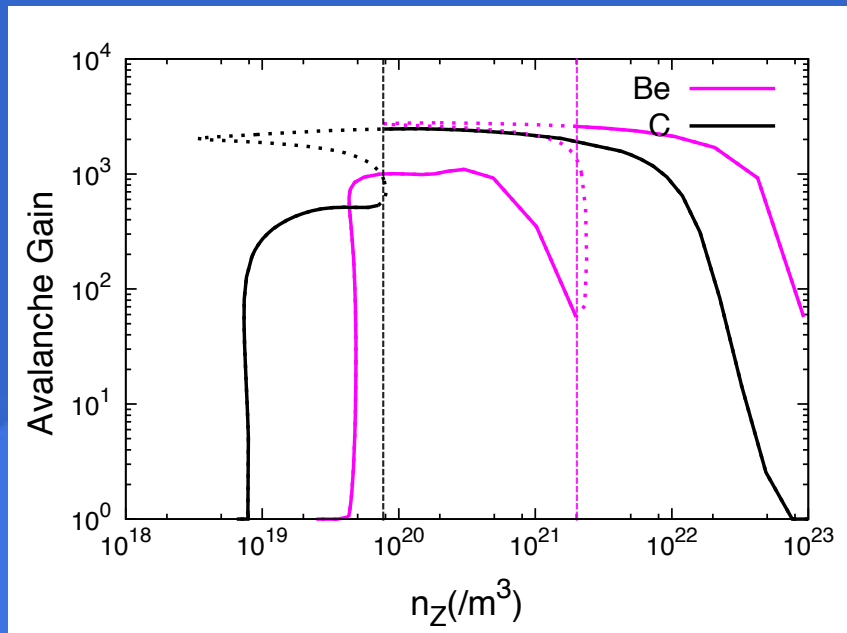


Dependence of the avalanche gain on impurity species - - low Z impurities (Be/C)

$$\text{Gain} = \frac{I_{\text{RE,max}}}{I_{\text{RE}}(t = 0)}$$

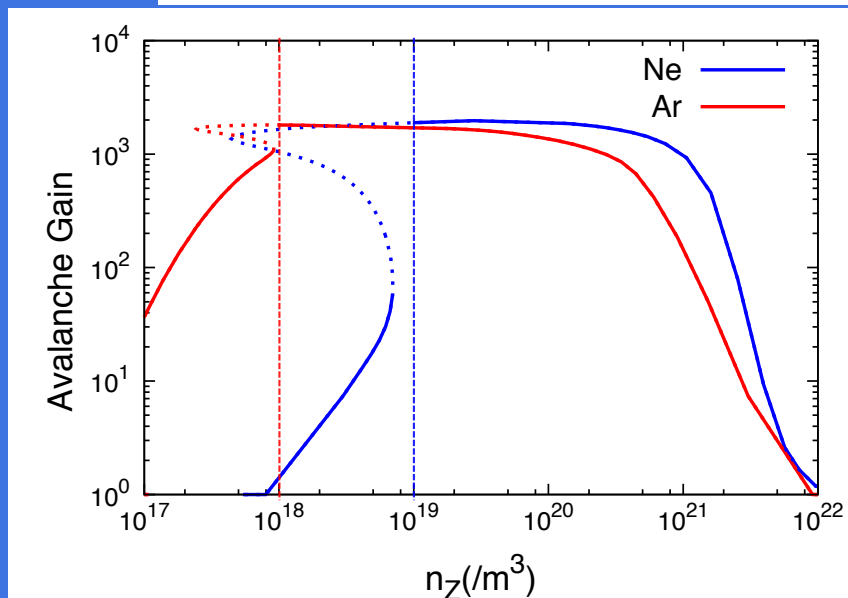


Impurity species characterize the parameter region where the avalanche generation becomes significant



✦ Threshold for strong avalanche with impurities

Species	threshold(/m ³)
Be	2x10 ²¹
C	1x10 ²⁰
Ne	1x10 ¹⁹
Ar	1x10 ¹⁸



✦ Threshold for decreasing avalanche gain

Species	threshold(/m ³)
Be	5x10 ²²
C	1x10 ²²
Ne	1x10 ²¹
Ar	5x10 ²⁰

Simulation of runaway beam current profile with MHD modes

Motivation: How MHD instability affects generation of runaway electrons?

- Runaway generation is affected by various processes of post-disruption plasmas in both direct and indirect ways:
 - ◆ MHD instability
 - ◆ impurity radiation
 - ◆ thermal & particle transport
 - ◆ control by external coils

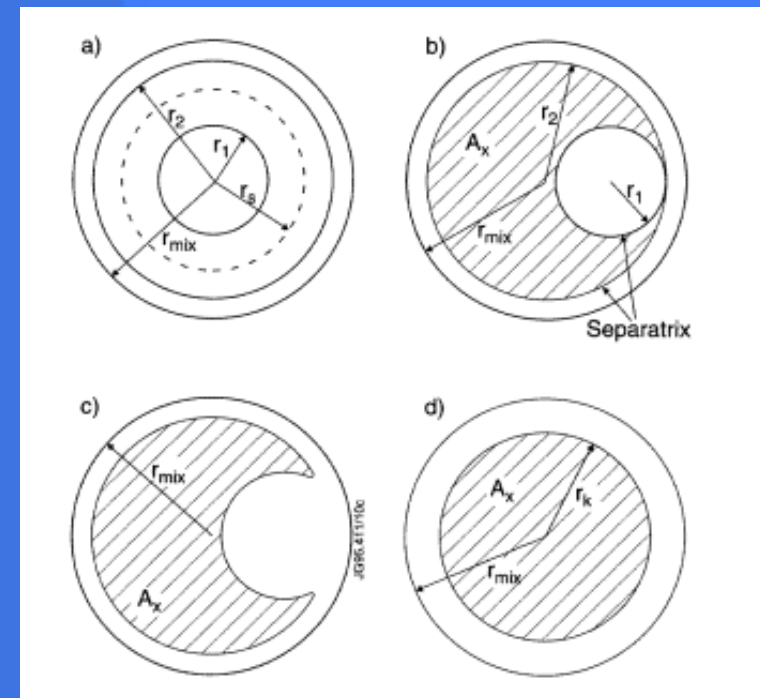
Motivation: How MHD instability affects generation of runaway electrons?

- Runaway generation is affected by various processes of post-disruption plasmas in both direct and indirect ways:
 - ◆ MHD instability
 - ◆ impurity radiation
 - ◆ thermal & particle transport
 - ◆ control by external coils

Motivation: How MHD instability affects generation of runaway electrons?

- Runaway generation is affected by various processes of post-disruption plasmas in both direct and indirect ways:
 - ◆ MHD instability
 - ◆ impurity radiation
 - ◆ thermal & particle transport
 - ◆ control by external coils
- Candidate mode: $m=1$ resistive kink

Cited from Porcelli 1996



complete reconnection due to $m = 1$ resistive kink (unstable when $q < 1$)

Motivation: How MHD instability affects generation of runaway electrons?

- Runaway generation is affected by various processes of post-disruption plasmas in both direct and indirect ways:

- ◆ MHD instability

- ◆ impurity radiation

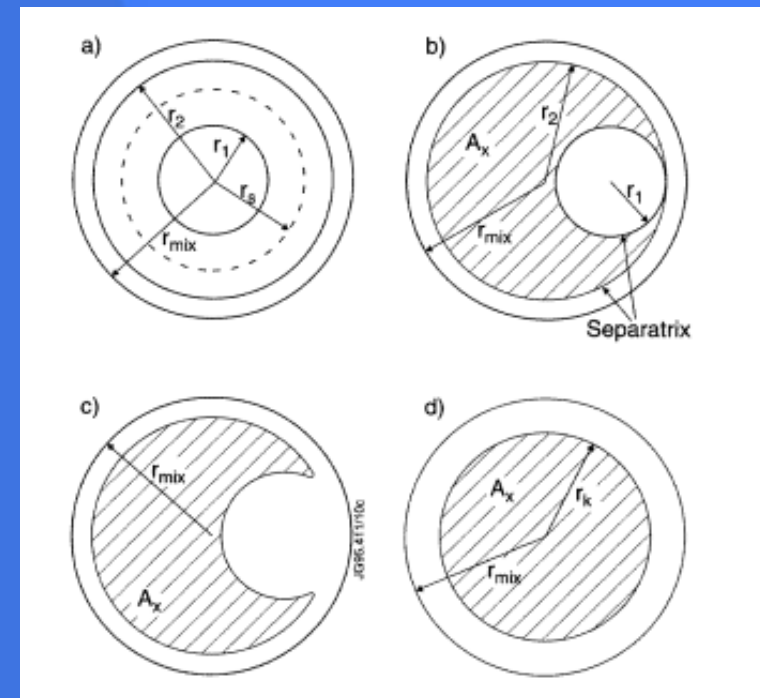
- ◆ thermal & particle transport

- ◆ control by external coils

- Candidate mode: $m=1$ resistive kink

- ◆ Runaway current profile tends to be more peaked than pre-disruption ohmic current profile.

Cited from Porcelli 1996

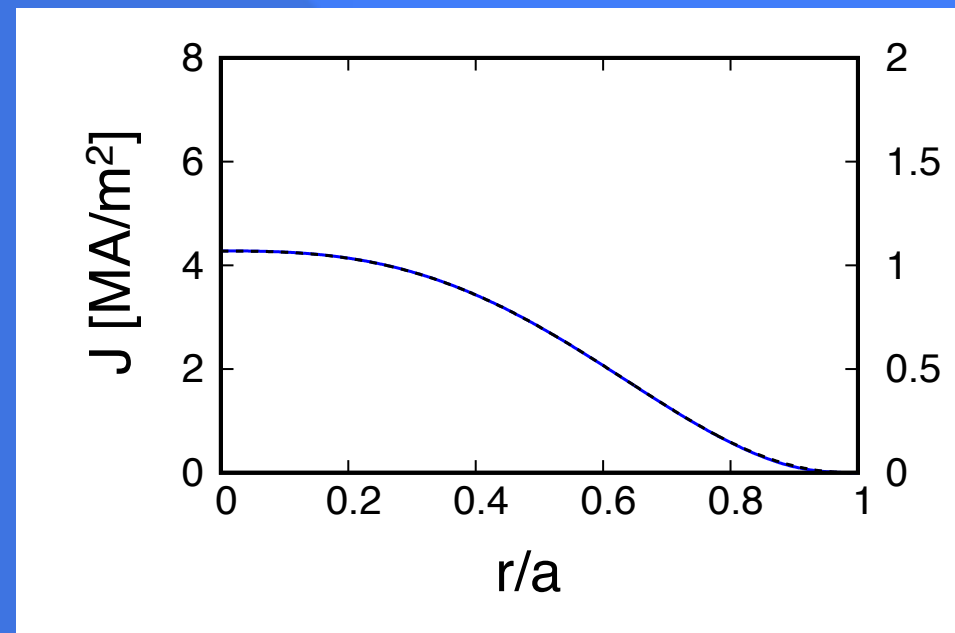


complete reconnection due to $m = 1$ resistive kink (unstable when $q < 1$)

Motivation: How MHD instability affects generation of runaway electrons?

- Runaway generation is affected by various processes of post-disruption plasmas in both direct and indirect ways:
 - ◆ MHD instability
 - ◆ impurity radiation
 - ◆ thermal & particle transport
 - ◆ control by external coils
- Candidate mode: $m=1$ resistive kink
 - ◆ Runaway current profile tends to be more peaked than pre-disruption ohmic current profile.

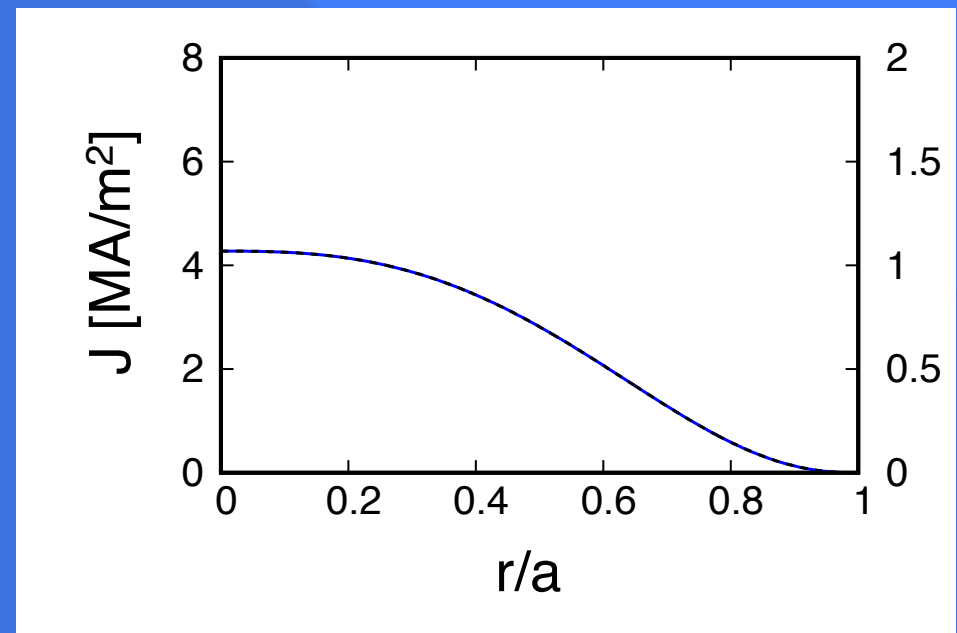
T=0.0 ms



Motivation: How MHD instability affects generation of runaway electrons?

- Runaway generation is affected by various processes of post-disruption plasmas in both direct and indirect ways:
 - ◆ MHD instability
 - ◆ impurity radiation
 - ◆ thermal & particle transport
 - ◆ control by external coils
- Candidate mode: $m=1$ resistive kink
 - ◆ Runaway current profile tends to be more peaked than pre-disruption ohmic current profile.

$T=1.32$ ms



Motivation: How MHD instability affects generation of runaway electrons?

- Runaway generation is affected by various processes of post-disruption plasmas in both direct and indirect ways:

- ◆ MHD instability

- ◆ impurity radiation

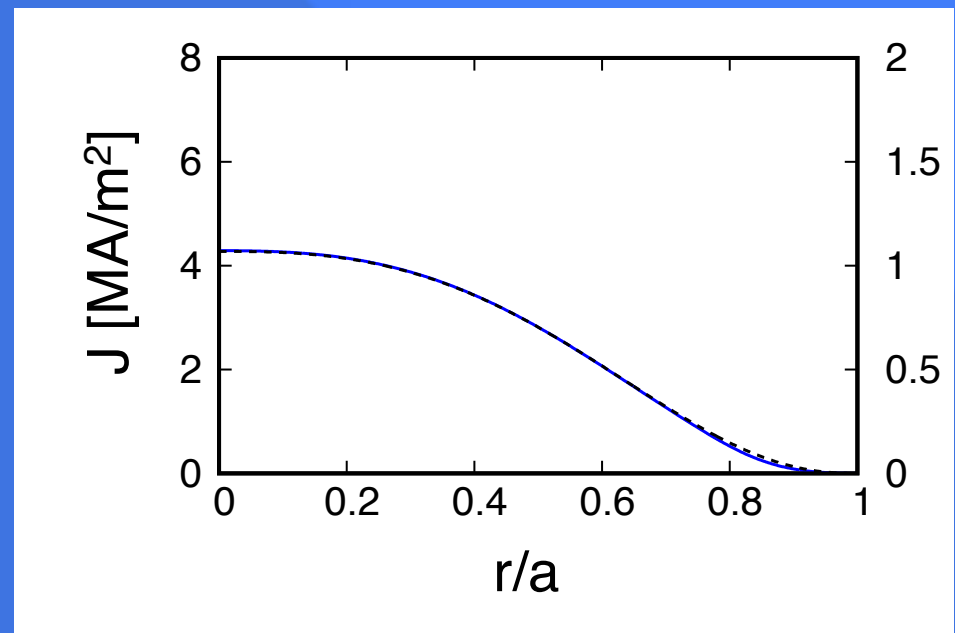
- ◆ thermal & particle transport

- ◆ control by external coils

- Candidate mode: $m=1$ resistive kink

- ◆ Runaway current profile tends to be more peaked than pre-disruption ohmic current profile.

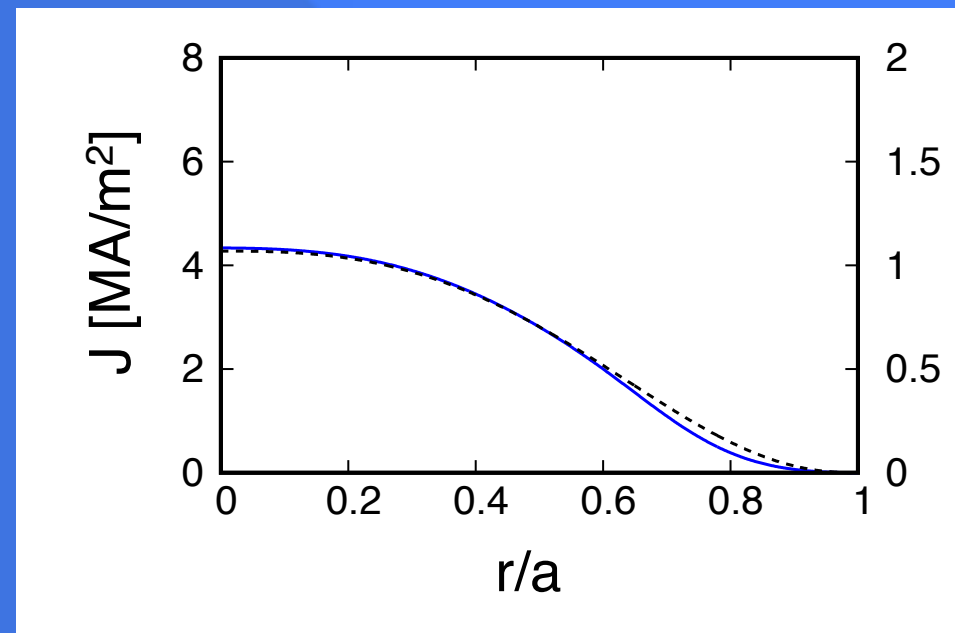
$T=2.64$ ms



Motivation: How MHD instability affects generation of runaway electrons?

- Runaway generation is affected by various processes of post-disruption plasmas in both direct and indirect ways:
 - ◆ MHD instability
 - ◆ impurity radiation
 - ◆ thermal & particle transport
 - ◆ control by external coils
- Candidate mode: $m=1$ resistive kink
 - ◆ Runaway current profile tends to be more peaked than pre-disruption ohmic current profile.

$T=3.97$ ms



Motivation: How MHD instability affects generation of runaway electrons?

- Runaway generation is affected by various processes of post-disruption plasmas in both direct and indirect ways:

- ◆ MHD instability

- ◆ impurity radiation

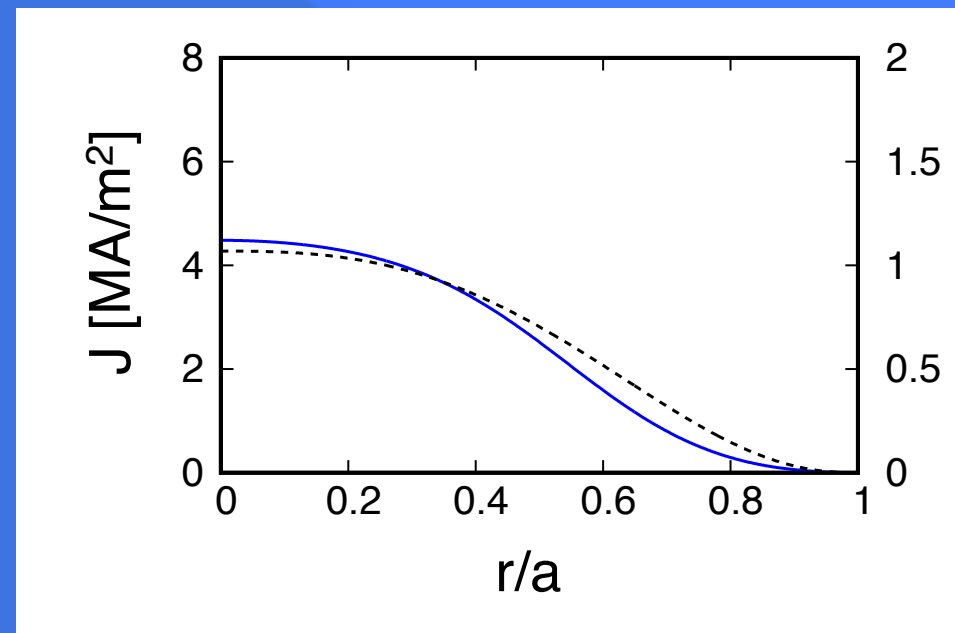
- ◆ thermal & particle transport

- ◆ control by external coils

- Candidate mode: $m=1$ resistive kink

- ◆ Runaway current profile tends to be more peaked than pre-disruption ohmic current profile.

$T=5.29$ ms



Motivation: How MHD instability affects generation of runaway electrons?

- Runaway generation is affected by various processes of post-disruption plasmas in both direct and indirect ways:

- ◆ MHD instability

- ◆ impurity radiation

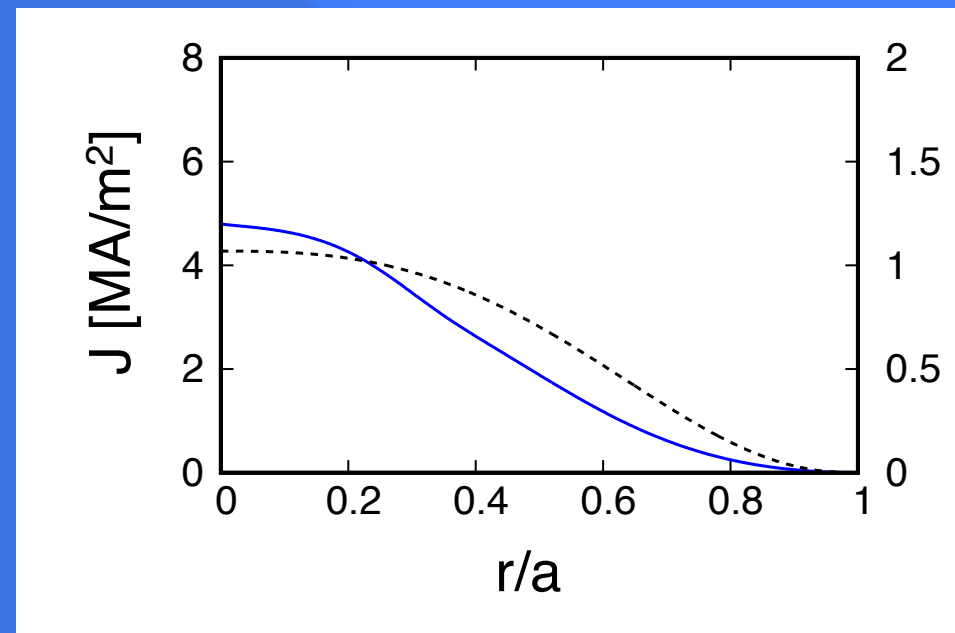
- ◆ thermal & particle transport

- ◆ control by external coils

- Candidate mode: $m=1$ resistive kink

- ◆ Runaway current profile tends to be more peaked than pre-disruption ohmic current profile.

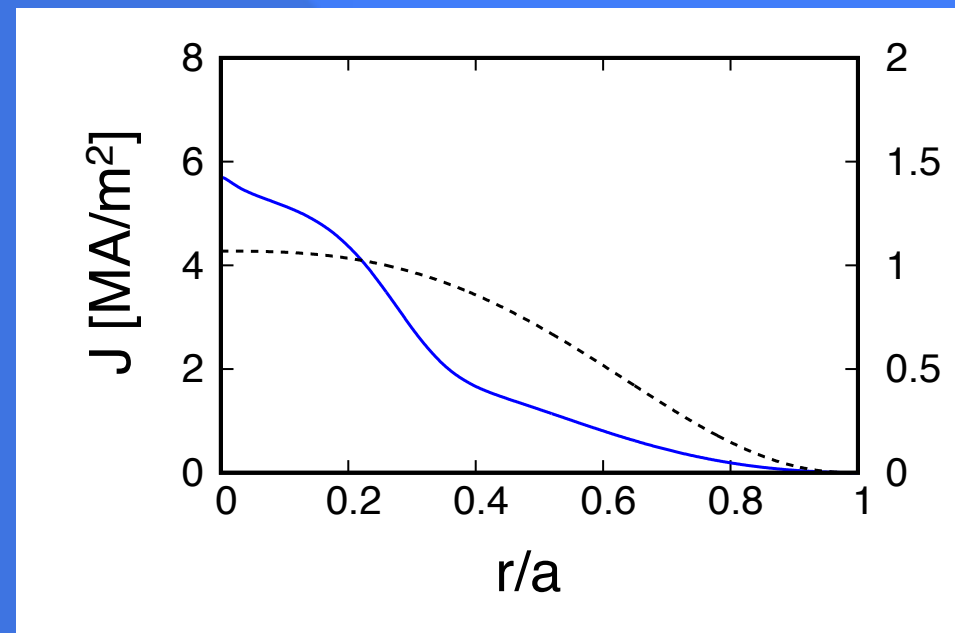
$T=6.61$ ms



Motivation: How MHD instability affects generation of runaway electrons?

- Runaway generation is affected by various processes of post-disruption plasmas in both direct and indirect ways:
 - ◆ MHD instability
 - ◆ impurity radiation
 - ◆ thermal & particle transport
 - ◆ control by external coils
- Candidate mode: $m=1$ resistive kink
 - ◆ Runaway current profile tends to be more peaked than pre-disruption ohmic current profile.

T=7.94 ms



Motivation: How MHD instability affects generation of runaway electrons?

- Runaway generation is affected by various processes of post-disruption plasmas in both direct and indirect ways:

- ◆ MHD instability

- ◆ impurity radiation

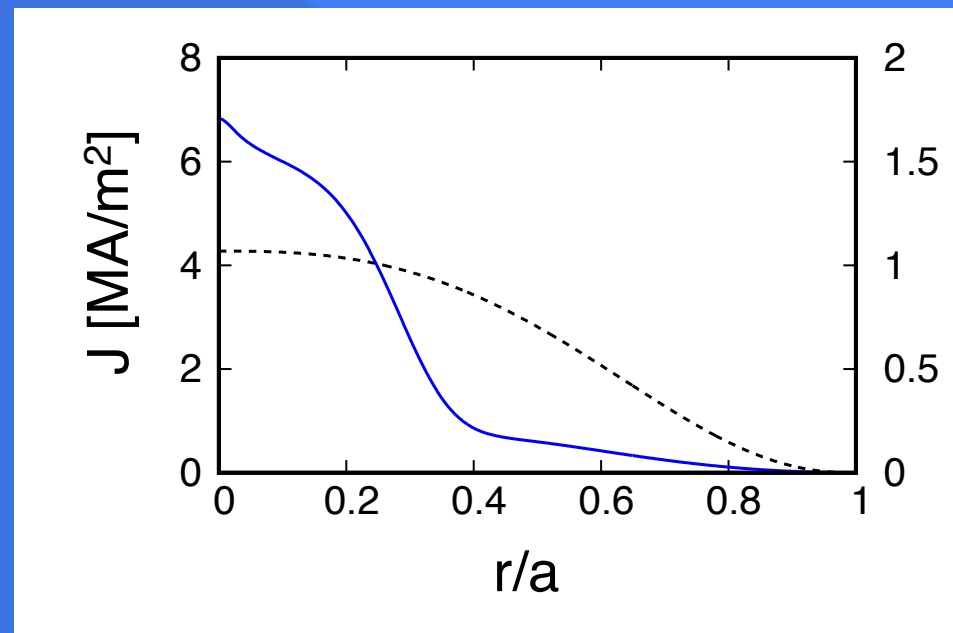
- ◆ thermal & particle transport

- ◆ control by external coils

- Candidate mode: $m=1$ resistive kink

- ◆ Runaway current profile tends to be more peaked than pre-disruption ohmic current profile.

T=9.26 ms



Motivation: How MHD instability affects generation of runaway electrons?

- Runaway generation is affected by various processes of post-disruption plasmas in both direct and indirect ways:

- ◆ MHD instability

- ◆ impurity radiation

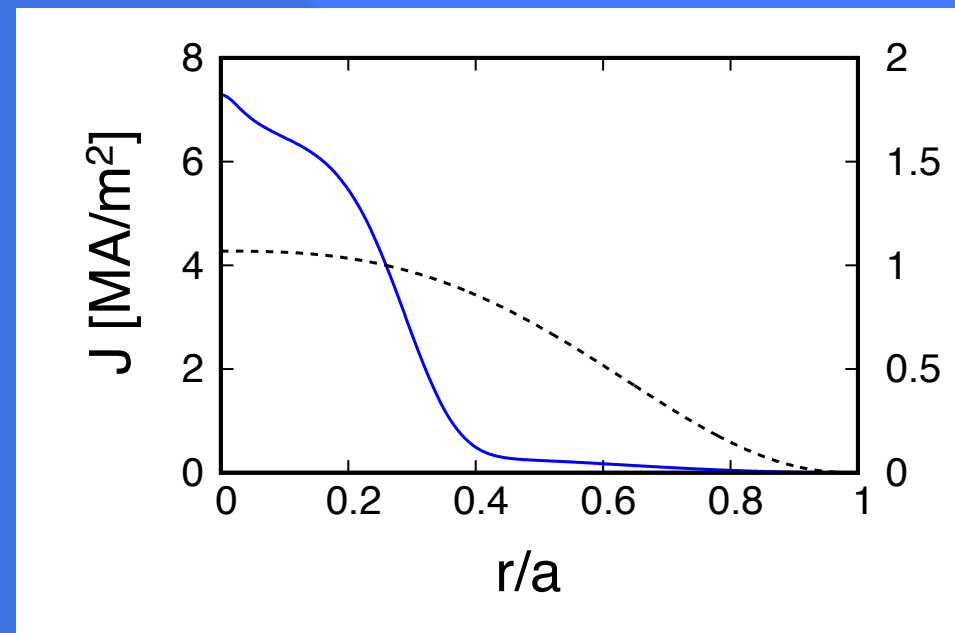
- ◆ thermal & particle transport

- ◆ control by external coils

- Candidate mode: $m=1$ resistive kink

- ◆ Runaway current profile tends to be more peaked than pre-disruption ohmic current profile.

$T=10.58$ ms



Motivation: How MHD instability affects generation of runaway electrons?

- Runaway generation is affected by various processes of post-disruption plasmas in both direct and indirect ways:

- ◆ MHD instability

- ◆ impurity radiation

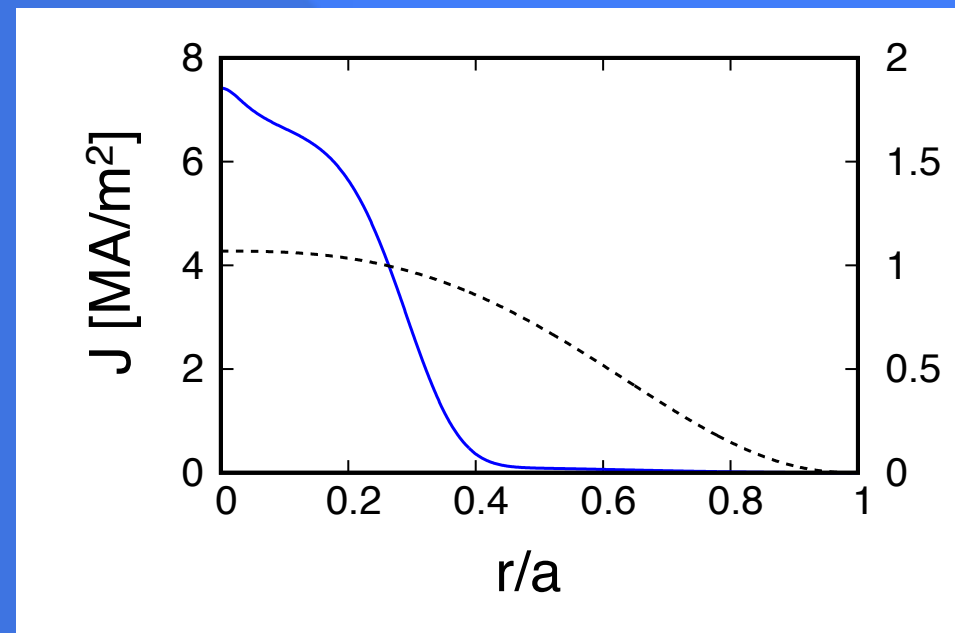
- ◆ thermal & particle transport

- ◆ control by external coils

- Candidate mode: $m=1$ resistive kink

- ◆ Runaway current profile tends to be more peaked than pre-disruption ohmic current profile.

$T=11.91$ ms



Motivation: How MHD instability affects generation of runaway electrons?

- Runaway generation is affected by various processes of post-disruption plasmas in both direct and indirect ways:

- ◆ MHD instability

- ◆ impurity radiation

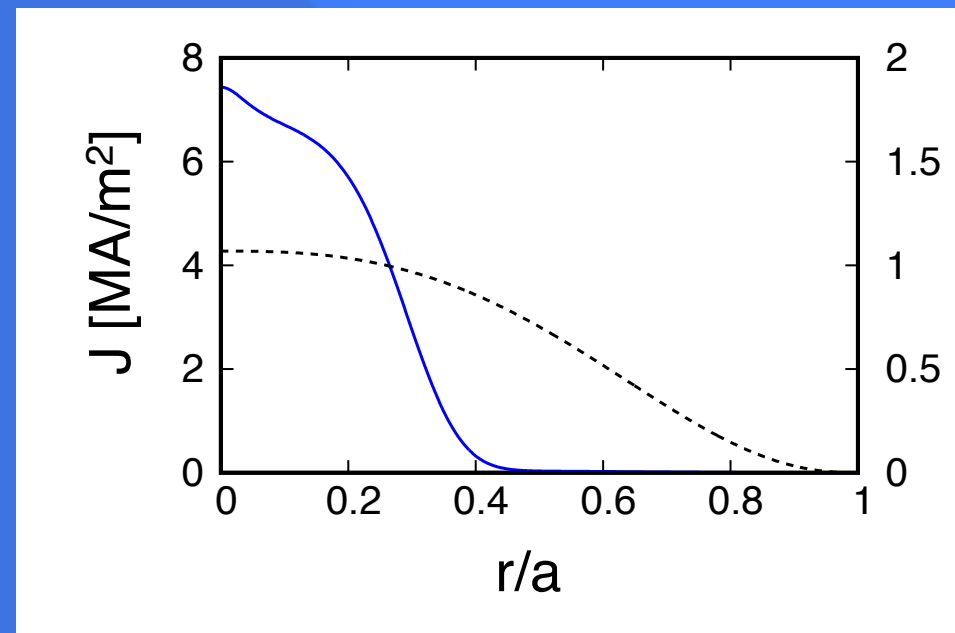
- ◆ thermal & particle transport

- ◆ control by external coils

- Candidate mode: $m=1$ resistive kink

- ◆ Runaway current profile tends to be more peaked than pre-disruption ohmic current profile.

$T=13.23$ ms



Simulation scheme for studying effects of MHD mode on the formation of runaway beam current profile

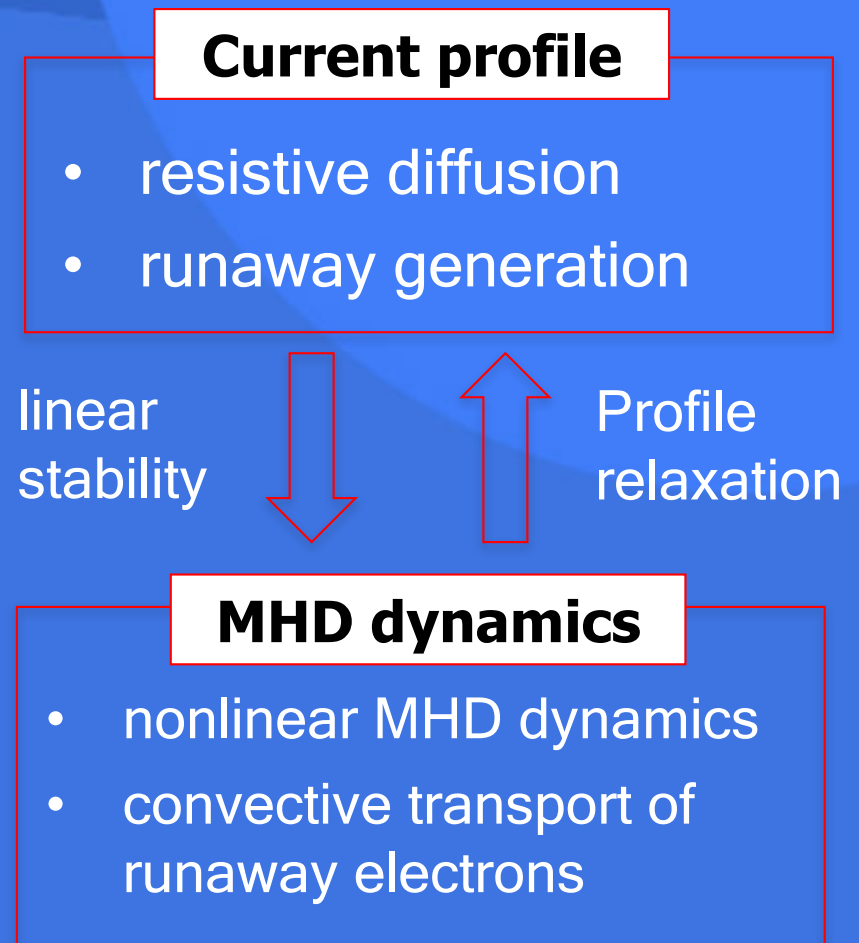
- **EXTREM code** (Matsuyama, et al., IAEA-FEC2016)

Previous work

- ◆ Analysis of runaway profile evolution with 1D current diffusion model [Eriksson, et al., PRL2004; Smith, et al., PoP2006]
- ◆ Analysis of linear/nonlinear stability of runaway plasma with given current profile [Helander, et al., PoP2007; Cai & Fu, NF2015; Aleynikova, et al., EPS2015]

Main feature of the EXTREM code

- ◆ By coupling RE generation mechanism with MHD codes, **EXTREM allows self-consistent description of current profile evolution and MHD instability.**



Method: Nonlinear resistive MHD model coupled to runaway electron generation

- EXTREM code (Matsuyama, et al., IAEA-FEC2016)

Bulk plasma

◆ reduced MHD in cylindrical tokamak

◆ $E \ll E_D = (n_e e^3 \ln \Lambda / 4 \pi \epsilon_0^2 T_e)$: thermal electrons do not runaway

$$U = \nabla_{\perp}^2 \phi$$

$$J = J_{\text{th}} + J_{\text{RE}} = \nabla_{\perp}^2 \psi$$

$$\mathbf{u} = \mathbf{e}_{\varphi} \times \nabla \phi$$

$$\mathbf{B} = B_0 \mathbf{e}_{\varphi} + \mathbf{e}_{\varphi} \times \nabla \psi$$

$$\frac{\partial U}{\partial t} = -\mathbf{u} \cdot \nabla U + \mathbf{B} \cdot \nabla J_{\text{th}}$$

$$\frac{\partial \psi}{\partial t} = \mathbf{B} \cdot \nabla \phi + \eta(T_e) J_{\text{th}}$$

Runaway electrons

◆ monoenergetic fluid

◆ convective runaway transport

◆ kinetic runaway generation mechanism is treated as density source

$$J_{\text{RE}} = \epsilon_a e c n_{\text{RE}} \quad \epsilon_a = \frac{J_{\text{RE}}}{e c n_{\text{RE}}} \simeq 1$$

$$\frac{\partial n_{\text{RE}}}{\partial t} + v_{\text{RE}}^{(\text{conv})} \mathbf{b} \cdot \nabla n_{\text{RE}} = S_{\text{Dreicer}} + S_{\text{Avalanche}}$$

$$S_{\text{Dreicer}} \simeq \frac{n_e}{\tau} \left(\frac{m_e c^2}{2T_e} \right)^{3/2} \left(\frac{E_D}{E} \right)^{3(1+Z_{\text{eff}}/16)} \times \exp \left(-\frac{E_D}{4E} - \sqrt{\frac{(1+Z_{\text{eff}})E_D}{E}} \right)$$

$$S_{\text{Avalanche}} \simeq n_{\text{RE}} \left(\frac{\pi}{2} \right)^{1/2} \frac{E/E_c - 1}{3\tau \ln \Lambda}$$

Method: Nonlinear resistive MHD model coupled to runaway electron generation

- EXTREM code (Matsuyama, et al., IAEA-FEC2016)

Bulk plasma

- reduced MHD in cylindrical tokamak
- $E \ll E_D = (n_e e^3 \ln \Lambda / 4\pi \epsilon_0^2 T_e)$: thermal electrons do not runaway

$$U = \nabla_{\perp}^2 \phi$$

$$J = J_{th} + J_{RE} = \nabla_{\perp}^2 \psi$$

$$\mathbf{u} = \mathbf{e}_{\varphi} \times \nabla \phi$$

Ampere's law

$$\mathbf{B} = B_0 \mathbf{e}_{\varphi} + \mathbf{e}_{\varphi} \times \nabla \psi$$

$$\frac{\partial U}{\partial t} = -\mathbf{u} \cdot \nabla U + \mathbf{B} \cdot \nabla J_{th}$$

$$\frac{\partial \psi}{\partial t} = \mathbf{B} \cdot \nabla \phi + \eta(T_e) J_{th}$$

Runaway electrons

- monoenergetic fluid
- convective runaway transport
- kinetic runaway generation mechanism is treated as density source

$$J_{RE} = \epsilon_a e c n_{RE} \quad \epsilon_a = \frac{J_{RE}}{e c n_{RE}} \simeq 1$$

$$\frac{\partial n_{RE}}{\partial t} + v_{RE}^{(conv)} \mathbf{b} \cdot \nabla n_{RE} = S_{Dreicer} + S_{Avalanche}$$

$$S_{Dreicer} \simeq \frac{n_e}{\tau} \left(\frac{m_e c^2}{2T_e} \right)^{3/2} \left(\frac{E_D}{E} \right)^{3(1+Z_{eff}/16)} \times \exp \left(-\frac{E_D}{4E} - \sqrt{\frac{(1+Z_{eff})E_D}{E}} \right)$$

$$S_{Avalanche} \simeq n_{RE} \left(\frac{\pi}{2} \right)^{1/2} \frac{E/E_c - 1}{3\tau \ln \Lambda}$$

Method: Nonlinear resistive MHD model coupled to runaway electron generation

- EXTREM code (Matsuyama, et al., IAEA-FEC2016)

Bulk plasma

- reduced MHD in cylindrical tokamak
- $E \ll E_D = (n_e e^3 \ln \Lambda / 4\pi \epsilon_0^2 T_e)$: thermal electrons do not runaway

$$U = \nabla_{\perp}^2 \phi$$

$$J = J_{th} + J_{RE} = \nabla_{\perp}^2 \psi$$

$$\mathbf{u} = \mathbf{e}_{\varphi} \times \nabla \phi$$

$$\mathbf{B} = B_0 \mathbf{e}_{\varphi} + \mathbf{e}_{\varphi} \times \nabla \psi$$

$$\frac{\partial U}{\partial t} = -\mathbf{u} \cdot \nabla U + \mathbf{B} \cdot \nabla J_{th}$$

$$\frac{\partial \psi}{\partial t} = \mathbf{B} \cdot \nabla \phi + \eta(T_e) J_{th}$$

Ampere's law

Electric field

Runaway electrons

- monoenergetic fluid
- convective runaway transport
- kinetic runaway generation mechanism is treated as density source

$$J_{RE} = \epsilon_a e c n_{RE} \quad \epsilon_a = \frac{J_{RE}}{e c n_{RE}} \simeq 1$$

$$\frac{\partial n_{RE}}{\partial t} + v_{RE}^{(conv)} \mathbf{b} \cdot \nabla n_{RE}$$

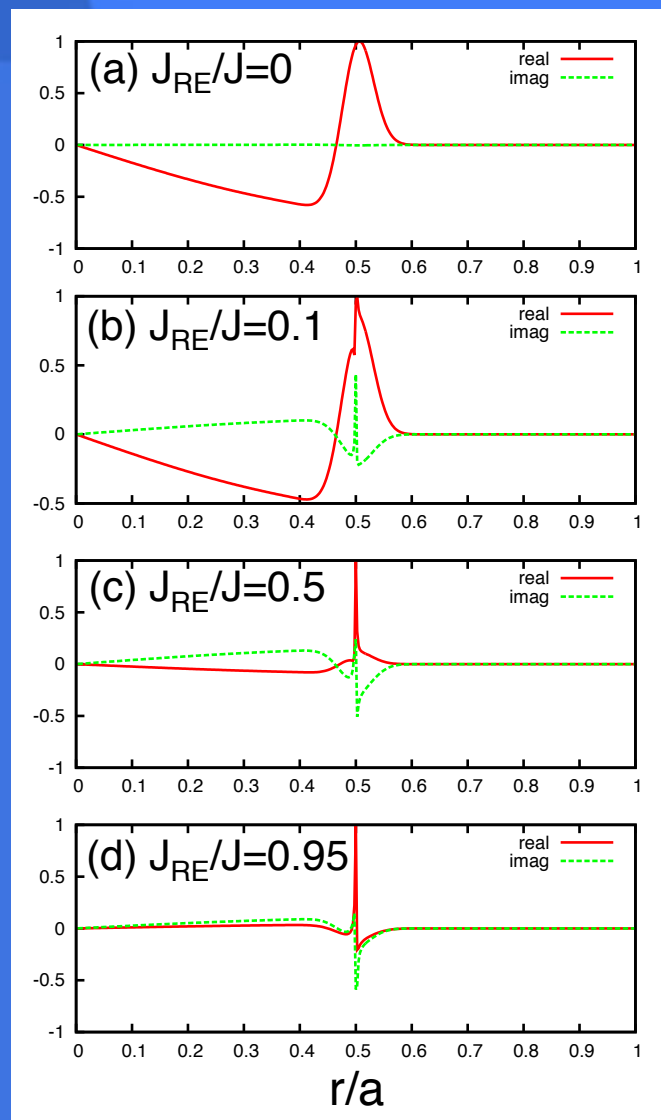
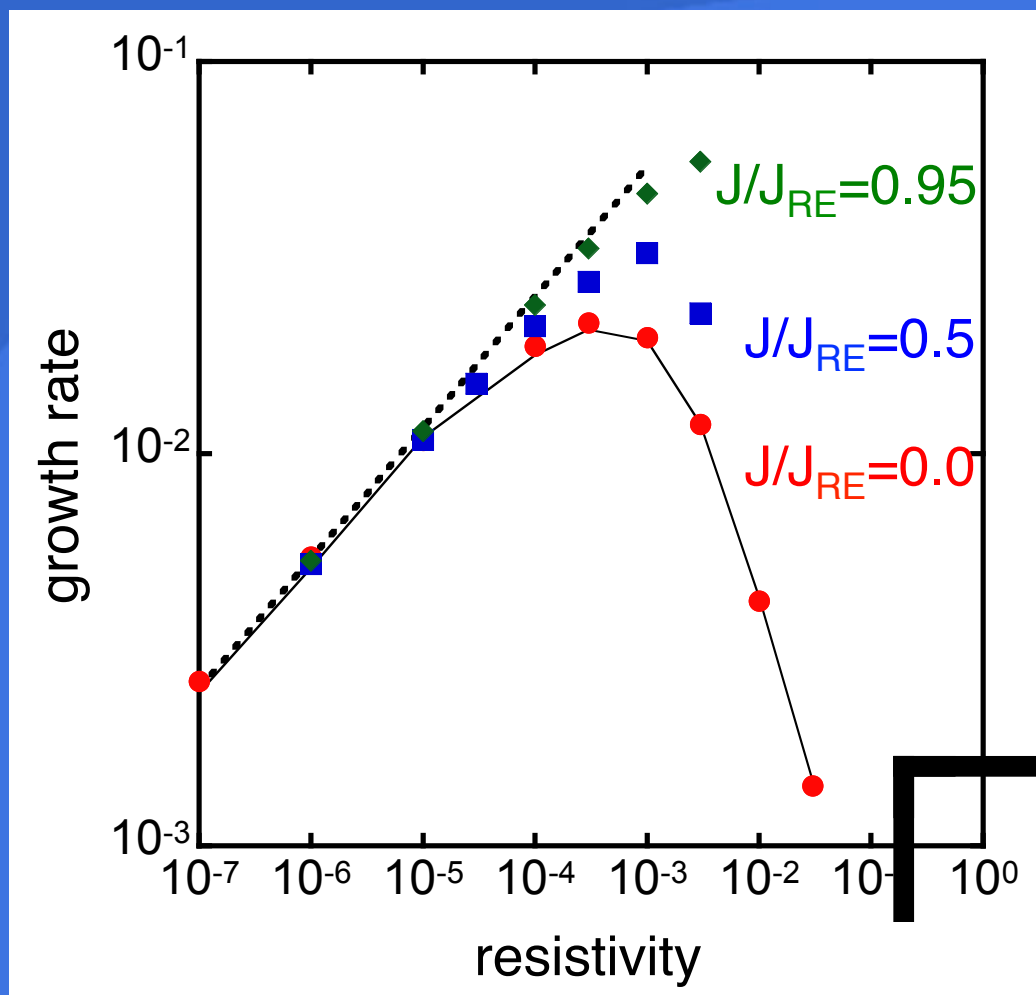
$$\Rightarrow S_{Dreicer} + S_{Avalanche}$$

$$S_{Dreicer} \simeq \frac{n_e}{\tau} \left(\frac{m_e c^2}{2T_e} \right)^{3/2} \left(\frac{E_D}{E} \right)^{3(1+Z_{eff}/16)} \times \exp \left(-\frac{E_D}{4E} - \sqrt{\frac{(1+Z_{eff})E_D}{E}} \right)$$

$$S_{Avalanche} \simeq n_{RE} \left(\frac{\pi}{2} \right)^{1/2} \frac{E/E_c - 1}{3\tau \ln \Lambda}$$

Linear growth rate of resistive kink mode including runaway electrons

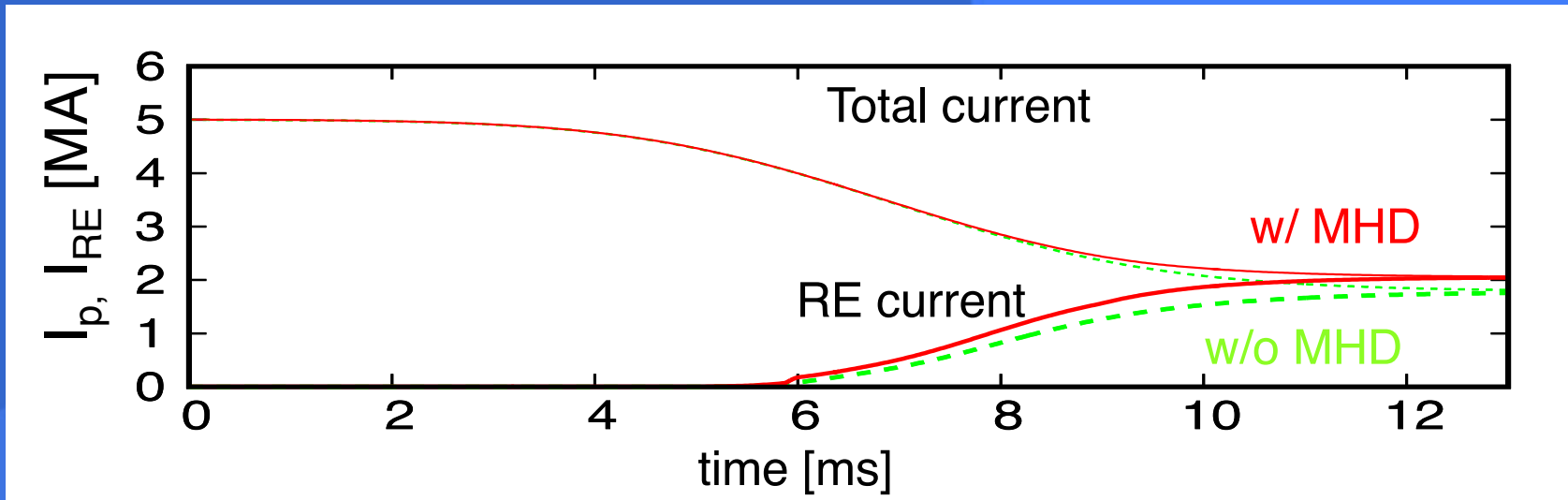
- Runaway-driven resistive MHD mode (Helander, et al., PoP2007; Cai & Fu, NF2015)



Simulation results

$I_p = 5\text{MA}$, $R=3\text{m}$, $a = 1\text{m}$, $T_e(0) = 3.1\text{ keV}$ to 10 eV , $n_e=1.2 \times 10^{20}/\text{m}^3$, $Z_{\text{eff}}=3$, $t_{\text{TQ}}=1\text{ ms}$

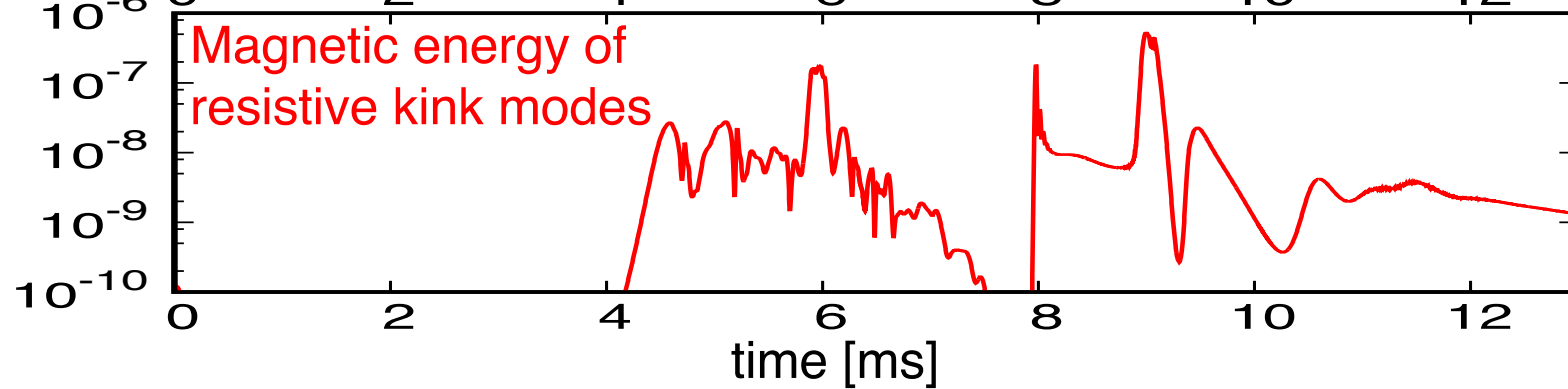
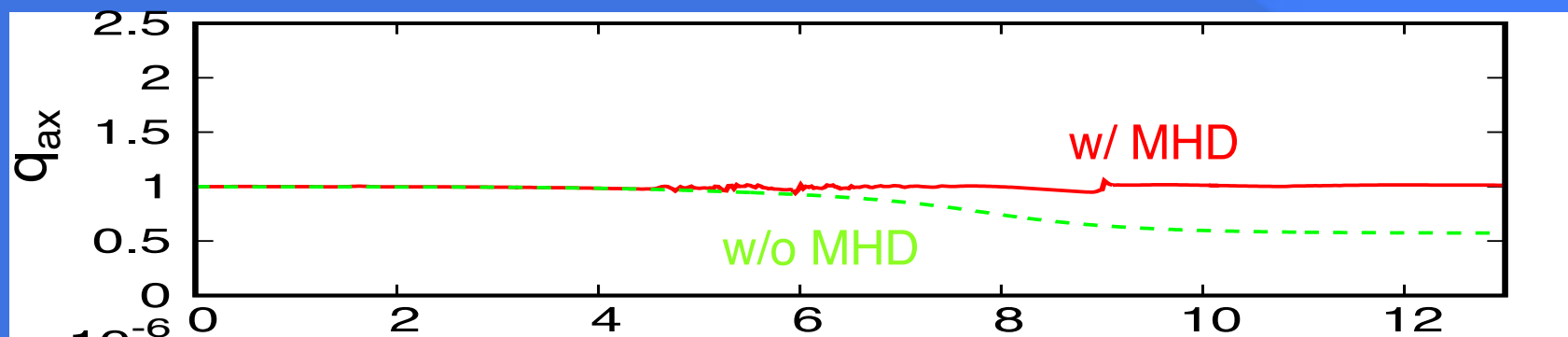
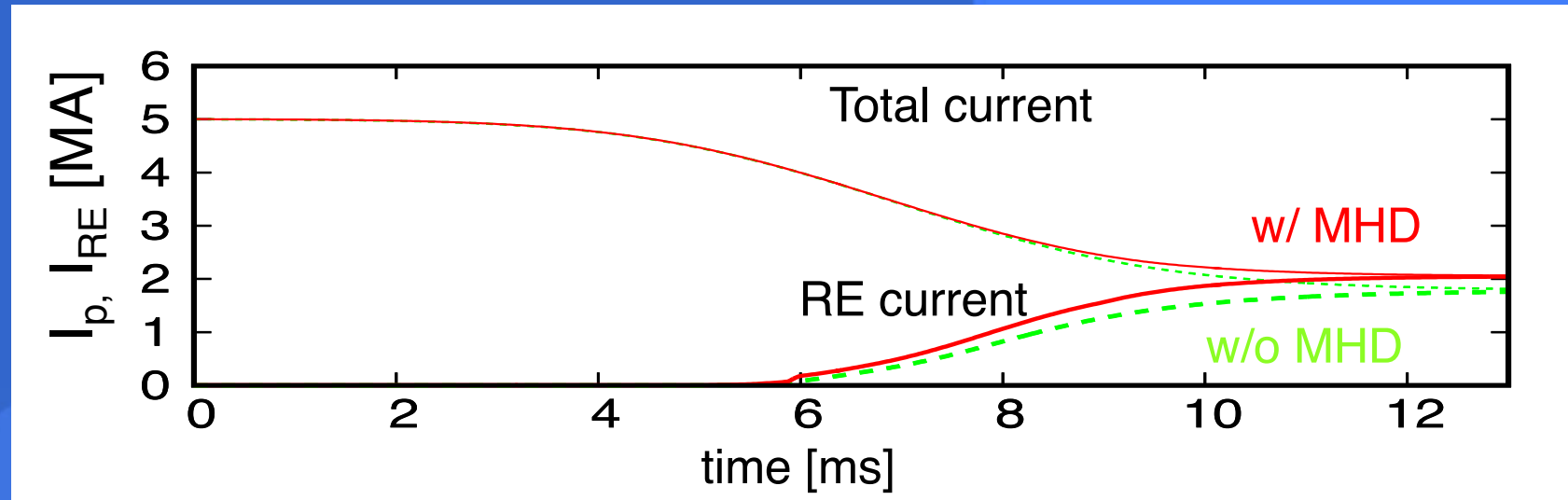
[*] B_t is adjusted for q_a to be 3.



Simulation results

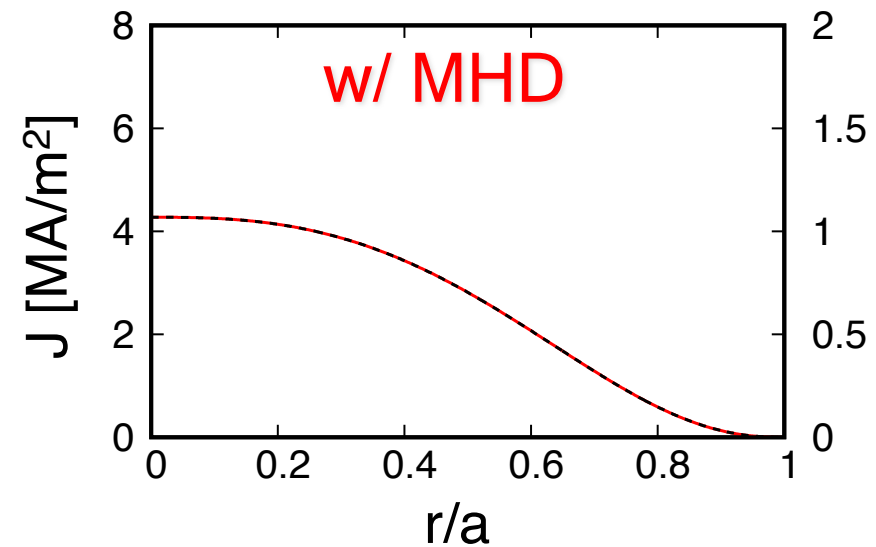
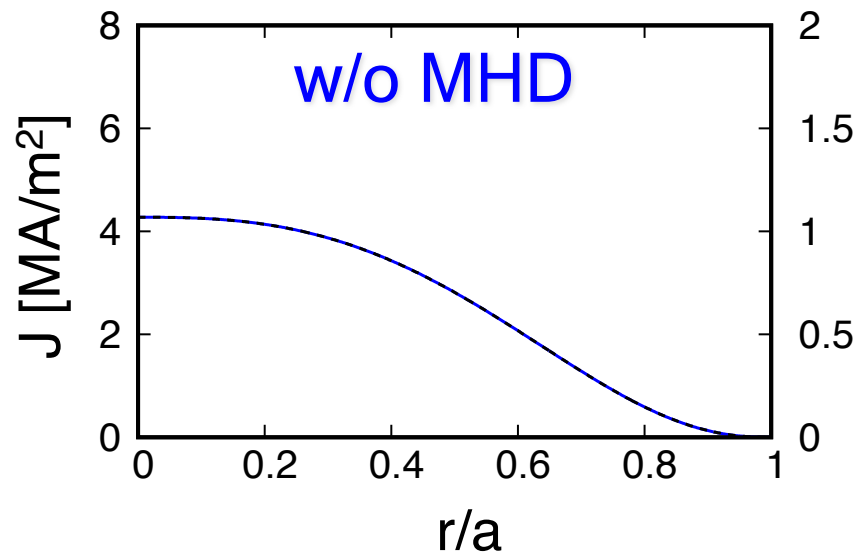
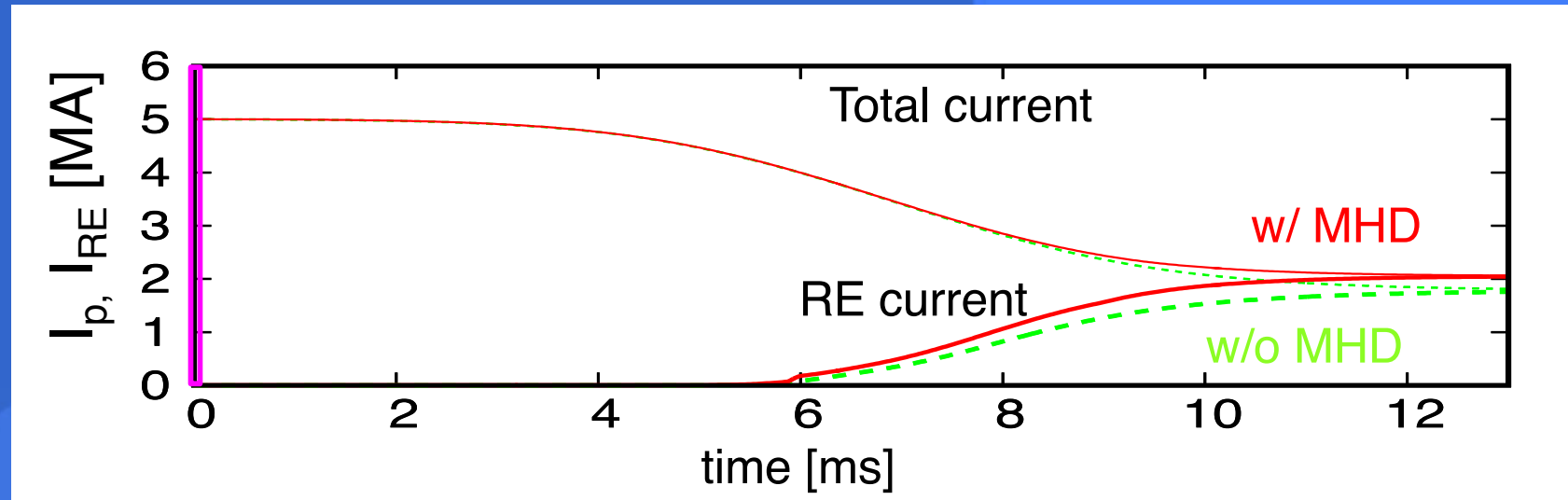
$I_p = 5\text{MA}$, $R=3\text{m}$, $a = 1\text{m}$, $T_e(0) = 3.1\text{ keV}$ to 10 eV , $n_e=1.2 \times 10^{20}/\text{m}^3$, $Z_{\text{eff}}=3$, $t_{\text{TQ}}=1\text{ ms}$

[*] B_t is adjusted for q_a to be 3.



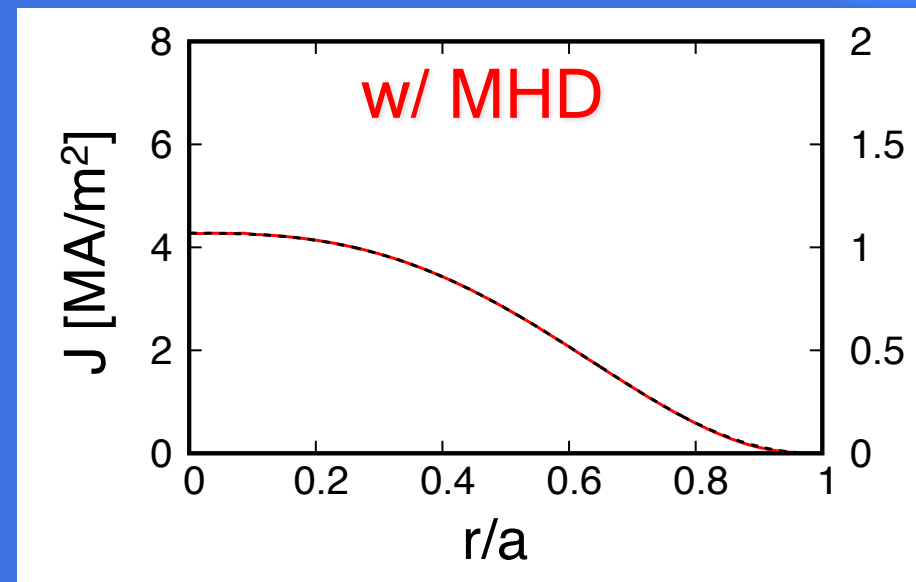
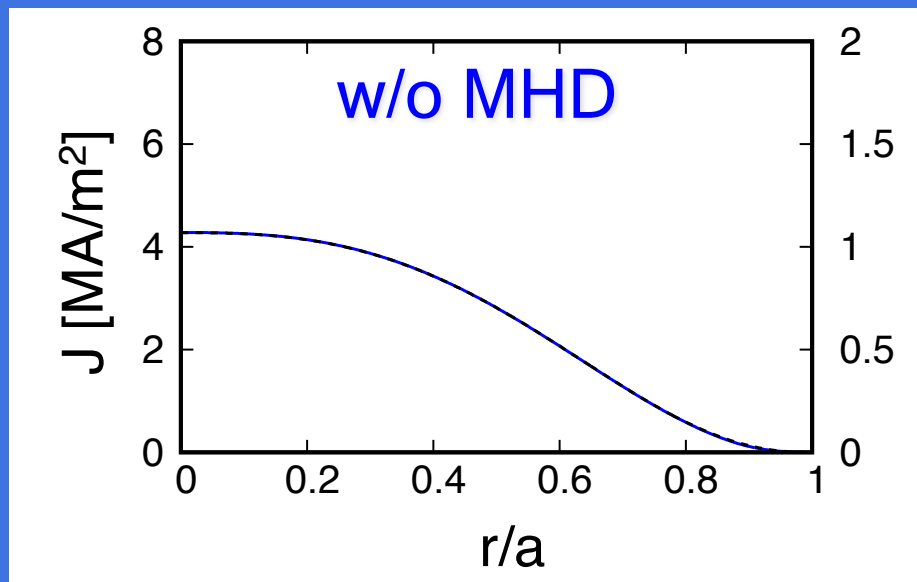
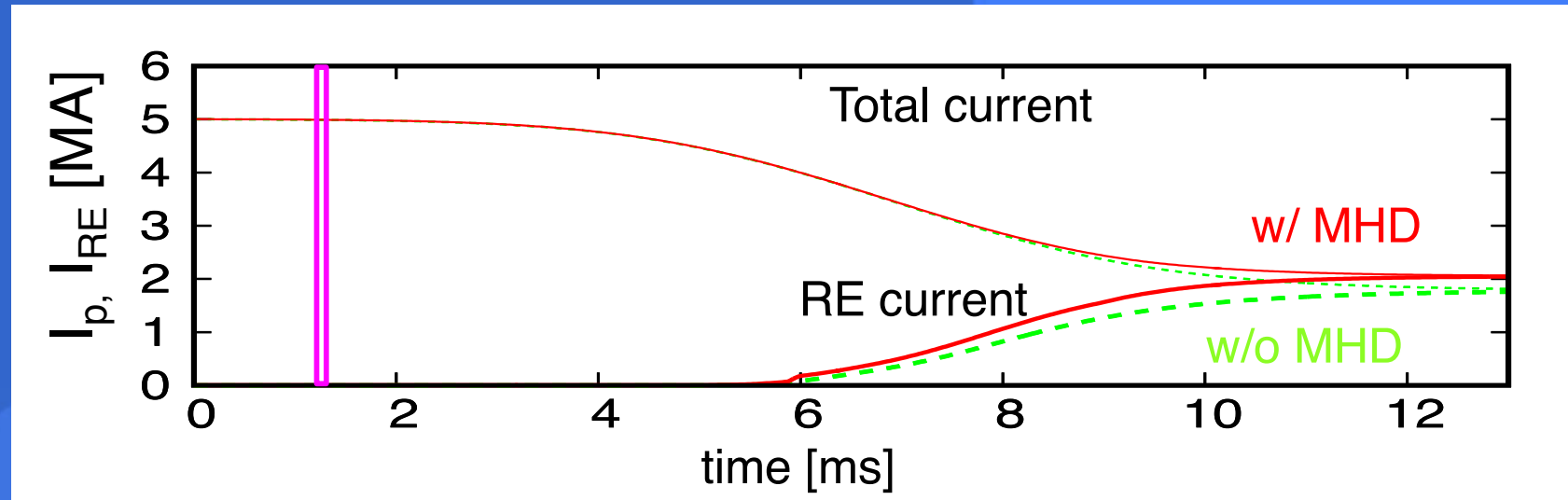
Simulation results

$I_p = 5\text{MA}$, $R=3\text{m}$, $a = 1\text{m}$, $T_e(0) = 3.1\text{ keV}$ to 10 eV , $n_e=1.2 \times 10^{20}/\text{m}^3$, $Z_{\text{eff}}=3$, $t_{\text{TQ}}=1\text{ ms}$
[*] B_t is adjusted for q_a to be 3.



Simulation results

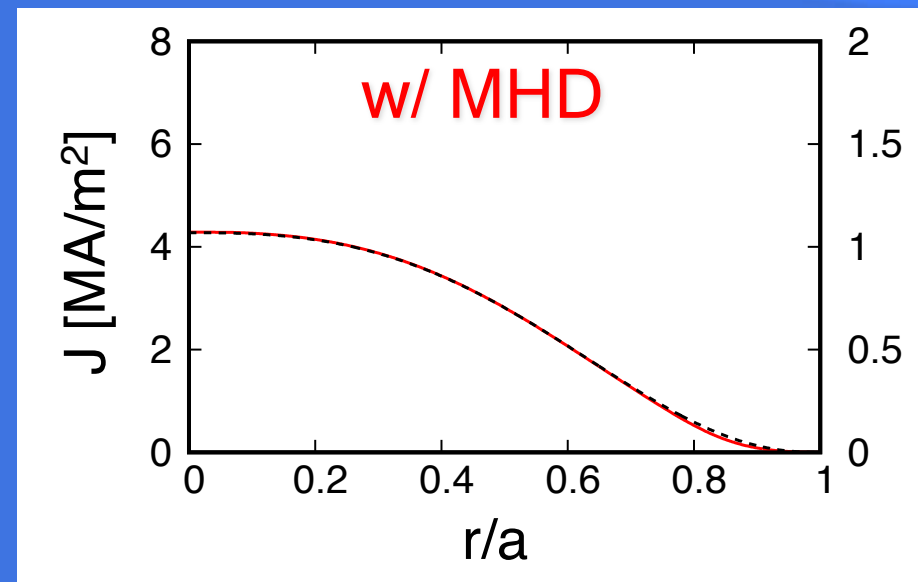
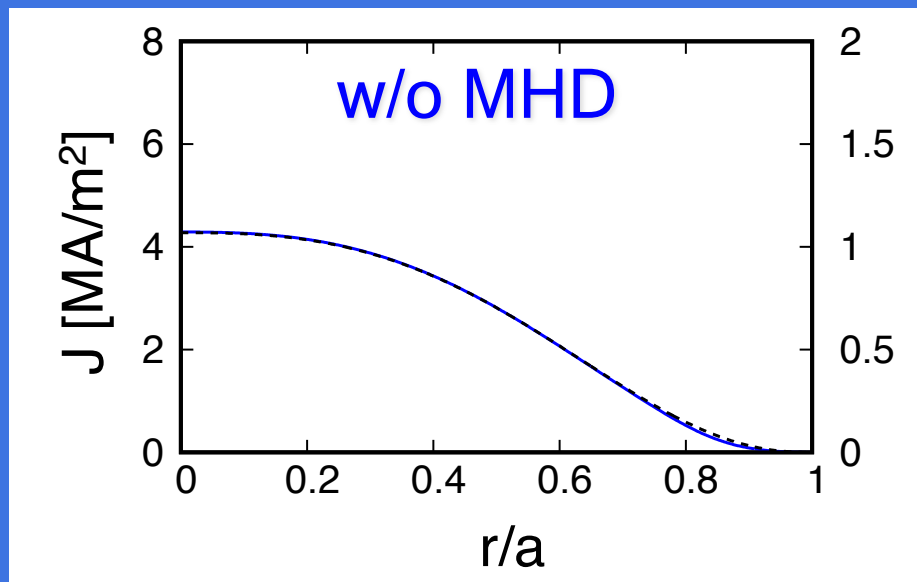
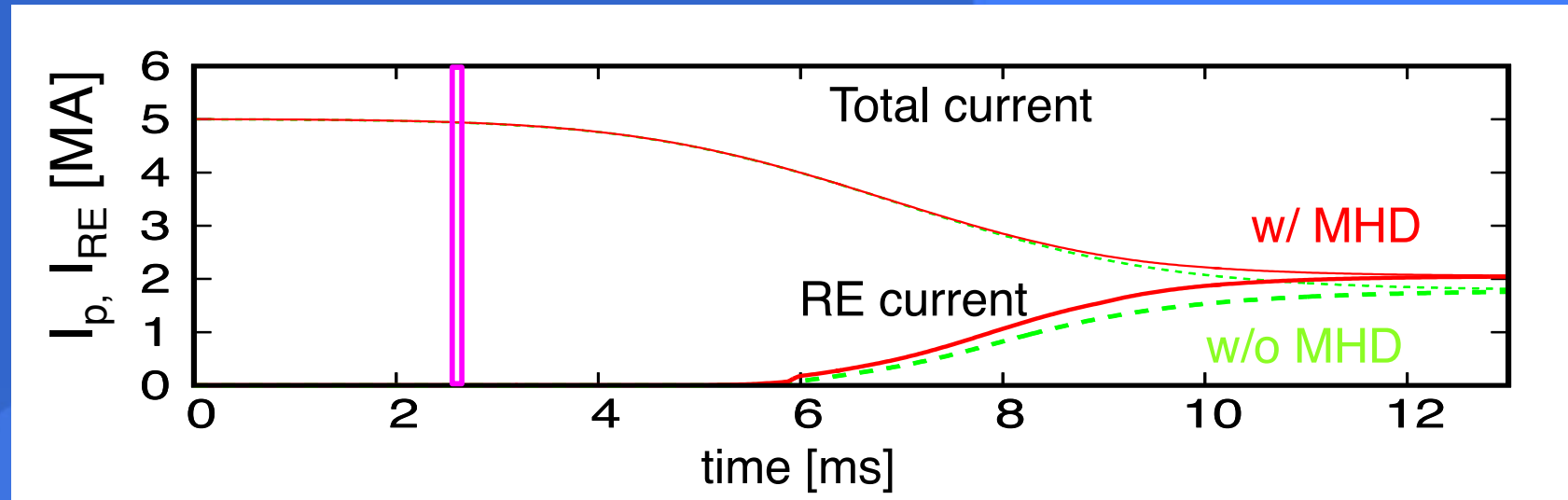
$I_p = 5\text{MA}$, $R=3\text{m}$, $a = 1\text{m}$, $T_e(0) = 3.1\text{ keV}$ to 10 eV , $n_e=1.2 \times 10^{20}/\text{m}^3$, $Z_{\text{eff}}=3$, $t_{\text{TQ}}=1\text{ ms}$
[*] B_t is adjusted for q_a to be 3.



Simulation results

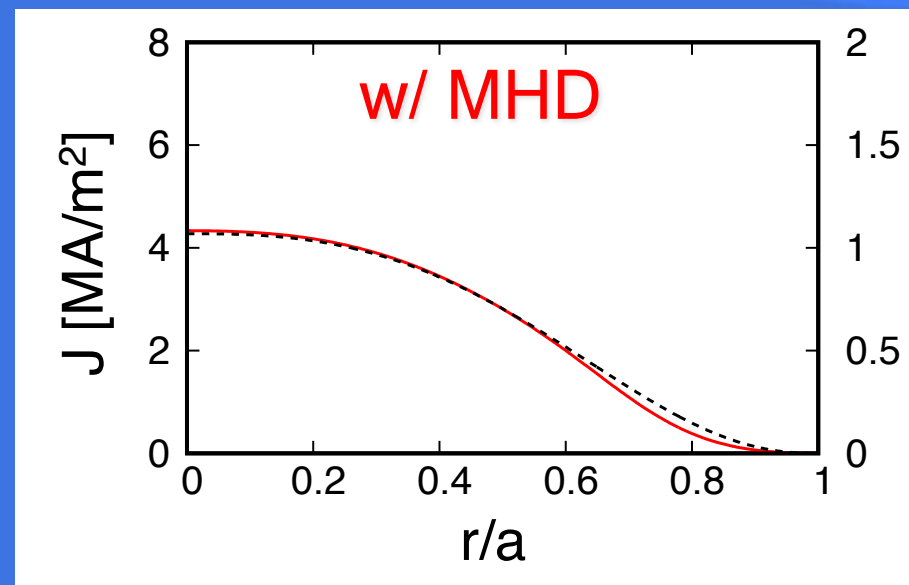
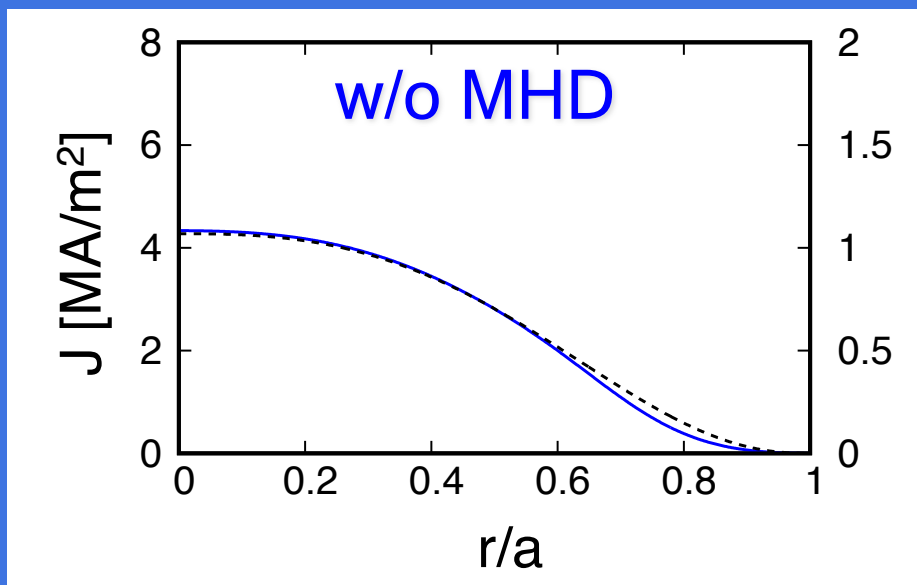
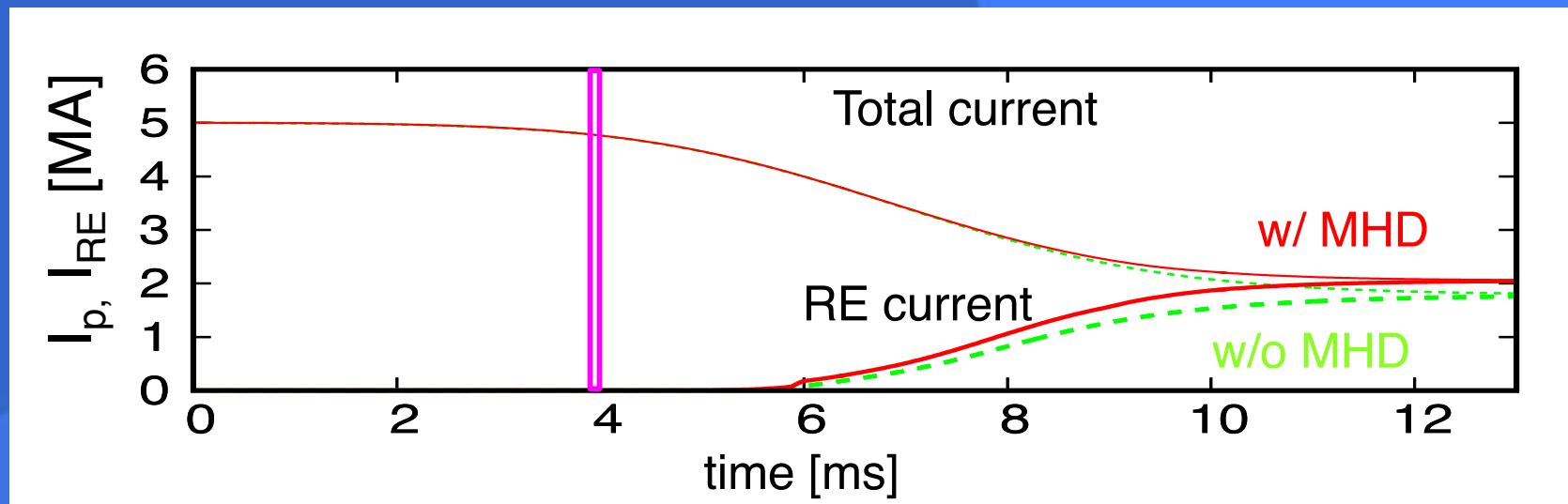
$I_p = 5\text{MA}$, $R=3\text{m}$, $a = 1\text{m}$, $T_e(0) = 3.1\text{ keV}$ to 10 eV , $n_e=1.2 \times 10^{20}/\text{m}^3$, $Z_{\text{eff}}=3$, $t_{\text{TQ}}=1\text{ ms}$

[*] B_t is adjusted for q_a to be 3.



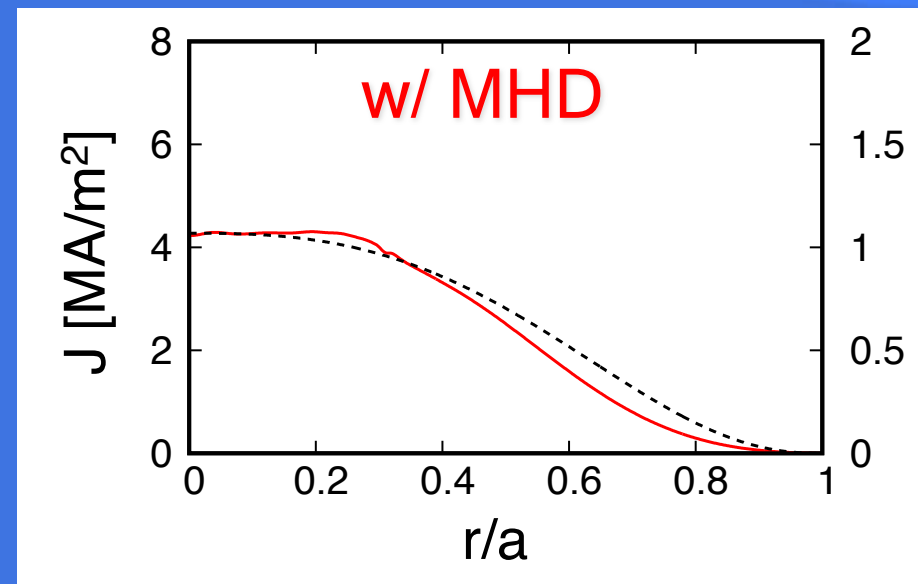
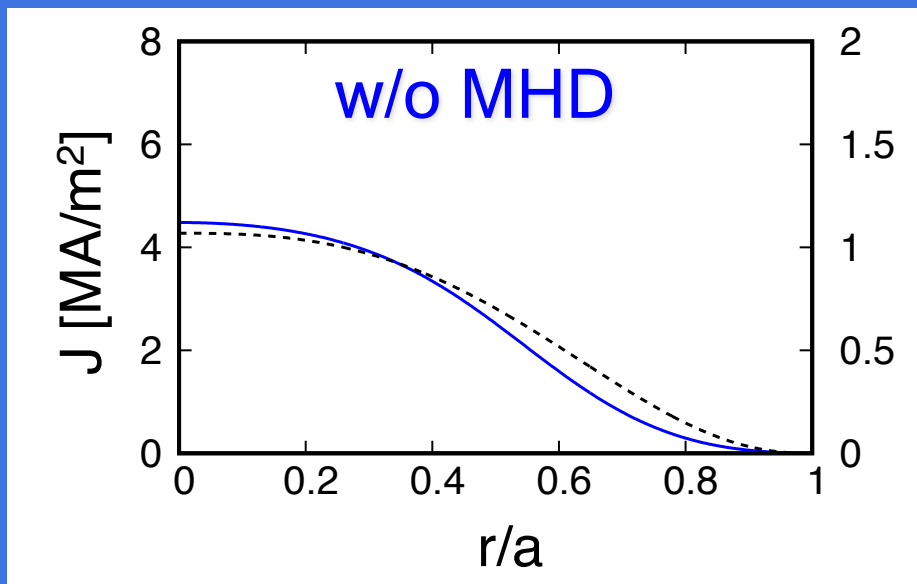
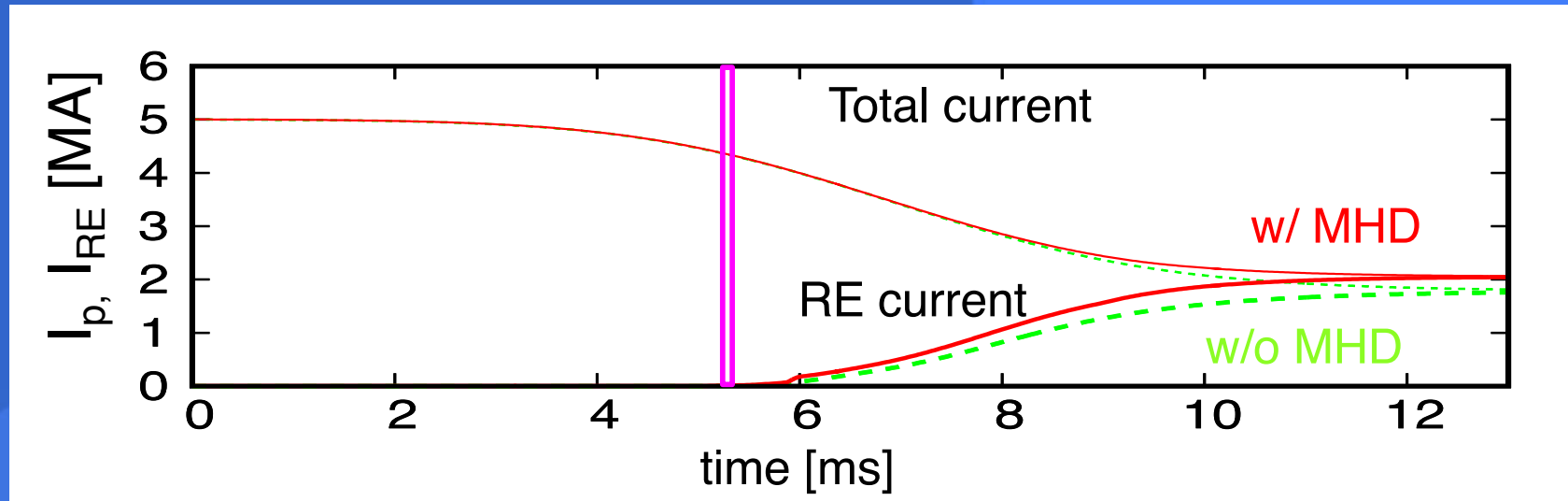
Simulation results

$I_p = 5\text{MA}$, $R=3\text{m}$, $a = 1\text{m}$, $T_e(0) = 3.1\text{ keV}$ to 10 eV , $n_e=1.2 \times 10^{20}/\text{m}^3$, $Z_{\text{eff}}=3$, $t_{\text{TQ}}=1\text{ ms}$
[*] B_t is adjusted for q_a to be 3.



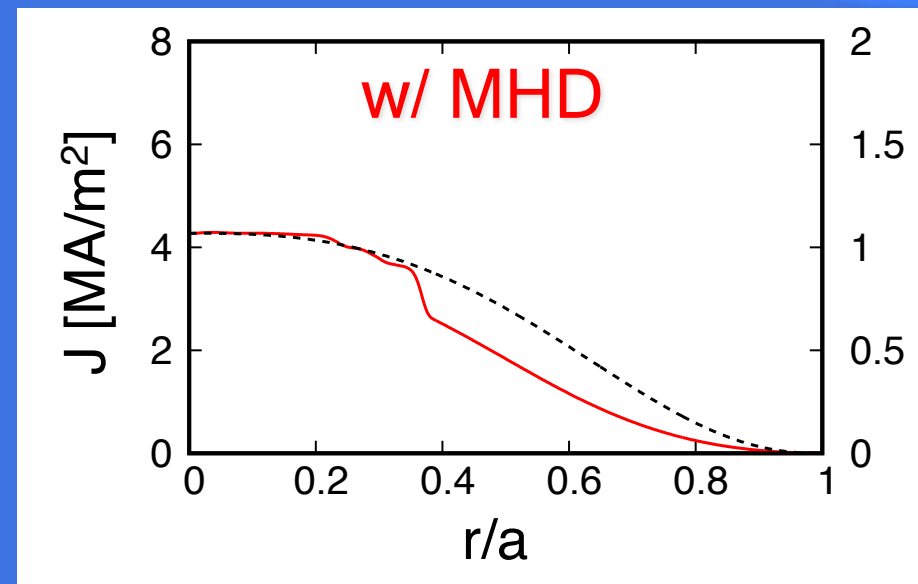
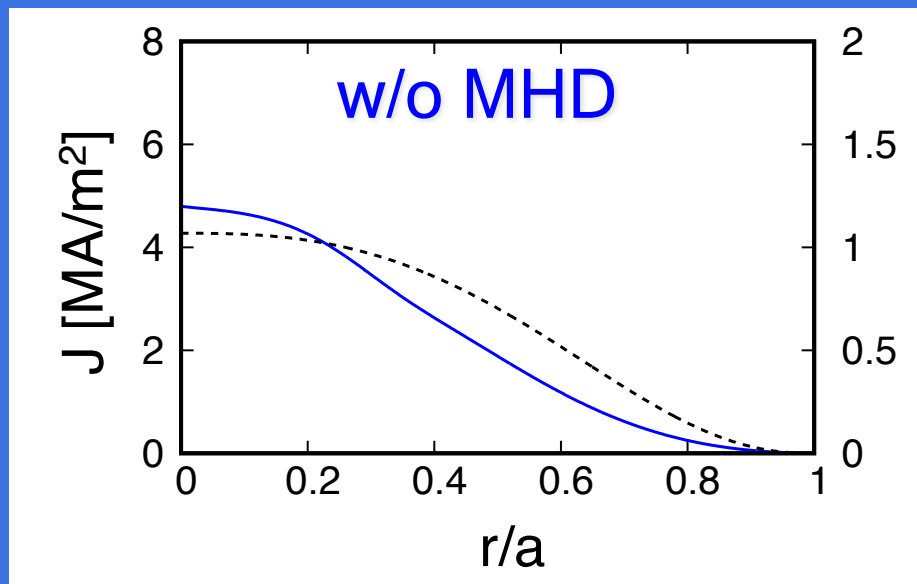
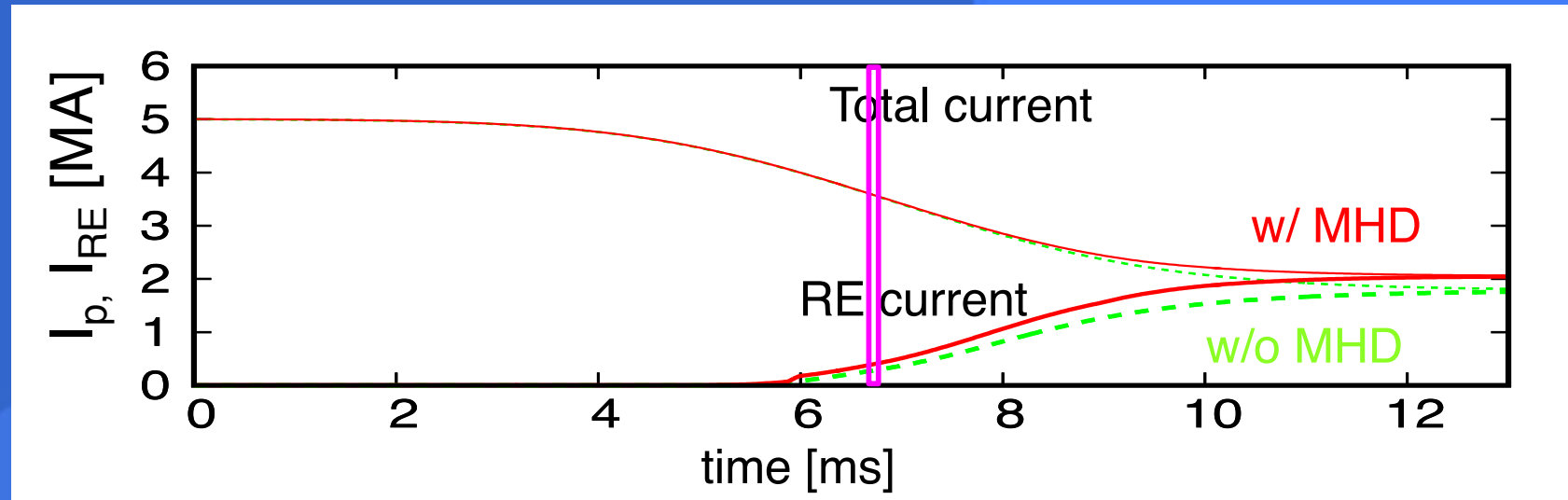
Simulation results

$I_p = 5\text{MA}$, $R=3\text{m}$, $a = 1\text{m}$, $T_e(0) = 3.1\text{ keV}$ to 10 eV , $n_e=1.2 \times 10^{20}/\text{m}^3$, $Z_{\text{eff}}=3$, $t_{\text{TQ}}=1\text{ ms}$
[*] B_t is adjusted for q_a to be 3.



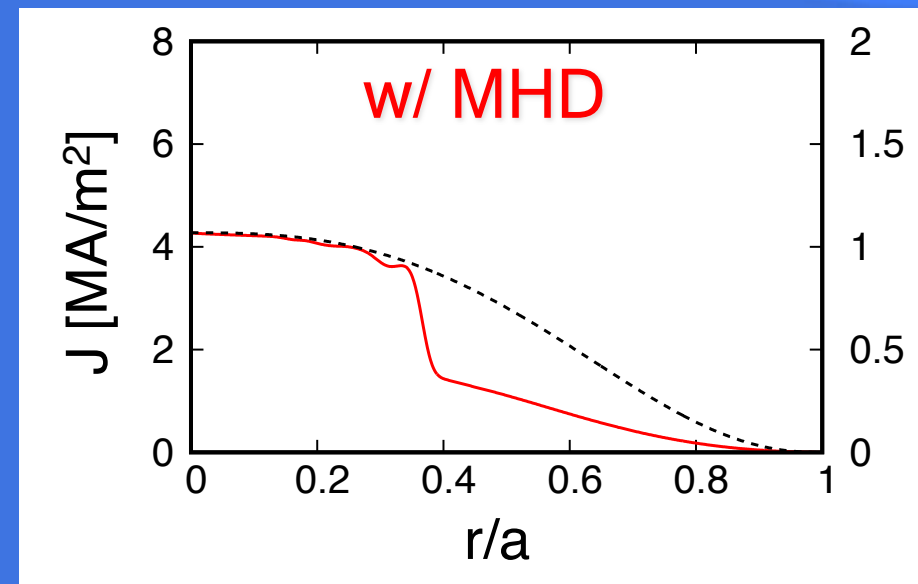
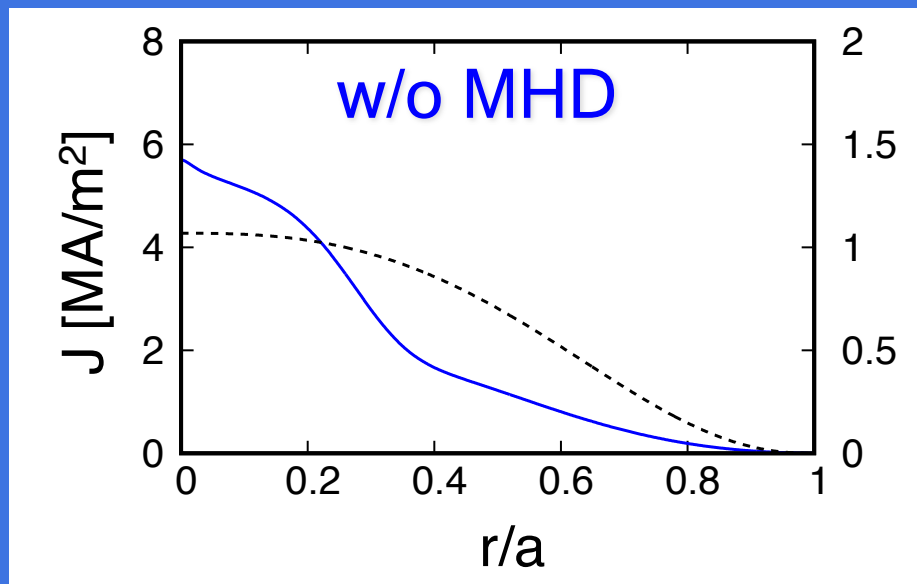
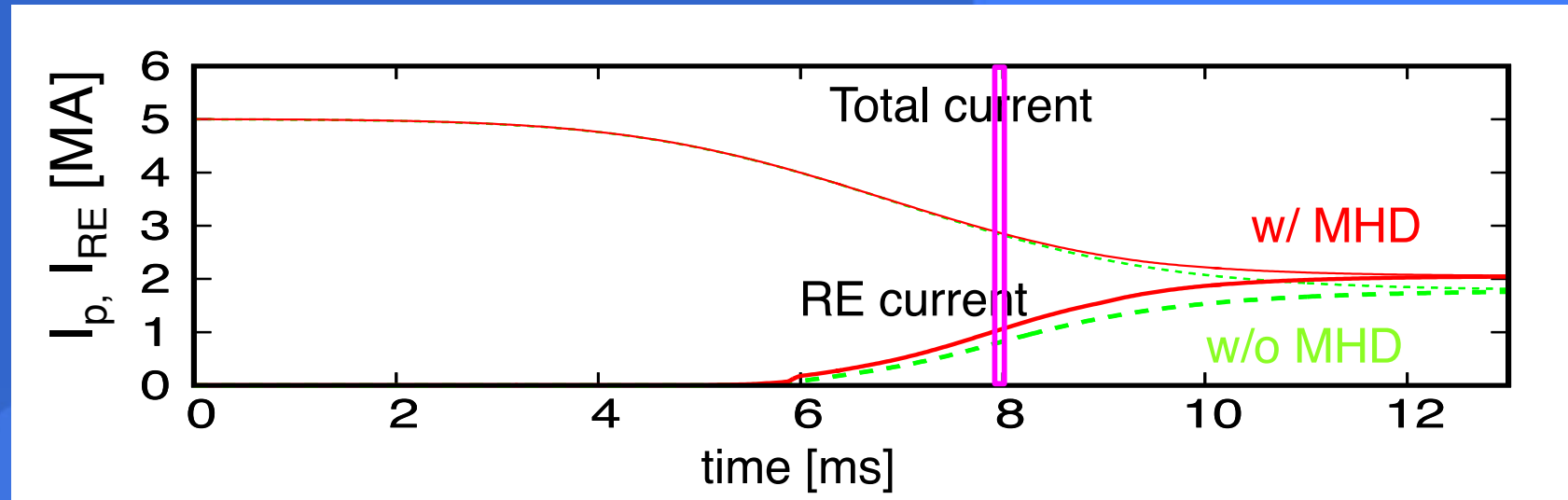
Simulation results

$I_p = 5\text{MA}$, $R=3\text{m}$, $a = 1\text{m}$, $T_e(0) = 3.1\text{ keV}$ to 10 eV , $n_e=1.2 \times 10^{20}/\text{m}^3$, $Z_{\text{eff}}=3$, $t_{\text{TQ}}=1\text{ ms}$
[*] B_t is adjusted for q_a to be 3.



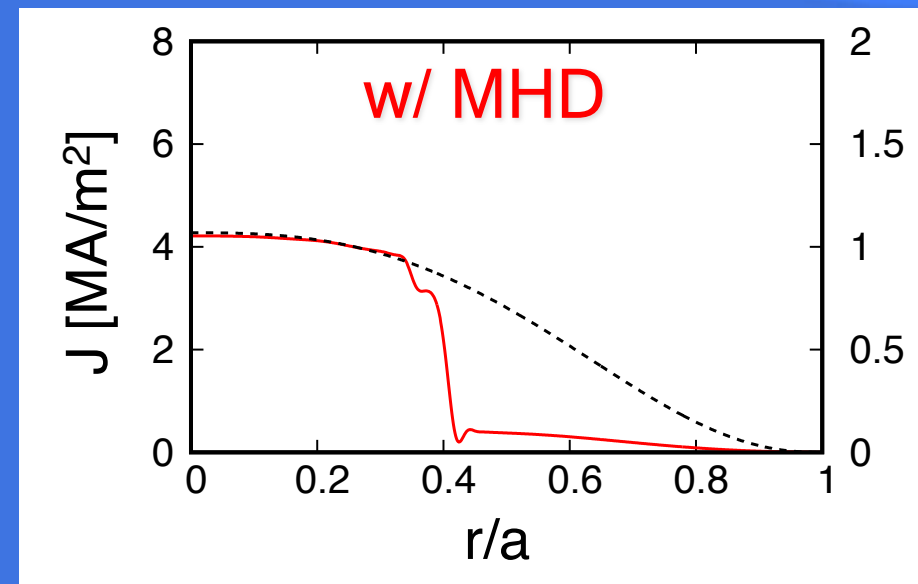
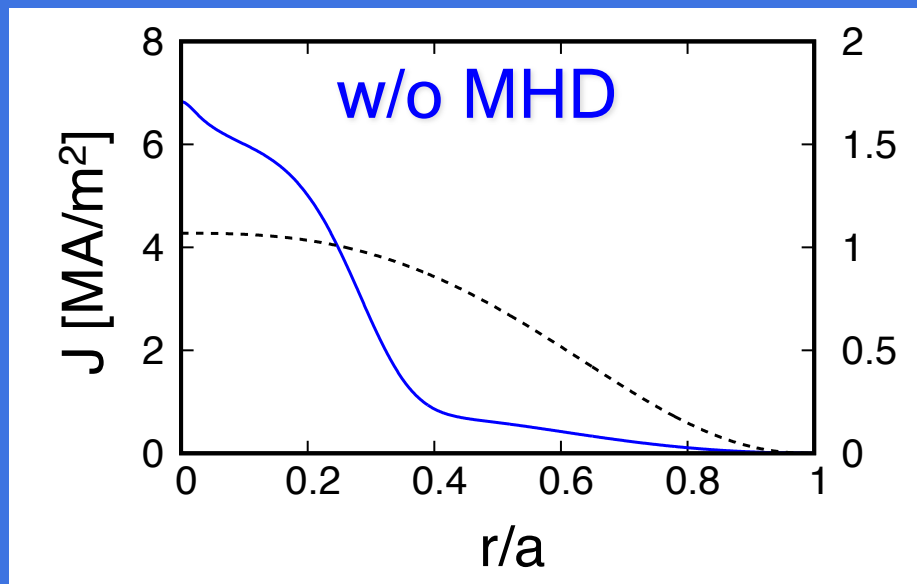
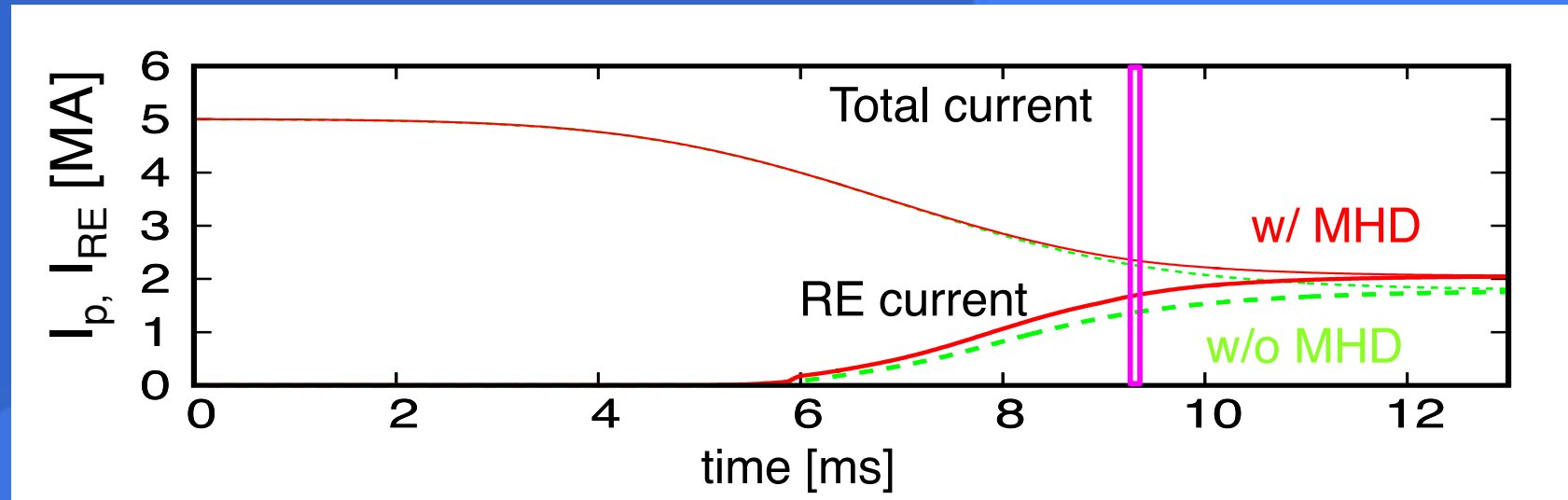
Simulation results

$I_p = 5\text{MA}$, $R=3\text{m}$, $a = 1\text{m}$, $T_e(0) = 3.1\text{ keV}$ to 10 eV , $n_e=1.2 \times 10^{20}/\text{m}^3$, $Z_{\text{eff}}=3$, $t_{\text{TQ}}=1\text{ ms}$
[*] B_t is adjusted for q_a to be 3.



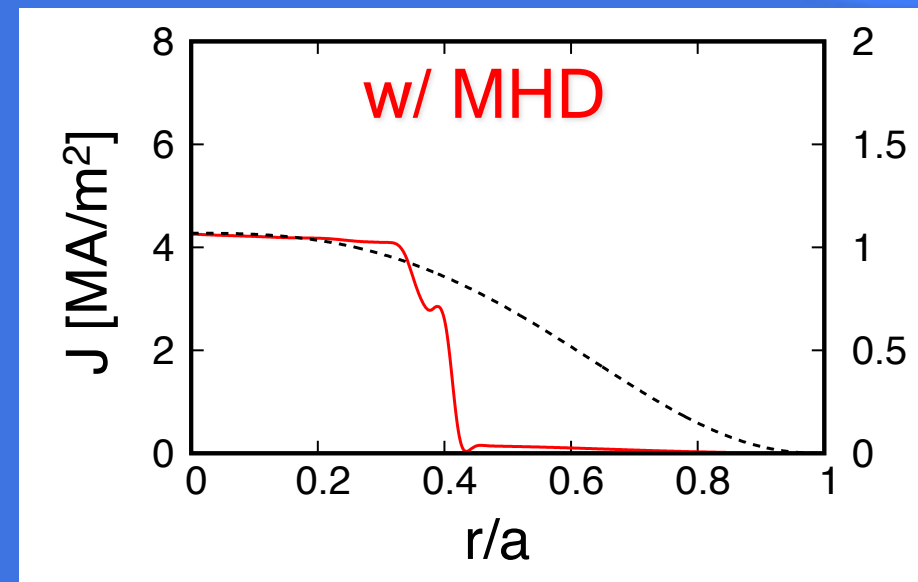
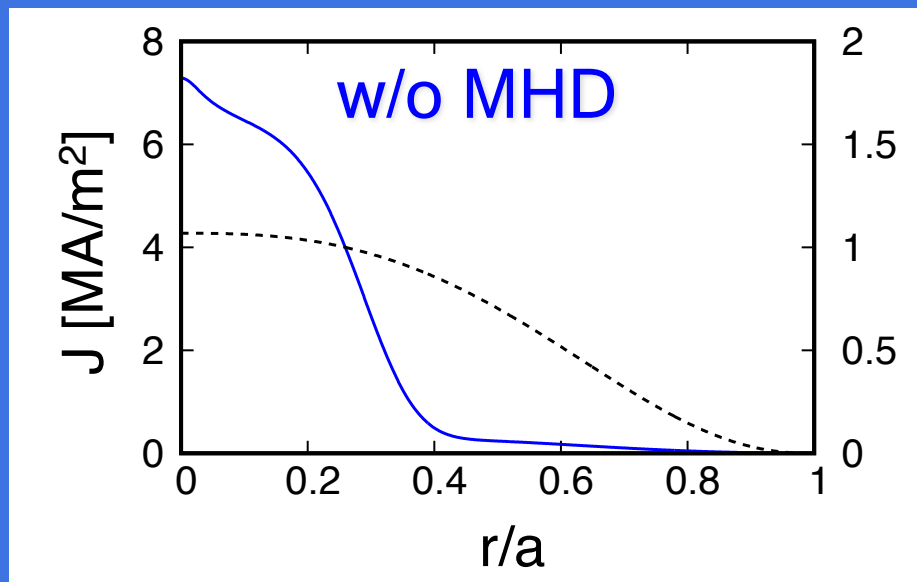
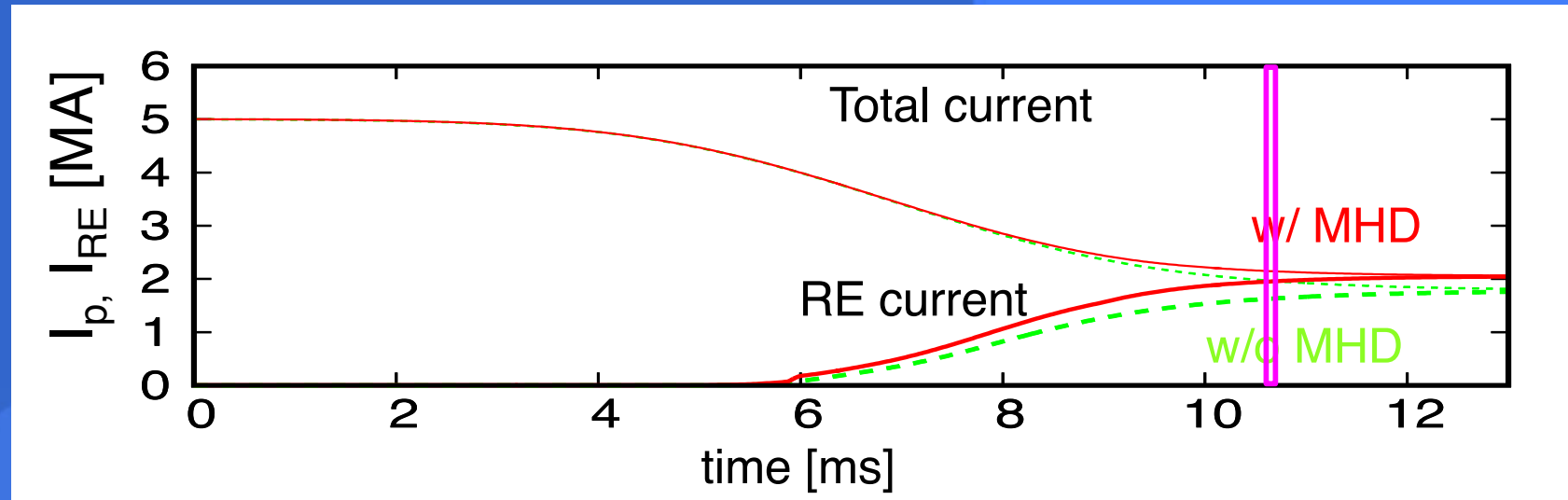
Simulation results

$I_p = 5\text{MA}$, $R=3\text{m}$, $a = 1\text{m}$, $T_e(0) = 3.1\text{ keV}$ to 10 eV , $n_e=1.2 \times 10^{20}/\text{m}^3$, $Z_{\text{eff}}=3$, $t_{\text{TQ}}=1\text{ ms}$
[*] B_t is adjusted for q_a to be 3.



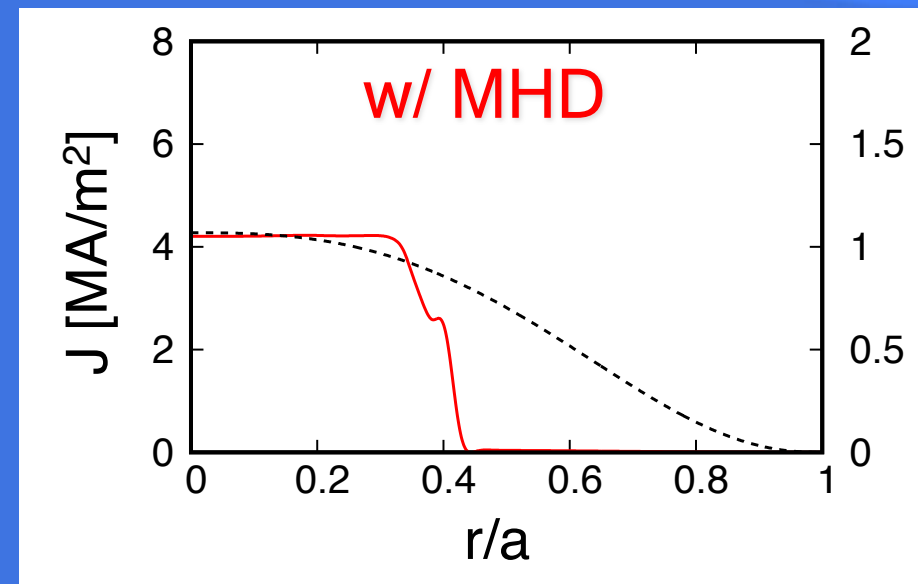
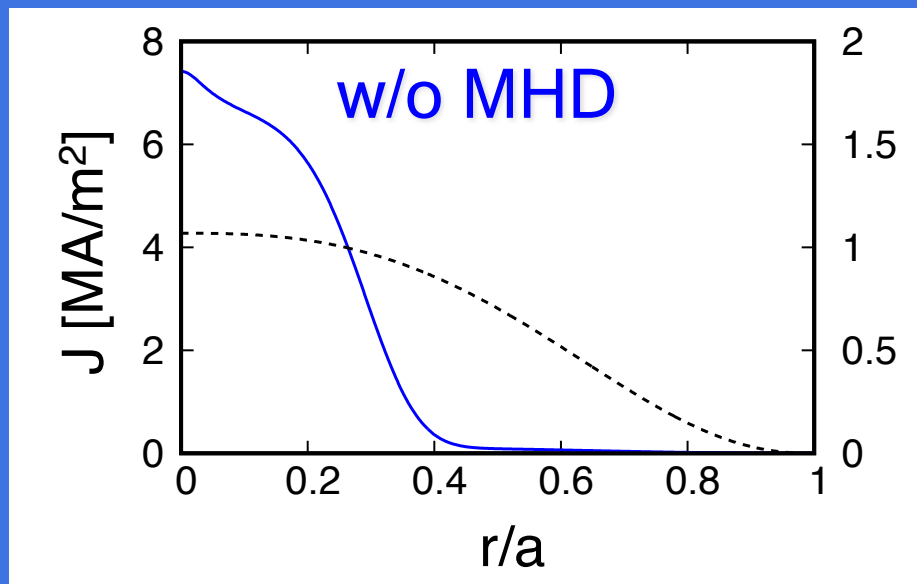
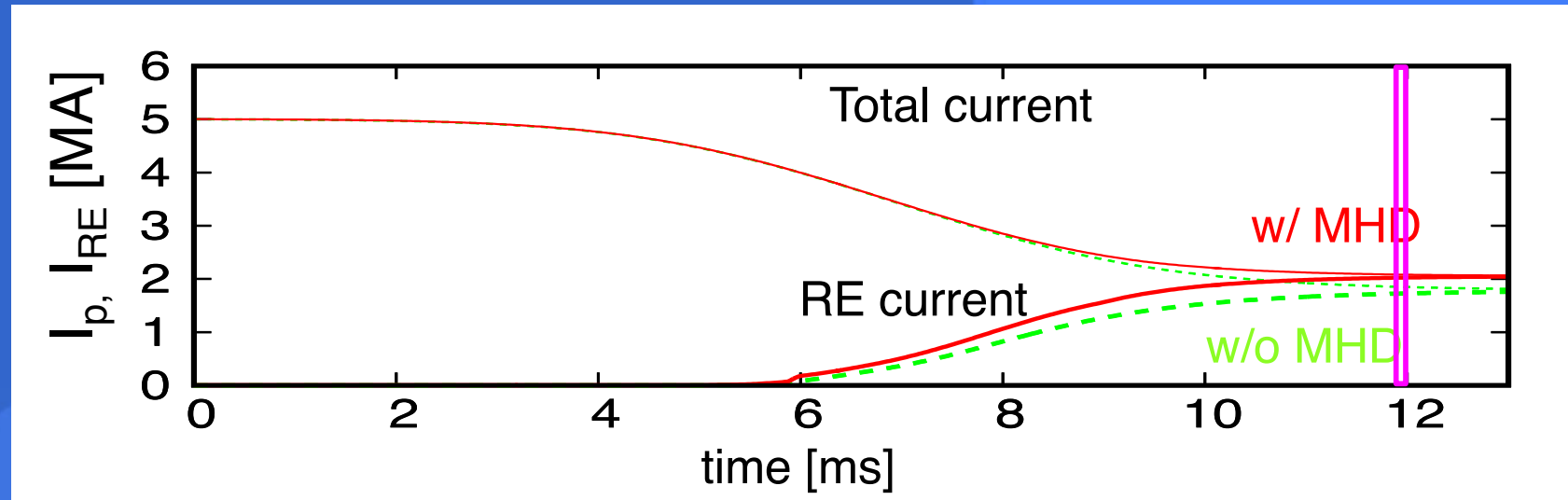
Simulation results

$I_p = 5\text{MA}$, $R=3\text{m}$, $a = 1\text{m}$, $T_e(0) = 3.1\text{ keV}$ to 10 eV , $n_e=1.2 \times 10^{20}/\text{m}^3$, $Z_{\text{eff}}=3$, $t_{\text{TQ}}=1\text{ ms}$
[*] B_t is adjusted for q_a to be 3.



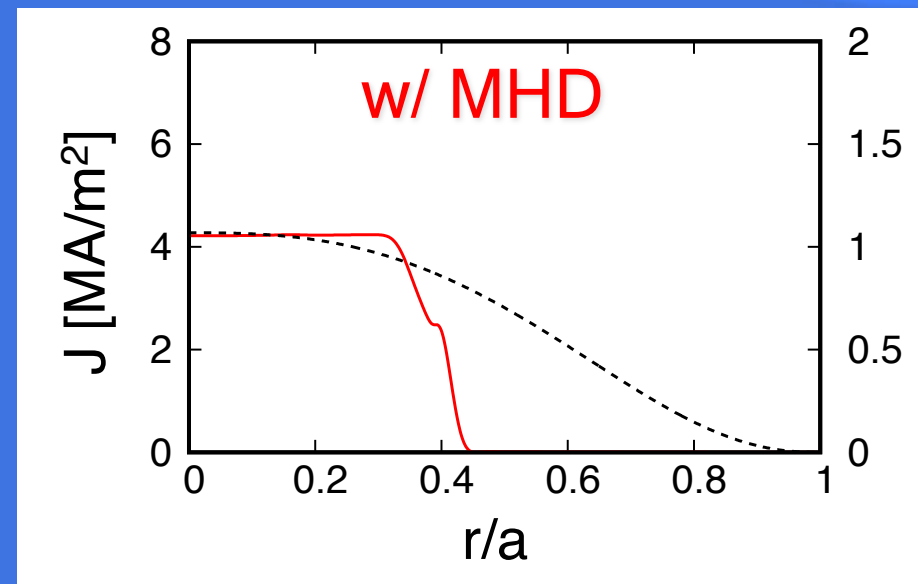
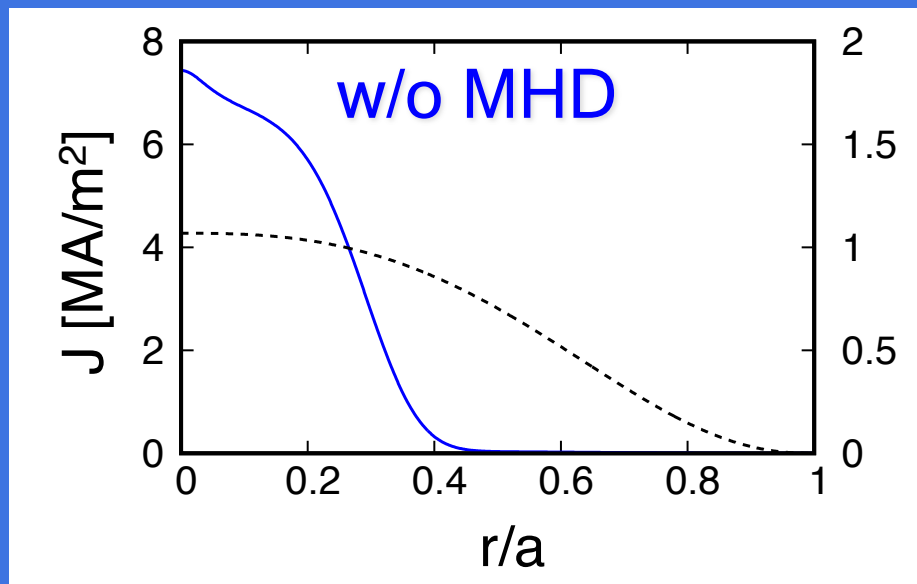
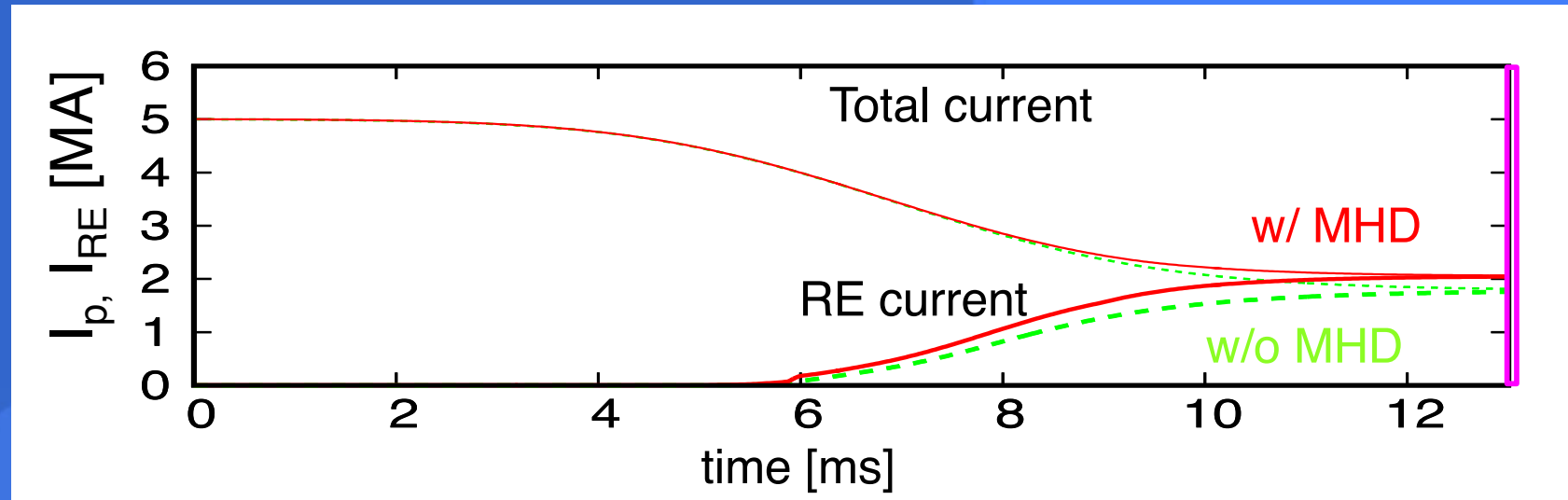
Simulation results

$I_p = 5\text{MA}$, $R=3\text{m}$, $a = 1\text{m}$, $T_e(0) = 3.1\text{ keV}$ to 10 eV , $n_e=1.2 \times 10^{20}/\text{m}^3$, $Z_{\text{eff}}=3$, $t_{\text{TQ}}=1\text{ ms}$
[*] B_t is adjusted for q_a to be 3.



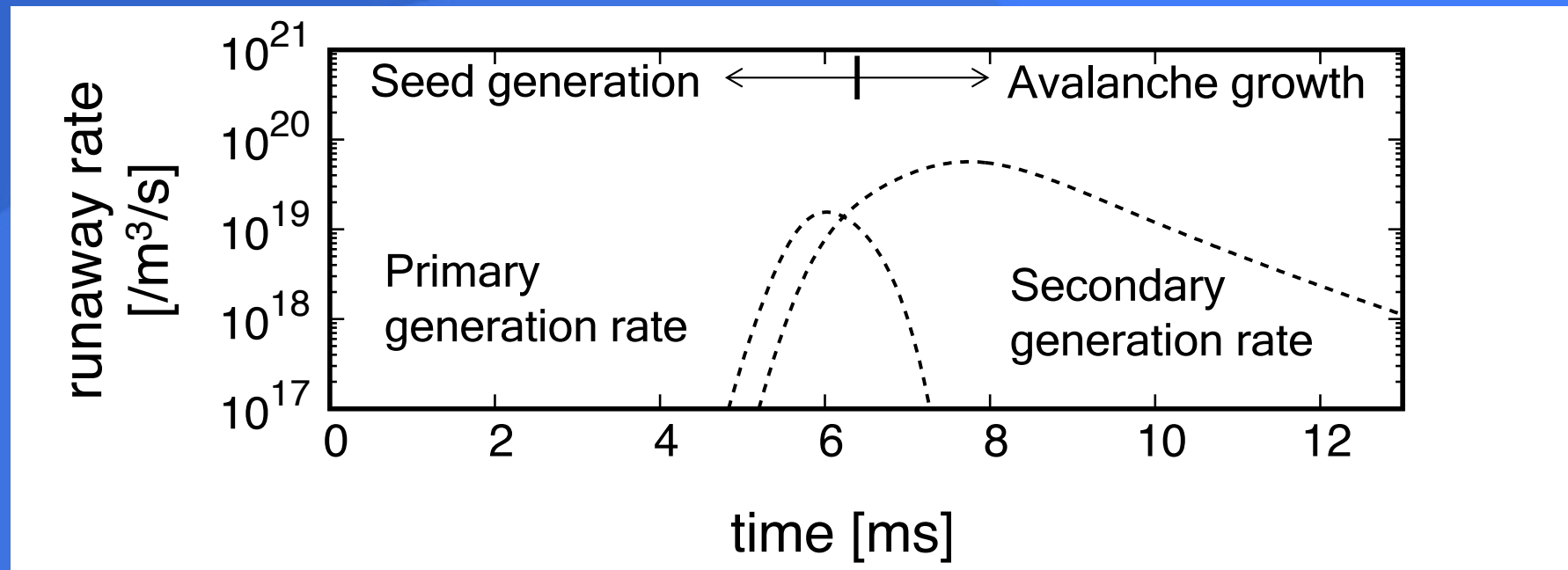
Simulation results

$I_p = 5\text{MA}$, $R=3\text{m}$, $a = 1\text{m}$, $T_e(0) = 3.1\text{ keV}$ to 10 eV , $n_e=1.2 \times 10^{20}/\text{m}^3$, $Z_{\text{eff}}=3$, $t_{\text{TQ}}=1\text{ ms}$
[*] B_t is adjusted for q_a to be 3.



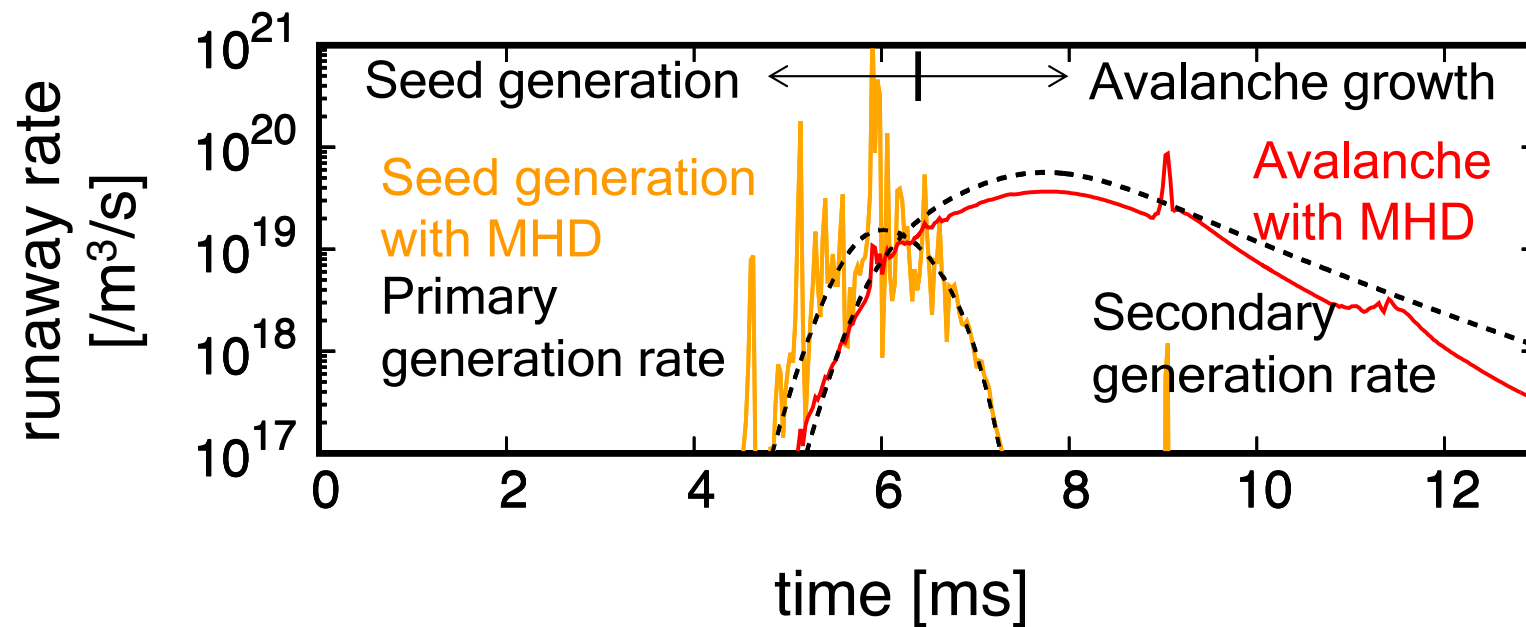
How MHD instability affects generation of runaway electrons?

- Compare runaway generation rate at the plasma center between MHD and non-MHD simulations



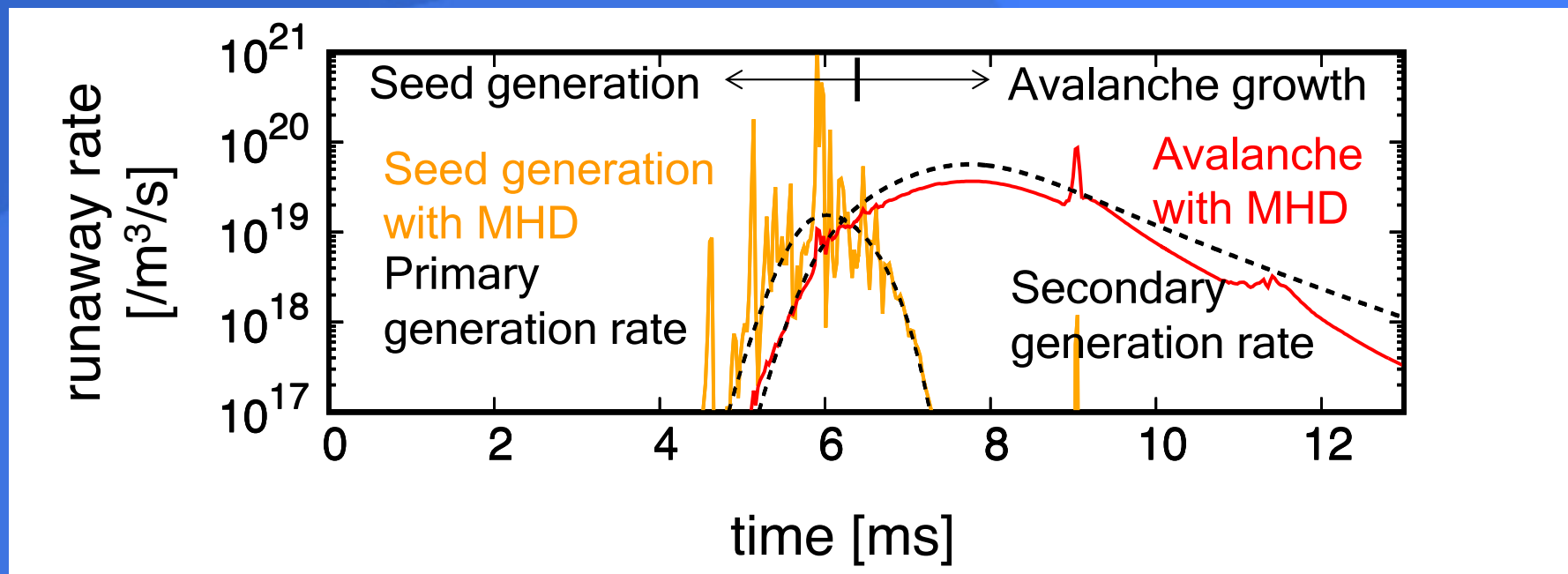
How MHD instability affects generation of runaway electrons?

- Compare runaway generation rate at the plasma center between MHD and non-MHD simulations



How MHD instability affects generation of runaway electrons?

- Compare runaway generation rate at the plasma center between MHD and non-MHD simulations



⇒ MHD modes have significant effects on the seed generation rate

In this case, $m=0/n=0$ voltage spike due to resistive kink (full reconnection) is responsible

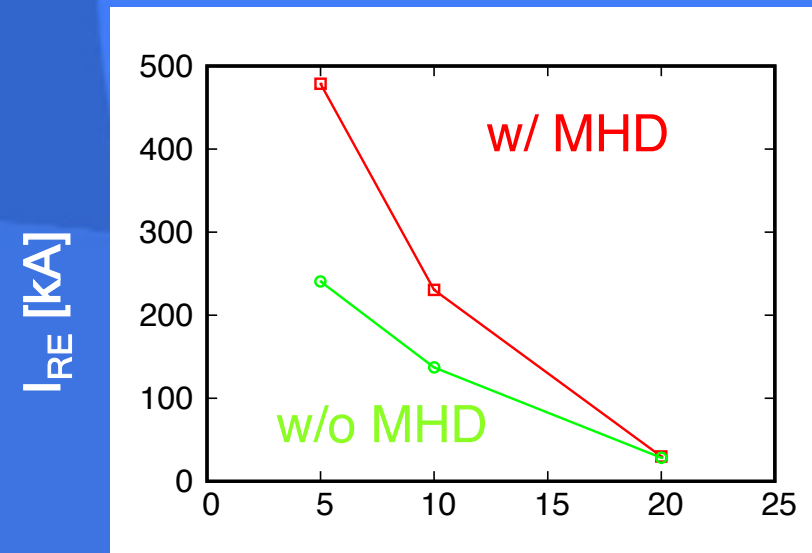
Net increase of both seed and plateau current is observed by MHD simulations

- Dreicer runaway rate is exponentially sensitive to electric field
- ⇒ Once electric field exceeds critical threshold, net production of seed electron can be sensitive to electric field fluctuation

$$S_{\text{Dreicer}} \simeq \frac{n_e}{\tau} \left(\frac{m_e c^2}{2T_e} \right)^{3/2} \left(\frac{E_D}{E} \right)^{3(1+Z_{\text{eff}}/16)} \times \exp \left(-\frac{E_D}{4E} - \sqrt{\frac{(1+Z_{\text{eff}})E_D}{E}} \right)$$

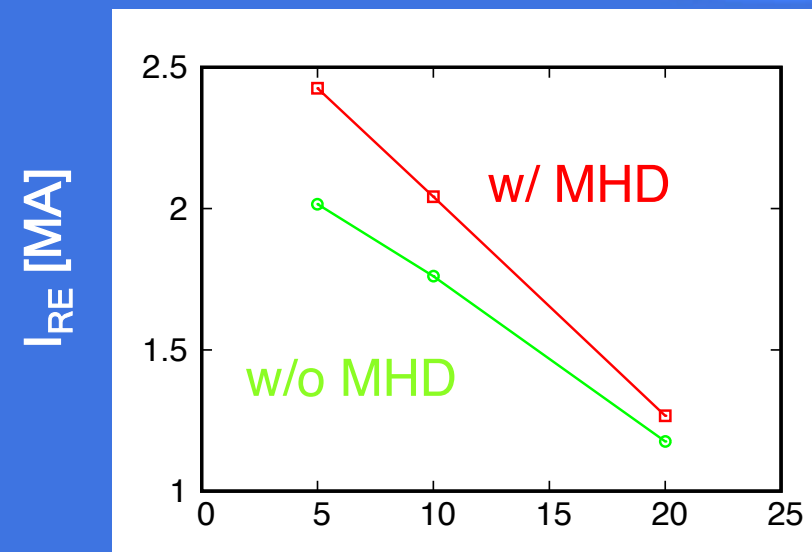
- Modification of internal inductance also affects net RE generation due to avalanche.

Seed current



post-TQ T_e [eV]

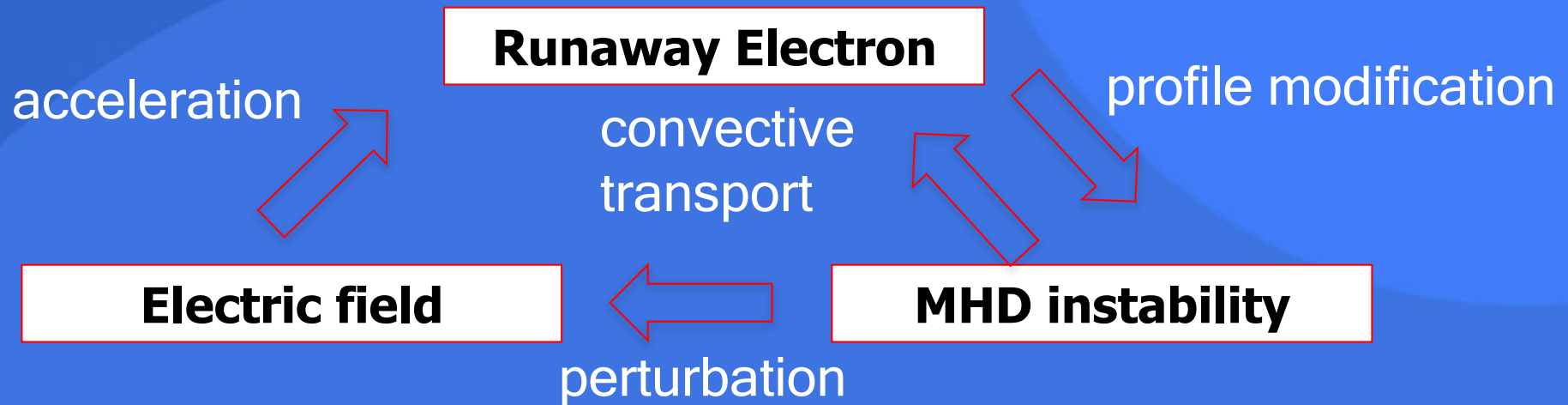
Plateau current



post-TQ T_e [eV]

Self-consistent coupling between RE, electric field, and MHD instabilities

- ◆ EXTREM code allows simulation of runaway current generation consistent with resistive stability.



- **Hybrid approach coupling MHD and runaway** would be important for our understanding of seed electron generation mechanisms in early phase of current quenches.

Effects of stochastic magnetic fields

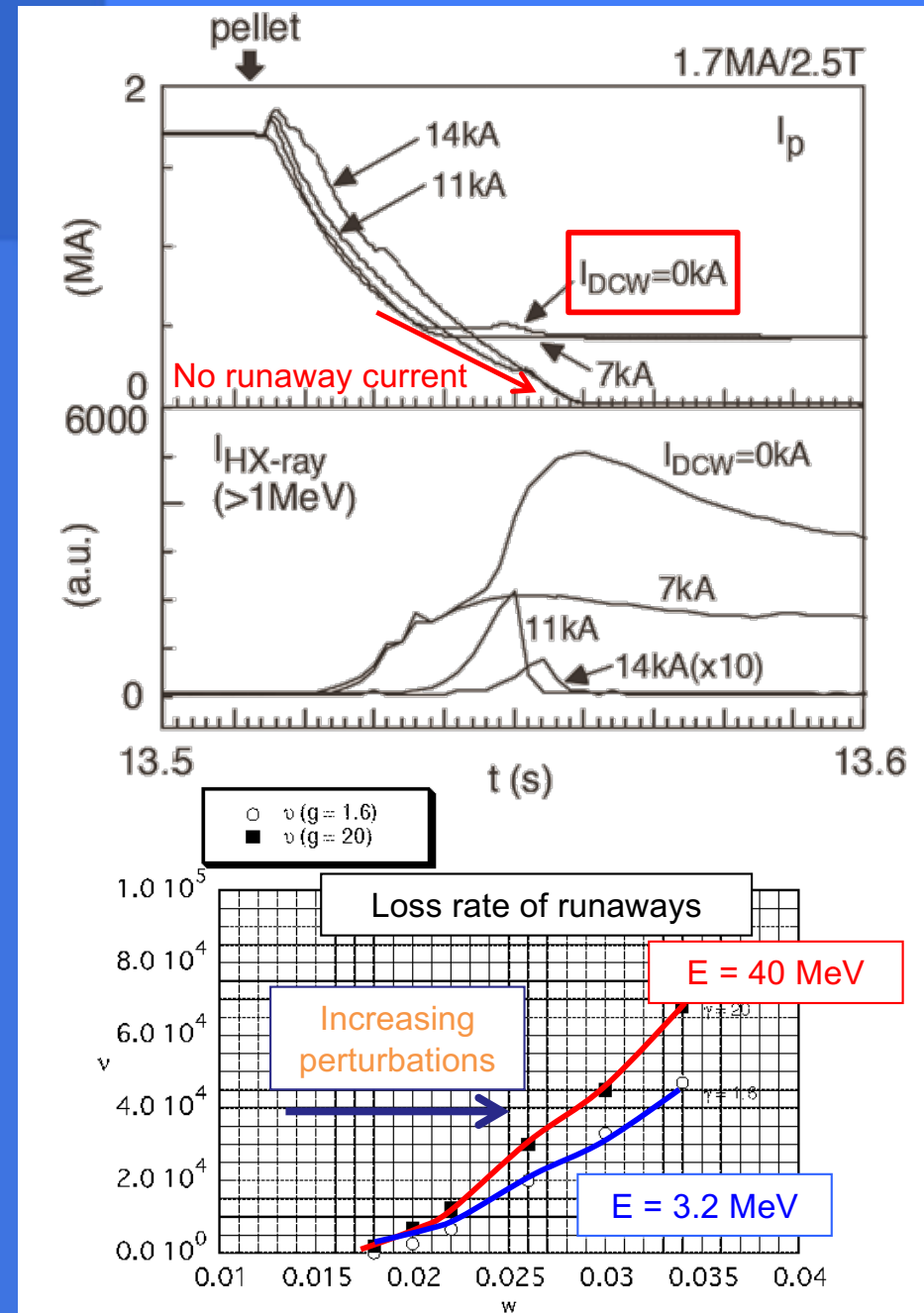
JT-60U experiments for suppression of runaway electrons with magnetic perturbations

Background

- Exp.: RE suppression with RMPs are demonstrated in JT-60U (Kawano, IAEA1996) & TEXTOR (Lehnen, PRL2008).
- Theory: REs are mitigated if the confinement time is much shorter than avalanche growth time (Helander, PPCF2002).

Issue on necessary fluctuation level

- Transport by microturbulence (Mynick & Strachan, PF1981) with $\delta B/B=10^{-4}-10^{-5}$ is too small for affecting avalanches.
- Overlapping of low-order islands ($\delta B/B=10^{-3}-10^{-2}$) can induce large transport with stochastization of core magnetic fields (Tokuda & Yoshino, NF1999).



Model magnetic perturbation

Flute-like perturbation: $\tilde{\mathbf{A}} = \varepsilon \alpha(\psi, \chi, \phi) \mathbf{B}_{eq}$

$$\alpha(\psi, \chi, \phi) = \sum_{m,n} \alpha_{m,n}(\psi) \cos(m\chi - n\phi + \nu_{m,n})$$

Axisymmetric coordinates:

$$\theta = \chi + G(\psi, \chi)$$

$$\zeta = \phi + qG(\psi, \chi)$$

ϕ : symmetric angle

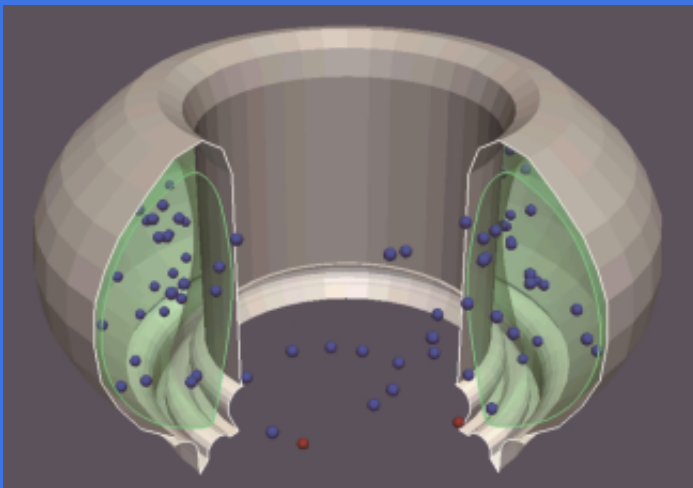
Radial mode structure:

$$\alpha_{m,n}(\psi) = \alpha_{m,n} \exp\left(-\frac{(s - s_{m,n})^2}{w_{m,n}^2}\right), \quad s^2 = \psi / \psi_0$$

ETC-Rel code

S. Tokuda & R. Yoshino, NF1999

A. Matsuyama, et al., APS-DPP 2013



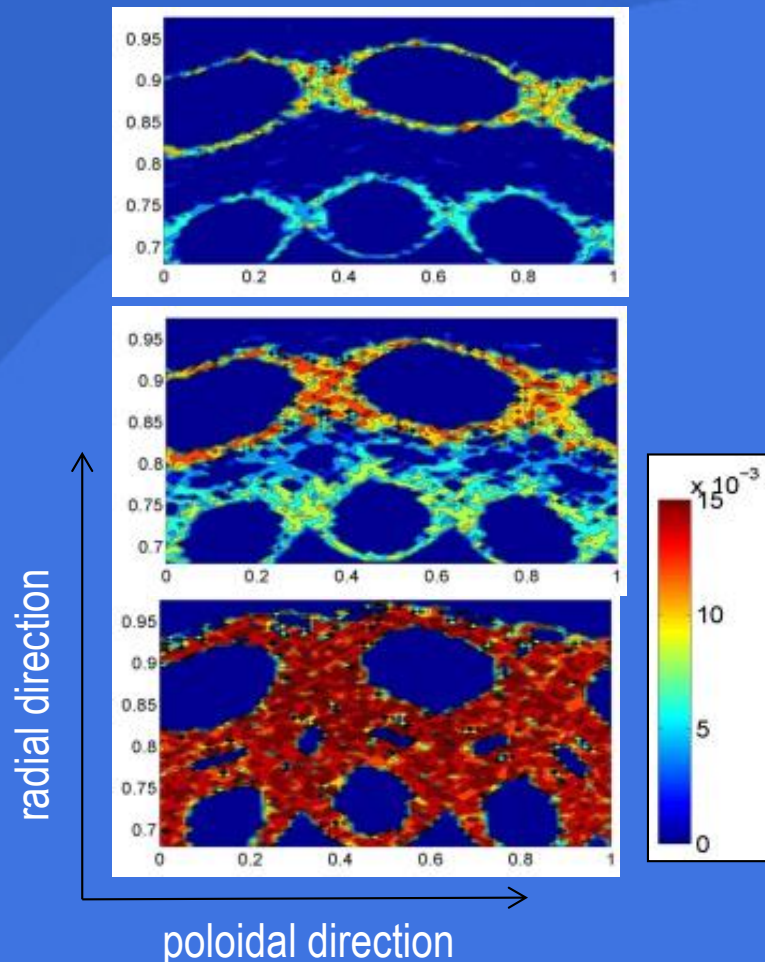
Island width:

$$\Delta s = \sqrt{\frac{2qJ_p \alpha_{mn}}{\psi_{edge} S_0 \frac{dq}{ds}}}$$

Chaotic orbit with magnetic island overlapping

Ex.) Consider overlapping of (2, 1) and (3, 2) islands

Spatial distribution of Liapunov exponents:
Electron orbit (25 MeV), JT-60U size



- REs freely move along the magnetic field
→ **Island overlapping is suggested to be most efficient cause of RE transport**

Quantitative study of runaway electron transport by stochastic magnetic field is still an open issue!

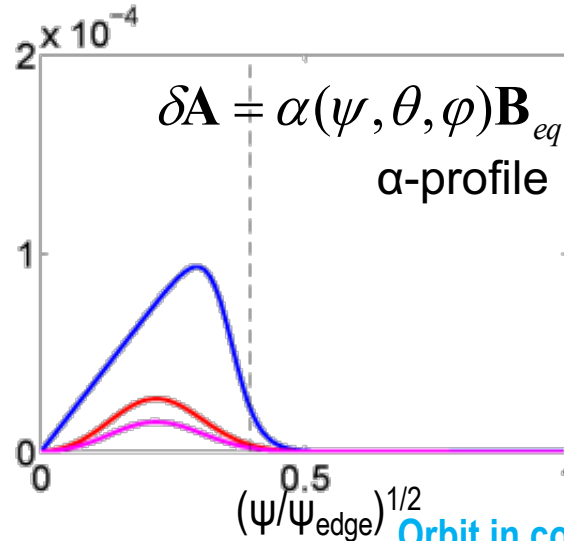
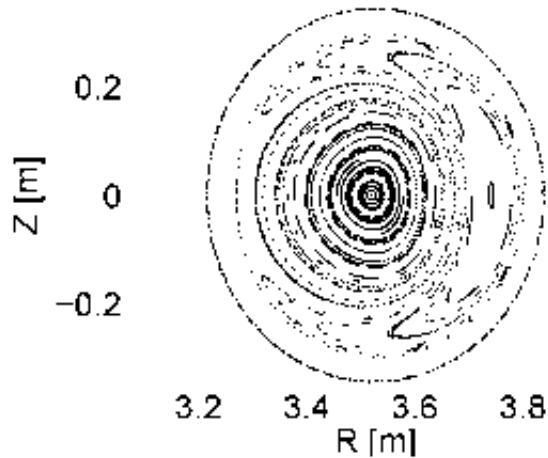
66

[Tokuda & Yoshino NF1999]

Effects of toroidal geometry - drift resonance due to finite orbit width of high energy runaway electrons

$R_0=3.4\text{m}$, $a=1.2\text{m}$, $B=3\text{T}$ (JT-60U grade)

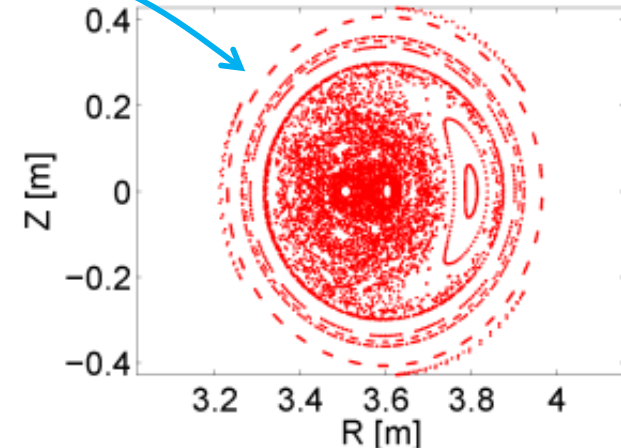
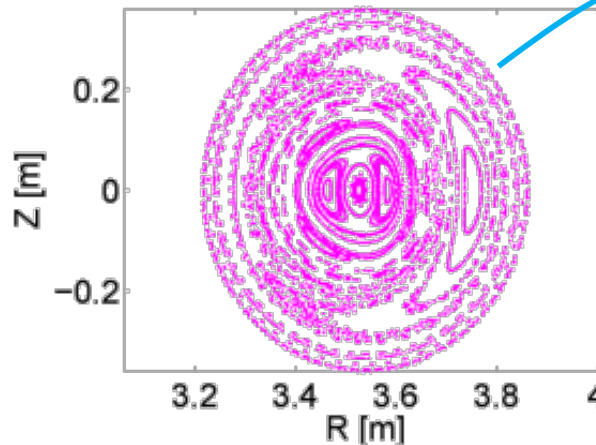
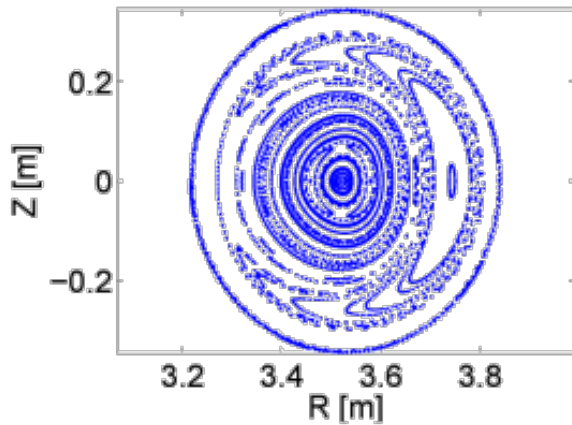
field lines



$$\delta\mathbf{A} = \alpha(\psi, \theta, \varphi)\mathbf{B}_{eq}$$

m/n	$\delta B/B(\%)$
1/1	0.1
2/2	0.02
3/3	0.015

Runaway orbit



Orbit in core region becomes stochastic even without magnetic stochasticity

1MeV

10MeV

50MeV

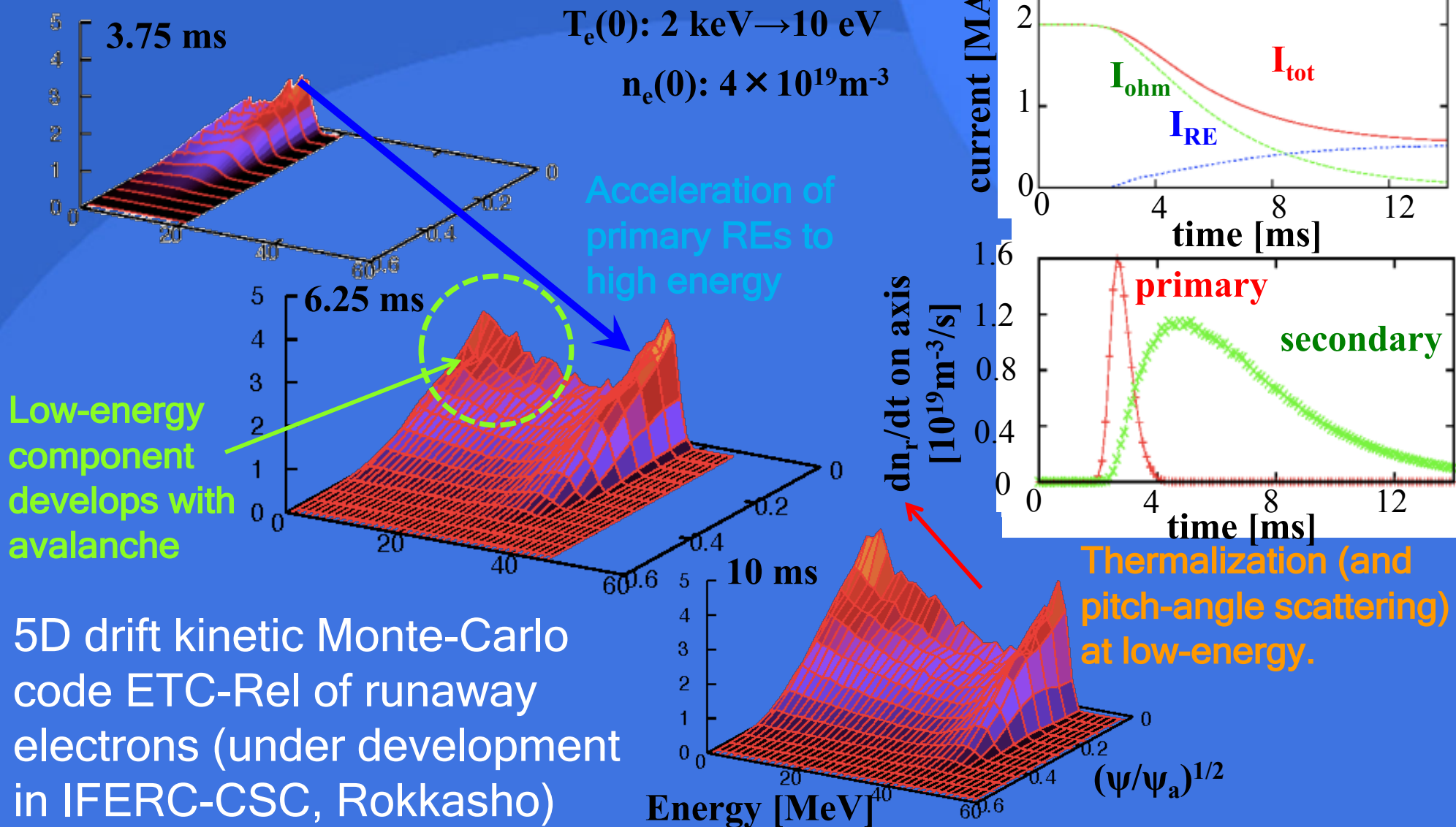
67

Summary and Conclusion

- Development of reliable mitigation scheme of runaway electrons on the basis of its physical understanding is important for extrapolation towards ITER.
- Avalanche amplification is a dominant mechanism for RE generation in ITER, which depends predominantly on the impurity species.
- Beam profile relaxation is studied by using a reduced beam fluid model. Enhancement of seed electrons with $m/n=1/1$ resistive kink modes is observed, which results in increase of net RE current as compared to non-MHD simulation.
- Transport of runaway electrons due to stochastic magnetic fields has been suggested to play a role in suppression of runaway avalanche. However, its detailed physical mechanisms and quantitative study are still open issue.

Future prospects of runaway electron simulation

Understanding of individual mechanisms of primary generation, avalanche, impurity, etc., needs to be combined into integrated large-scale simulation for ITER prediction.



Helander, PPCF 2002

Boozer, POP 2015

Dreicer Electric Field (non relativistic)

In tokamak, a toroidal electric field is applied to drive plasma current

$$E = \frac{V_{loop}}{2\pi R}$$

$$m \frac{dv}{dt} = eE - mv\nu \quad \nu(v) = \frac{e^4 n \ln \Lambda}{4\pi\epsilon_0^2 m^2 v^3}$$

If $eE > mv\nu$ Acceleration of electron

$$E > E_D \equiv \frac{e^3 n \ln \Lambda}{4\pi\epsilon_0^2 m v^2} = \frac{e^3 n \ln \Lambda}{4\pi\epsilon_0^2 T_e}$$

Primary runaway generation

Kruskal and Bernstein PPPL Rep. 1962

$$S_{KB} \equiv \frac{dn_r}{dt} = kn_e \nu \left(\frac{E}{E_D} \right)^{-3/8} \exp \left(-\frac{E_D}{4E} - \sqrt{\frac{2E_D}{E}} \right)$$

Relativistic effect

Connor & Hastie, NF1975

$$E_c = \frac{e^3 n \ln \Lambda}{4\pi\epsilon_0^2 m c^2} = \frac{T_e}{m c^2} E_D$$

$$S_{CH} = S_{KB} \times O\left(\exp\left(-\left(T_e/m_e c^2\right)\left(E_D/E\right)^2\right)\right) \quad E \gg E_c$$

Secondary runaway generation (Avalanche)

Rosenbluth & Putvinski, NF 1997

orbit-average of the relativistic drift-kinetic equation

$$\left\langle \frac{\partial f}{\partial t} \right\rangle - \left\langle \frac{e\mathbf{E}}{m} \cdot \frac{\partial f}{\partial \mathbf{v}} \right\rangle = \langle C(f) \rangle + \langle S \rangle \quad S: \text{the avalanche source of runaway electron}$$

The source comes from close collisions of a primary relativistic electron with low energy electrons from the background plasma

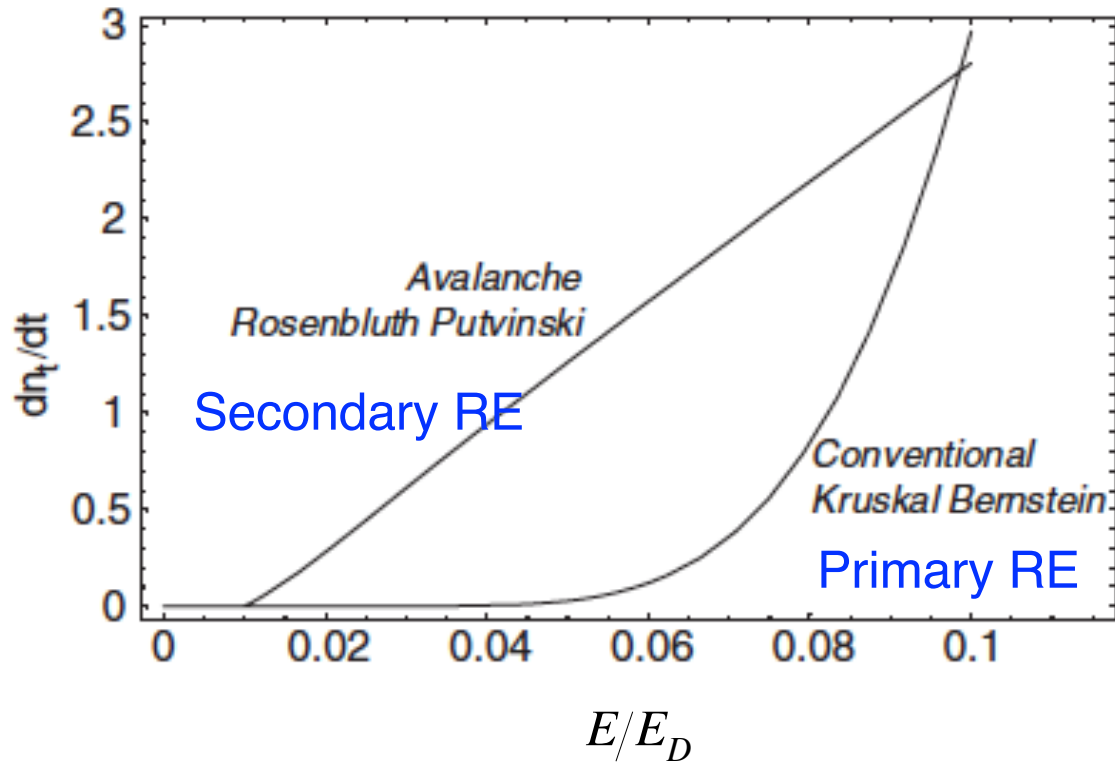


Figure 1. Conventional (4) and avalanche (8) runaway generation rates versus electric field strength.
 $E_c/E_D = T_e/m_e c^2 = 0.01$.

Helander, PPCF 2002

Fokker-Planck simulation for runaway electron generation including the hot-tail effect

H. Nuga¹ A. Matsuyama² M. Yagi² A. Fukuyama¹

¹Kyoto University ²Japan Atomic Energy Agency

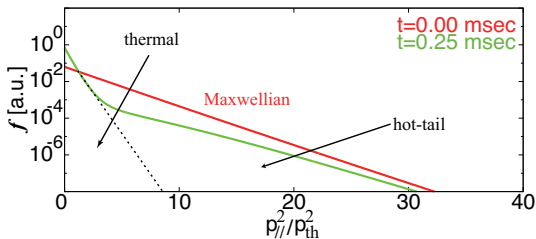


Introduction (RE generation in disruptions)

- Runaway Electrons (REs) are generated in tokamak disruptions.
- The impact of REs to the first wall leads intolerable heat load especially in ITER.
- The high electron density plasma achieved by MGI may suppress the RE generation because of high collisionality.
- **MGI shortens the thermal quench** and might enhance the RE generation through the **hot-tail effect**.
 - This requires the kinetic treatment.
- The estimation of the amount of REs generated in tokamak disruption is required for the development of the mitigation method.

Introduction (hot-tail effect)

- Non-thermal effect should be included for RE gen. simulation
 - If the drop of T is sufficiently fast, the plasma cools down so quickly that fast electrons do not have enough time to be thermalized.
 - The rapid cooling forms the high velocity tail of f_e .
 - It enhances **the primary RE generation** and this effect is called as **hot-tail effect**.



- For mitigated disruptions, the thermal quench time tends to be shortened.

Equations

Electric field diffusion

$$\frac{1}{r} \frac{\partial}{\partial r} \left(r \frac{\partial E}{\partial r} \right) = \mu_0 \frac{\partial j}{\partial t}$$

Ohm's law

$$j = \sigma_{sp} E + ec n_r, \quad n_r = n_{rp} + n_{rs}$$

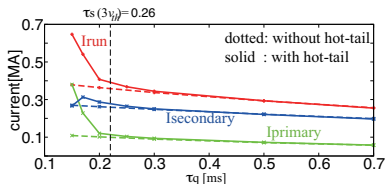
Primary and secondary RE generation rate

$$\frac{dn_{rp}}{dt} = - \int \frac{\partial f}{\partial t} d\mathbf{p}, \quad (p_{max}^2/m \sim 0.5\text{MeV}), \quad \frac{dn_{rs}}{dt} = S_{avalanche}(n_r, E/E_C)$$

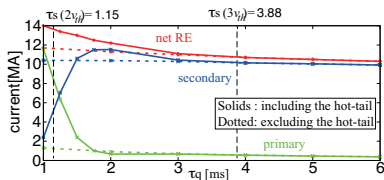
Temperature

$$T(t) = (T(0) - T(t_{max})) \exp(-t/\tau_q) + T(t_{max}), \quad T(t_{max}) = 10\text{eV}$$

Threshold of the hot-tail effect



JT-60U like ($I_p=1\text{MA}$)



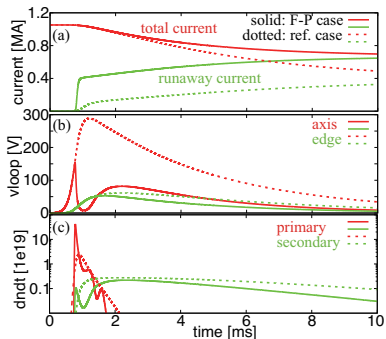
ITER like ($I_p=15\text{MA}$)

- If the thermal quench time τ_q is shorter than $\tau_s^{ee}(2 - 3v_{th})$, the hot-tail effect becomes remarkable.

$$\tau_s^{ee}(v) = \frac{2\pi\epsilon_0^2 m_e^2 v^3}{n_e q^4 \ln \Lambda}$$

- The hot-tail effect enhances the **primary** RE current.
- The high primary RE current reduces the **secondary** RE current.

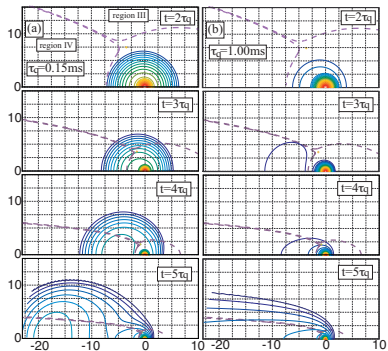
Evolutions (JT-60U case)



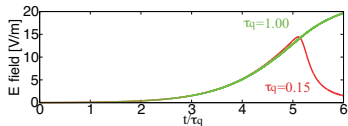
- Evolutions of current, loop voltage, and RE gen. rate on magnetic axis
- $\tau_q = 0.15$ ms ($\tau_s^{ee}(3v_{th}) = 0.26$ ms)
- dotted: excluding the hot-tail
- solid: including the hot-tail

- The hot-tail effect enhances the RE current. (fig. a)
- the peak value of the primary RE gen. rate is an order magnitude greater. (fig. (c))
- The E field including the hot-tail sharply drops (fig. (b))
 - owing to the high primary RE gen. rate.
- Once the E field decreases, it re-increases gradually. (fig. (b))
 - The hollow E profile is filled by E diffusion.

Hot-tail affects the RE distribution (JT-60U case)

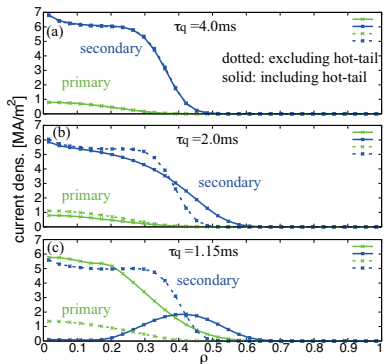


- left: $\tau_q = 0.15$ ms (hot-tail effective)
- right: $\tau_q = 1.0$ ms (ineffective)
- dashed curve: RE-nonRE boundary derived by Fussmann[NF 19, 327, (1979)]



- E field is similar until $t = 5\tau_q$ in both cases.
- The hot-tail effect makes f_e broad to the p_{\perp} direction.
- There are a lot of hot-tail electrons, which have finite perpendicular momentum (See $t = 2 - 3\tau_q$)
- Collisional pitch angle scattering also affects the broadening.

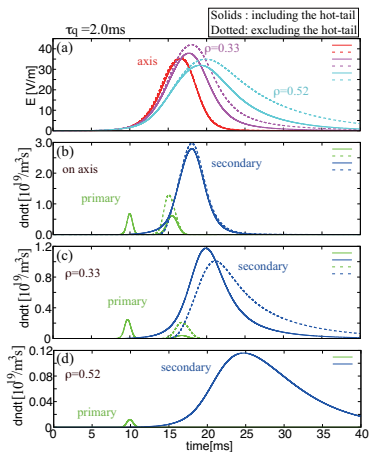
RE current density profile (ITER like)



■ $\tau_s^{ee}(3v_{th}) = 3.88\text{ms}$

- RE j profiles are in good agreement for $\tau_q < \tau_s(3v_{th})$.
- For $\tau_q = 2.0$ ms, the secondary RE j profile including the hot-tail effect becomes broader.
 - The hot-tail effect reduces the primary RE j around $\rho = 0$ and enhances it in outer region ($\rho > 0.4$) in invisible magnitude.
- For $\tau_q = 1.15$ ms, the hot-tail effect dominates the primary RE j on-axis.
- The secondary RE j has a hollowed profile.

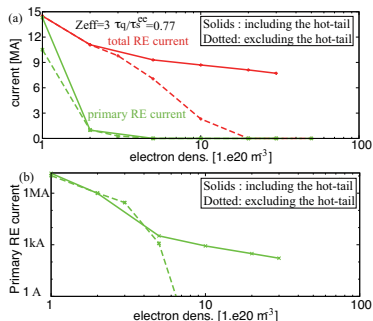
Evolutions of E and dn/dt for $\tau_q = 2.0\text{ms}$ (ITER)



- (a): E field at several radial point.
- (b)-(d): RE gen. rate.

- The hot-tail effect divides the peak of the primary RE gen. into two. ($t \sim 10$ and $t \sim 15\text{ms}$)
 - Former is the hot-tail generation.
- The hot-tail electrons can be REs even with the weak E ($E/E_C \sim 20$ at $t = 10\text{ms}$).
- REs generated at the earlier time trigger the secondary gen.
- Earlier onset on the secondary gen. maintains E weaker.
- Subsequent primary gen. decreases
 - The primary gen. is sensitive to E .

Density dependence



- (a) Primary and secondary RE current against electron density.
 - (b) Focused on the primary RE
 - $\tau_q/\tau_s = 0.77$ (fixed)
 - Evolution of n_e is omitted.
- The high density $n_e \sim 10^{21} \text{ m}^{-3}$ may suppress RE current (excluding hot-tail).
 - If $\tau_q/\tau_s < 1$ is kept
 - Hot-tail maintains 0.1 – 1kA even if $n_e > 10^{21} \text{ m}^{-3}$
 - Primary REs are multiplied to $\sim \text{MA}$.
 - Reliable τ_q in mitigated plasma is required.

Summary

- RE generation including hot-tail effect has been investigated.
- The hot-tail effect affects to the RE current, the evolution of E , j profile, RE velocity distribution, and density dependence even in secondary dominant case.
- There are potentials that
 - RE velocity distribution affects to synchrotron rad.
 - If the mitigation shortens the thermal quench sufficiently, hot-tail effect makes innegligible RE current.